VAPOR-LIQUID EQUILIBRIA PERTAINING TO THE STUDY OF ALTERNATIVE FUELS AND THE FORENSIC ANALYSIS OF CHEMICAL EVIDENCE

by

MEGAN ELIZABETH HARRIES

B.A., Fordham University, 2012

A thesis submitted to the

Faculty of the Graduate School of the

University of Colorado in partial fulfilment

of the requirements for the degree of

Doctor of Philosophy

Department of Chemistry and Biochemistry

2018

This thesis entitled:

Vapor-Liquid Equilibria Pertaining to the Study of Alternative Fuels

and the Forensic Analysis of Chemical Evidence

written by Megan Elizabeth Harries

has been approved for the Department of Chemistry and Biochemistry

---

Jose-Luis Jimenez, Ph.D.

Tara Lovestead, Ph.D.

Date _____

The final copy of this thesis has been examined by the signatories, and we find that both the content and the form meet acceptable presentation standards of scholarly work in the above mentioned discipline.

Harries, Megan Elizabeth (Ph.D., Chemistry, Department of Chemistry and Biochemistry)

Vapor-Liquid Equilibria Pertaining to the Study of Alternative Fuels and the Forensic Analysis of Chemical Evidence

Thesis directed by Dr. Thomas J. Bruno and Professor Jose-Luis Jimenez

Measurement of the vapor-liquid equilibrium (VLE) of fluid mixtures with many components presents a challenge. Data describing such mixtures, like fuels, are important for the development of alternative energy sources and to support forensic science, but there is a lack of suitable instrumentation to provide data with reasonable uncertainty for mixtures with many components. In this thesis, three different techniques for fluid characterization are explored: the advanced distillation curve (ADC), the advanced distillation curve with reflux (ADCR), and PLOT-cryoadsorption.

Two pyrolysis fuels similar to gasoline and diesel fuel made from polypropylene were studied with respect to volatility, composition, and energy content using the advanced distillation curve. The diesel fuel demonstrated volatility very similar to previously measured diesel fuels. The gasoline was less volatile than petroleum-derived counterparts and did not meet specifications. Two pyrolysis crude oils made from ponderosa pine and dairy manure were assessed using the ADC coupled to an approach for characterizing fluids with multiple, immiscible liquid phases. Both oils contained high water levels and would require further refinement before use. The organic phases of each oil contained components indicative of the feedstock used.

A modification of the ADC method, the advanced distillation curve with reflux, was introduced as an approach to measuring the VLE of fluids with many components. The ADCR

additionally approximates the weathering of an ignitable liquid that occurs during an arson fire and measures VLE across a range of weathered conditions. The method was demonstrated using two simple mixtures. The measurements agreed well with models, indicating that ADCR is a suitable VLE metrology.

Vapor-liquid equilibrium data are crucial for interpreting the results of headspace characterization used often in forensic science. One headspace method, portable PLOT-cryoadsorption, was tested in a series of experiments in the laboratory and then deployed for the first time in a field environment that simulated a cargo container. The technology was found to be rapid and sensitive to a variety of compounds of interest to forensic science. Each of the three techniques described in this thesis contribute valuable property data for multicomponent mixtures, towards the development of high-quality predictive models.

ACKNOWLEDGMENTS

Sue Ballou, M.S., and the NIST Special Programs Office, for funding support

Lt. Mark Evans and Boulder Fire-Rescue Station 4

Chris Hamilton

Barbara and Rick Harries

Adam Holewinski, Ph.D.

Jose-Luis Jimenez, Ph.D.

Darron King

Tatiana Popovitchenko, M.S.

Wes Utsler

NIST Applied Chemicals and Materials Division, especially:

Elba Aguirre

Tom Bruno, Ph.D.

Jessica Burger, Ph.D.

Tara Fortin, Ph.D.

Gary Hardin, Ph.D.

Marcia Huber, Ph.D.

Kavita Jeerage, Ph.D.

Tara Lovestead, Ph.D.

Stephanie Outcalt

Jody Sandel

Kim Urness, Ph.D.

Jason Widegren, Ph.D.

CONTENTS

LIST OF TABLES

LIST OF FIGURES

LIST OF PUBLICATIONS

First author:

Harries, M. E.; McDonald, A. G.; Bruno, T. J., Measuring the distillation curves of non-homogeneous fluids: Method and case study of two pyrolysis oils. *Fuel* 2017, *204*, 23-27.

Harries, M.; Bukovsky-Reyes, S.; Bruno, T. J., Field portable low temperature porous layer open tubular cryoadsorption headspace sampling and analysis part II: Applications. *Journal of Chromatography A* 2016, *1429*, 72-78.

Harries, M. E.; Kunwar, B.; Sharma, B. K.; Bruno, T. J., Application of the advanced distillation curve method to characterize two alternative transportation fuels prepared from the pyrolysis of waste plastic. *Energy & Fuels* 2016, *30*, (11), 9671-9678.

Co-author:

Burger, J.; Harries, M.; Bruno, T. J., Characterization of four diesel fuel surrogates by the advanced distillation curve method. *Energy & Fuels* 2016, *30*, (4), 2813–2820.

Chapter 1: Introduction

The work presented in this thesis explores the measurement of vapor-liquid equilibria (VLE) of fluid mixtures both to enable the development of high quality equations of state and to better understand the two most important applications in energy and forensic science which are dependent on VLE. First, the volatility of fuels and oils made by pyrolysis of waste feedstocks, which might help supplement or replace petroleum-based fuels, is characterized with advanced distillation curve measurements. Second, a new approach to measuring VLE of fluids like these and other mixtures containing many components is introduced and demonstrated. Finally, headspace (vapor) characterization, which fully depends on principles of VLE, is investigated using a portable vapor sampler, called PLOT-cryoadsorption, developed to be deployed in the field for environmental testing and forensic science. The study of multicomponent mixtures, especially fuels, is important for the increased rigor of forensic science called for by the National Academy of Sciences in 2009, and for the informed development of non-petroleum energy sources.[1]

1.1. Fuel property measurement and modeling

Alternative liquid fuels to supplement or replace petroleum derived gasoline and diesel fuel are an important area of research. There are both economic and environmental considerations motivating the search for such fuels, made from a variety of feedstocks and by different processes. Road freight transport by truck used 54.3 billion gallons of gasoline and diesel fuel combined in 2016, costing about $90 billion and emitting 293 billion pounds of carbon dioxide from gasoline (E10) and 869 billion pounds from diesel.[2] The creation of liquid

transportation fuels made from sources other than petroleum to replace or blend with today's fuels addresses some of the concerns with our current energy resources. These fuels must be characterized, including measuring properties like volatility. New fuels which behave similarly to existing fuels are desirable, because they may be easily blended with petroleum-derived gasoline or diesel, for instance, and operate in existing engines and other infrastructure. This topic is further discussed in Chapter 2.

A popular route to produce liquid fuels is pyrolysis, the decomposition of solid hydrocarbon-containing feedstocks by application of extreme heat and pressure, often in the presence of catalysts that enhance efficiency. Common materials that have been used to create pyrolysis fuels are biomass and plastic.[3-8] These fuels are still combusted and therefore have their own global warming potential; however, they are sometimes considered carbon neutral, and they address the separate societal challenge of how to dispose of all the trash generated by modern life.

The caveat to alternative fuels is that their properties must be compatible with the engines they are used in; if the fuels are to run in existing cars, their volatility, density, viscosity, and other properties must be adequately similar to existing fuels. Volatility is an especially important property for combustion and is often the first thing measured in assessing a fuel. Volatility is measured in the laboratory using distillation, a process of separating the components of a mixture based on their volatilities which yields a distillation curve, a plot of boiling temperature as a function of the fraction distilled (usually in terms of volume).

Chapters 2 and 3 of this thesis describe the measurement of fuels made from the pyrolysis of polypropylene plastic, dairy manure, and ponderosa pine shavings, all otherwise considered waste products. Collaborators at the University of Illinois and University of Idaho synthesized

the fuels and crude oils respectively. The particular method used to measure fuel volatility in this thesis is the advanced distillation curve (ADC), a modified distillation protocol that addresses the shortcomings and systematic error in the current standard fuel volatility measurement method, ASTM D86, and adds information to the measurement.[9]

1.2. Vapor-liquid equilibria of fluid mixtures

The common thread that connects the previous and next sections, the measurement of fuel volatility and the application of vapor analysis to condensed phase samples, is their dependence on our understanding of vapor-liquid equilibrium (VLE). Complex fluid mixtures containing more than two components present a measurement challenge: their VLE are, in best cases, difficult and resource-intensive to characterize by currently accepted methods used for pure fluids and binary mixtures. Reports of research specific to VLE of fuels and crude oils disregard the complexity of the individual component interactions in favor of treating the fuel as a single component in a binary mixture of hydrocarbons and carbon dioxide, for instance.[10, 11] Such simplification renders this type of measurement irrelevant to applications like arson fire debris analysis, in which the analyte is known to be a fuel, and it must be determined precisely which fuel was used.

VLE measurements are needed in part to contribute to models for multicomponent mixtures, which currently use estimated interaction parameters or binary parameters measured for individual pairs of components. High-quality, low uncertainty measurements of binary mixtures are possible with existing metrologies, although they tend to take months of data collection on different mixture compositions to build a complete VLE diagram. The complex fluid VLE metrology introduced in Chapter 4 is a more efficient way to measure these simpler

mixtures (depending on the acceptable level of uncertainty for the application) as well as an appropriate method to measure the mixtures containing many components that are relevant to real life situations in forensic science.

1.3. Headspace analysis

Headspace analysis is the characterization of a condensed phase sample by collecting and analyzing the vapor that surrounds it. The sample is held inside a closed container, where some of it lofts into the vapor phase in the headspace above it. This vapor is collected on an adsorbent material then desorbed thermally or with solvent prior to introduction to an analytical instrument. The vapor sample can be in equilibrium with the condensed phase but does not have to be for qualitative applications. The methods and instruments used for headspace collection can be applied to equilibrium samples, nonequilibrium samples, or even vapor mixtures without a condensed phase. Headspace analysis is only briefly described in this section; extensive further discussion of the theory and practice of headspace analysis is available in the Encyclopedia of Analytical Sciences entries in the Appendix.

The two major types of headspace methods are static and dynamic. As its name implies, static sampling involves an adsorbent trap passively exposed to the headspace of a sample with no moving parts. Dynamic sampling, also called purge and trap, uses a purge gas flowing over the sample to push vapor out of the sample and through the adsorbent trap. Static methods are simple, best for equilibrium applications, and lend themselves to portability. Dynamic methods tend to have better sensitivity limits because a large quantity of vapor can be collected. Dynamic methods can also be made portable and used for equilibrium measurements, depending on the quantity of vapor removed from the sample container.

Headspace methods have been in use since the 1970s and since used for a wide spectrum of applications. Standards organizations like ASTM International and the US Environmental Protection Agency have adopted standard test methods that use headspace science.[6, 12] Applications of the approach include:

- aroma analysis, including the creation of artificial flavors and fragrances[13-16]
- foods, including contamination, the differences between strains of fruit, and meat spoilage[17, 18]
- forensics, including clandestine graves, arson fire debris, explosives, and drug compounds/precursors[19-22]
- environmental monitoring[23, 24]
- industrial hygiene and process control[25, 26]
- medicine, including blood, breath, and urine testing[27-29]
- vapor pressure measurements of challenging analytes[30, 31]

There are several advantages to vapor sampling as an alternative to direct analysis of the condensed phase sample or other methods of extraction. Solvent extraction, for example, is destructive to the sample, generates more hazardous waste, and solvent choice requires foreknowledge of the types of compounds present in the sample. Targets of vapor analysis can often also be damaging to instrumentation, as in the cases of arson fire debris or soil, and analyzing the vapor is much cleaner while still yielding information about the sample itself. One drawback of vapor analysis, however, is that the composition of the headspace vapor, even in equilibrium with the condensed phase, will be different from the composition of the condensed phase. When the condensed phase sample is the article of interest, and explicit or quantitative

knowledge of its composition is required, good, validated thermodynamic models must exist for the vapor-liquid or vapor-solid equilibrium of the sample contents. In many cases, these models do not yet exist because of the difficulty of measuring the vapor-liquid equilibrium of such complex mixtures. The previous section of this chapter and Chapter 4 of this thesis describe this challenge and one solution to it.

The specific headspace sampling approach discussed in this thesis is porous layer open tubular (PLOT) cryoadsorption, or PLOT-cryo. PLOT-cryo, a dynamic headspace sampling method that uses adsorbent-coated capillary traps operated under cold conditions (to enhance collection of volatile compounds), was developed at NIST for laboratory-based experiments in 2009.[32] The benchtop apparatus has been used to analyze explosive vapors for the Department of Homeland Security, to study poultry spoilage markers, and to measure vapor pressures of cannabinoids, to name a few.[30, 31, 33-36] A portable version of the technology was developed in response to demand from stakeholders in forensic science interested in field capability.[37, 38] Chapters 5 and 6 describe two sets of experiments representing the initial testing of portable PLOT-cryo.

1.4. Thesis overview

This thesis encompasses research in forensic vapor sampling, the characterization of alternative fuels, and the vapor-liquid equilibrium behavior of complex fluid mixtures, their unifying measurement need.

In Chapter 2, the volatility of two alternative liquid fuels is measured and their compositions analyzed. These fuels, made by pyrolysis of polypropylene plastic, are a promising use of waste material to provide energy for transportation applications. To determine how both

gasoline and diesel fuel analogue formulations would perform compared to conventional petroleum derived fuels, the advanced distillation curve method was used to characterize the volatility and composition of the fuels.

In Chapter 3, the advanced distillation curve is applied again, this time to two crude pyrolysis oils made from two different sources of waste: pine shavings and dairy manure.

In Chapter 4, an approach to measuring the vapor-liquid equilibrium of fluids containing more than two components is developed and demonstrated using two simple mixtures. This approach, the advanced distillation curve with reflux, is particularly suitable for measurements relevant to the headspace analysis of arson fire debris. The method simultaneously weathers the fuels to produce mixtures like those found on fire debris evidence and relates the composition of that evidence to the composition profile found as a result of headspace analysis of the sample.

In Chapter 5, portable PLOT-cryo, a new technology for in-the-field collection of headspace vapors, is demonstrated with some applications in forensic science and environmental monitoring.

Chapter 6 describes the first field deployment of portable PLOT-cryo technology. It is tested using a simulated cargo shipping container containing several analytes of forensic interest.

In Chapter 7, the thesis work is summarized and discussed as a whole. The importance of technology transfer and education about these metrologies is emphasized, and recommendations for continued research are made. The progress of science is incremental and never complete.

1.5. References

1. National Research Council, *Strengthening Forensic Science in the United States: A Path Forward*. The National Academies Press: Washington, DC, 2009.

2. American Trucking Association, Reports, trends & statistics: fuel consumption. http://www.trucking.org/News_and_Information_Reports_Energy.aspx.

3. Sharma, B. K., Moser, B. R., Vermillion, K. E., Doll, K. M., Rajagopalan, N., Production, characterization and fuel properties of alternative diesel fuel from pyrolysis of waste plastic grocery bags. *Fuel Processing Technology* 2014, *122*, 79-90.

4. Kunwar, B., Chandrasekaran, S. R., Moser, B. R., Deluhery, J., Kim, P., Rajagopalan, N., Sharma, B. K., Catalytic thermal cracking of postconsumer waste plastics to fuels: 2. Pilot-scale thermochemical conversion. *Energy & Fuels* 2017, *31* (3), 2705-2715.

5. Han, Y., McIlroy, D. N., McDonald, A. G., Hydrodeoxygenation of pyrolysis oil for hydrocarbons production using nanosprings based catalysts. *J Anal Appl Pyrolysis* 2016, *117*, 94-105.

6. Anuar Sharuddin, S. D., Abnisa, F., Wan Daud, W. M. A., Aroua, M. K., A review on pyrolysis of plastic wastes. *Energy Conversion and Management* 2016, *115*, 308-326.

7. Elliott, D. C., Wang, H., French, R., Deutch, S., Iisa, K., Hydrocarbon liquid production from biomass via hot-vapor-filtered fast pyrolysis and catalytic hydroprocessing of the bio-oil. *Energy & Fuels* 2014, *28* (9), 5909-5917.

8. Zacher, A. H., Elliott, D. C., Olarte, M. V., Santosa, D. M., Preto, F., Iisa, K., Pyrolysis of woody residue feedstocks: Upgrading of bio-oils from mountain-pine-beetle-killed trees and hog fuel. *Energy & Fuels* 2014, *28* (12), 7510-7516.

9. *ASTM D86, Standard test method for distillation of petroleum products at atmospheric pressure*. ASTM International: West Conshohocken, PA, 2004.

10. Al Ghafri, S. Z., Maitland, G. C., Trusler, J. P. M., Experimental and modeling study of the phase behavior of synthetic crude oil+CO2. *Fluid Phase Equilibria* 2014, *365*, 20-40.

11. Turek, E. A., Metcalfs, R. S., Yarborough, L., Robinson, R. L., Jr., Phase Equilibria in CO2 - Multicomponent Hydrocarbon Systems: Experimental Data and an Improved Prediction Technique. *Society of Petroleum Engineers Journal* 1984, *24* (3).

12. US Environmental Protection Agency, Method 5021A: Volatile organic compounds in various sample matrices using equilibrium headspace analysis. July 2014.

13. Li, Z., Suslick, K. S., A hand-held optoelectronic nose for the identification of liquors. *ACS Sensors* 2018, *3* (1), 121-127.

14. Baránková, E., Dohnal, V., Effect of additives on volatility of aroma compounds from dilute aqueous solutions. *Fluid Phase Equilibria* 2016, *407*, 217-223.

15. Omar, J., Olivares, M., Alonso, I., Vallejo, A., Aizpurua-Olaizola, O., Etxebarria, N., Quantitative analysis of bioactive compounds from aromatic plants by means of dynamic headspace extraction and multiple headspace extraction-gas chromatography-mass spectrometry. *Journal of Food Science* 2016, *81* (4), C867-C873.

16. Kaiser, R., Environmental Scents at the Ligurian Coast. *Perfumer & Flavorist* 1997, *22*, 7–18.

17. Zhang, C.-Y., Zhang, Q., Zhong, C.-H., Guo, M.-Q., Analysis of volatile compounds responsible for kiwifruit aroma by desiccated headspace gas chromatography–mass spectrometry. *Journal of Chromatography A* 2016, *1440*, 255-259.

18. Sghaier, L., Vial, J., Sassiat, P., Thiebaut, D., Watiez, M., Breton, S., Rutledge Douglas, N., Cordella Christophe, B. Y., An overview of recent developments in volatile compounds analysis from edible oils: Technique-oriented perspectives. *European Journal of Lipid Science and Technology* 2016, *118* (12), 1853-1879.

19. Hargather, M. J., Staymates, M. E., Madalis, M. J., Smith, D. J., Settles, G. S., The internal aerodynamics of cargo containers for trace chemical sampling and detection. *IEEE Sensors Journal* 2011, *11* (5), 1184-1193.

20. Holland, P. M., Mustacich, R. V., Everson, J. F., Foreman, W., Leone, M., Sanders, A. H., Naumann, W. J., *Correlated column micro gas chromatography instrumentation for the vapor detection of contraband drugs in cargo containers*. SPIE's 1994 International Symposium on Optics, Imaging, and Instrumentation, SPIE: 1994; p 8.

21. Neudorfl, P., Hupe, M., Pilon, P., Lawrence, A. H., Drolet, G., Su, C.-W., Rigdon, S. W., Kunz, T. D., Ulwick, S., Hoglund, D. E., Wingo, J. J., Demirgian, J. C., Shier, P., *Detection of cocaine in cargo containers by high-volume vapor sampling: field test at Port of Miami*. Enabling Technologies for Law Enforcement and Security, SPIE: 1997; p 9.

22. Staples, E. J., Viswanathan, S., Detection of contrabands in cargo containers using a high-speed gas chromatograph with surface acoustic wave sensor. *Industrial & Engineering Chemistry Research* 2008, *47* (21), 8361-8367.

23. Truong, T., Porter, N., Lee, E., Thomas, R. J., The applicability of field-portable GC–MS for the rapid sampling and measurement of high-boiling-point semivolatile organic compounds in environmental samples. *Spectroscopy* 2016, *14* (3), 20-26.

24. Bellar, T. A., Lichtenberg, J. J., Kroner, R. C., The occurrence of organohalides in chlorinated drinking waters. *Journal - American Water Works Association* 1974, *66* (12), 703-706.

25. Hu, H.-C., Chai, X.-S., Determination of methanol in pulp washing filtrates by desiccated full evaporation headspace gas chromatography. *Journal of Chromatography A* 2012, *1222* (Supplement C), 1-4.

26. Hu, H.-C., Chai, X.-S., Wei, C.-H., Barnes, D., Increasing the sensitivity of headspace analysis of low volatility solutes through water removal by hydrate formation. *Journal of Chromatography A* 2014, *1343*, 42-46.

27. Mills, G. A., Walker, V., Headspace solid-phase microextraction procedures for gas chromatographic analysis of biological fluids and materials. *Journal of Chromatography A* 2000, *902* (1), 267-287.

28. Hryniuk, A., Ross, B. M., Detection of acetone and isoprene in human breath using a combination of thermal desorption and selected ion flow tube mass spectrometry. *International Journal of Mass Spectrometry* 2009, *285* (1), 26-30.

29. Di Francesco, F., Fuoco, R., Trivella, M. G., Ceccarini, A., Breath analysis: trends in techniques and clinical applications. *Microchemical Journal* 2005, *79* (1), 405-410.

30. Lovestead, T. M., Bruno, T. J., Determination of cannabinoid vapor pressures to aid in vapor phase detection of intoxication. *Forensic Chemistry* 2017, *5* (Supplement C), 79-85.

31. Lovestead, T. M., Bruno, T. J., Trace headspace sampling for quantitative analysis of explosives with cryoadsorption on short alumina porous layer open tubular columns. *Analytical Chemistry* 2010, *82*, 5621-5627.

32. Bruno, T. J., Simple, quantitative headspace analysis by cryoadsorption on a short alumina PLOT column. *J Chromatogr Sci* 2009, *47* (7), 569-74.

33. Burger, J. L., Lovestead, T. M., Bruno, T. J., Composition of the C6+ fraction of natural gas by multiple porous layer open tubular capillaries maintained at low temperatures. *Energy & Fuels* 2016, *30* (3), 2119-2126.

34. Lovestead, T. M., Bruno, T. J., Detecting gravesoil with headspace analysis with adsorption on short porous layer open tubular (PLOT) columns. *Forens Sci Int* 2011, *204*, 156-161.

35. Nichols, J. E., Harries, M. E., Lovestead, T. M., Bruno, T. J., Analysis of arson fire debris by low temperature dynamic headspace adsorption porous layer open tubular columns. *Journal of Chromatography A* 2014, *1334*, 126-138.

36. Lovestead, T. M., Bruno, T. J., Detection of poultry spoilage markers from headspace analysis with cryoadsorption on a short alumina PLOT column. *Food Chem* 2010, *121*, 1274-1282.

37. Bruno, T. J., Field portable low temperature porous layer open tubular cryoadsorption headspace sampling and analysis Part I: Instrumentation. *Journal of Chromatography A* 2016, *1429*, 65-71.

38. Harries, M., Bukovsky-Reyes, S., Bruno, T. J., Field portable low temperature porous layer open tubular cryoadsorption headspace sampling and analysis Part II: Applications. *Journal of Chromatography A* 2016, *1429*, 72-78.

Chapter 2: Application of the Advanced Distillation Curve Method to Characterize Two Alternative Transportation Fuels Prepared from the Pyrolysis of Waste Plastic

Reprinted from Harries, M. E., Kunwar, B., Sharma, B.K., Bruno, T.J. Application of the Advanced Distillation Curve Method to Characterize Two Alternative Transportation Fuels Prepared from the Pyrolysis of Waste Plastic. Energy & Fuels *30(11), 9671-9678, 2016. doi: 10.1021/acs.energyfuels.6b02068.*

2.1. Introduction

There is a great deal of interest in the development of alternative liquid fuels for transportation and heating applications, both to extend petroleum stocks and to improve performance. One of the primary impediments to the adoption of new fuel sources is the cost of modifying or replacing existing fuel-burning infrastructure to use a fuel with different combustion and thermophysical properties. For this reason, fuels with characteristics similar to existing fuels are desirable. Thus, it is important to measure and compare the fuel properties (chemical and thermophysical) of alternative fuels to those of conventional fuels. The degree of similarity in the major properties can indicate whether the fuel could be used directly (as a drop-in replacement) or blended with conventional fuel for use in existing combustion engines.

Fuel properties are fundamentally determined by composition, but not all properties are equally sensitive to varying composition. Volatility is one property that is very sensitive to composition; as such, it is frequently used as a fuel design tool.[39] The volatility measurement in the laboratory is expressed as the distillation (or boiling) curve. The alternative fuels evaluated in this study, a gasoline and a diesel fuel refined from polypropylene pyrolysis crude oil, were measured using the advanced distillation curve (ADC) method, which combines the volatility

measurement with a composition-explicit data channel that provides chemical information for each distillate volume fraction (DVF).

The ADC method was developed at NIST as a robust, data-rich volatility measurement approach that has been described in depth in previous publications.[40-45] The ADC improves on the well-known ASTM International D86 distillation standard in several significant ways.[9] The ADC provides: (1) a composition-explicit data channel for each distillate fraction (for qualitative, quantitative and trace analysis), (2) temperature, volume and pressure measurements of low uncertainty that are true thermodynamic state points that can be modeled with an equation of state, (3) consistency with a century of historical data measured using ASTM D86, and (4) an assessment of the energy content of each distillate fraction. Sampling very small volumes of the distillate yields a composition-explicit data channel with nearly instantaneous composition measurements. Chemical analysis of the distillate fractions provides some understanding of how the composition of the fluid varies with volume fraction and distillation temperature, even for complex fluids. The significant advantage offered by the ADC method is the ability to model the distillation curve with an equation of state.[46]

Currently, numerous feedstocks are used in pyrolysis reactors and gasifiers, including municipal refuse, various types of plastic, agricultural waste, and other biomass.[47] For example, our lab previously performed ADC characterization on a crude oil produced from pyrolysis of swine manure.[43, 48] The appeal of alternative fuels sourced from waste is clear: the widespread use of feedstocks like plastic trash would simultaneously reduce the need for fossil fuels and the demand placed on landfills. Plastics constituted only 0.5 wt.% of municipal solid waste (MSW) in United States in 1960 but were 12.5 wt. % (18 % by volume) in 2010.[49] According to a 2012 EPA report, 251 million tons of municipal solid waste was generated in the US, of which only

34.5 % gets recycled or composted. Even after MSW recovery through recycling and composting, plastic was the second largest component (18 %, 29 million tons) behind food waste (21 %) of the 164 million tons of waste discarded in 2012. Less than 10 % of plastic waste is recovered, recycled or utilized for energy production, with the remainder ending up in landfills.[49] More than 50 % of waste plastic is polyethylene (#2 HDPE and #4 LDPE) and polypropylene (#5).[50] In addition to decreasing the use of landfills, life cycle analyses have demonstrated that pyrolysis of MSW is net energy positive.[51]

In prior work, fuels derived from polypropylene (PP) corrugated advertisement plastic (for example, political campaign signage) were synthesized in a semi-pilot-scale continuous auger pyrolysis reactor.[4] PP was thermally cracked at 500 °C, producing a crude pyrolysis oil. Subsequently, the crude pyrolysis oil was distilled in an automated stainless steel spinning band distillation system, resulting in two fractions: one resembling the volatility of automotive gasoline (collected at vapor temperatures 35-185 °C) and the other, diesel fuel (185-350 °C).[4] In this report, these fuels will be referred to as PP gasoline and PP diesel fuel.

2.2. Materials and methods

Both polypropylene-based fuels described in the above paragraph were stored at room temperature before measurement. No phase separation was observed in the fluids, which were transparent and light yellow to light green in color, but they were still mixed by manual agitation before each distillation. For each distillation curve measurement, 200 mL of fuel were first measured into a boiling flask at atmospheric pressure using a 200 mL volumetric pipet. The flask was heated in an aluminum enclosure controlled by a model-predictive temperature controller. The temperature program was designed to lead the kettle temperature by about 20 °C.

Temperatures were measured with two thermocouples, one submerged in the boiling liquid (recording the kettle temperature or T_k) and one suspended in the bottom of the take-off position of the distillation head (recording the head temperature or T_h). The thermocouples had been previously calibrated in fixed point cells. The temperature T_k is the thermodynamically consistent value that is characteristic of the extant mixture in the kettle as it changes throughout distillation. Recording T_h serves three purposes: (1) it allows comparison with historical measurements made using the D86 distillation method, and the relationship between T_h and T_k provides (2) diagnostic information about apparatus performance and (3) an indication of potential azeotropy.[52, 53] The distillations were performed at ambient atmospheric pressure in a laboratory located 1655 m above sea level, where typical atmospheric pressure is 83 kPa. The electronic barometer used to measure the ambient pressure had been previously calibrated by use of a fixed cistern mercury barometer, temperature-corrected for the density of mercury and the expansion of the brass scale. Its uncertainty was 0.03 kPa. The temperatures reported here were adjusted to standard atmospheric pressure (101.325 kPa) using the modified Sydney Young equation, a correction that is approximately 7 – 8 °C.[54, 55] The correction term in this equation is based on a correlation of n-alkanes. The PP gasoline and PP diesel fuel studied here do not have compositions strictly comparable to conventional gasoline and diesel fuel; however, as will be seen, the component vapor pressures for the fuels are comparable to those in conventional fuels. Thus, the correction term for PP gasoline corresponded to a carbon chain of 8 and that for diesel fuel corresponded to a carbon chain of 12, as has been our practice with gasolines and diesel fuels in the past.[56]

For each of the two fuels, we performed three replicate distillations, one of which included sampling for composition. While more extensive measurements would decrease uncertainty to

some extent (discussed below), sample availability was a limiting factor in this work. During each sampling distillation, samples of approximately 7 μL were taken at 10 % DVF intervals (every 20 mL) using a 10 μL chromatographic syringe.

Preliminary characterization of the composite (undistilled) fuels informed the choice of a solvent that would not interfere with a chromatographic analysis of the components of the fuels. Samples from the PP gasoline distillations were diluted in chromatographic grade *n*-dodecane. Samples from the PP diesel fuel distillations were diluted in chromatographic grade *n*-hexane. Both solvents were tested for purity using protocols established at NIST.[57] All samples were analyzed using gas chromatography-mass spectrometry (GC-MS). Peaks were identified by analyzing their mass spectra with assistance from the NIST/EPA/NIH Mass Spectral Database and on the basis of retention indices.[58] A calibrant solution containing known concentrations of three representative hydrocarbons, alkenes with carbon chain lengths 6, 10 and 14, was used to calibrate the instrument by external standardization and calculate molar concentration from raw area counts.[59] The GC-MS methods used are detailed in Table 2.1. Baseline resolution was attained in both chromatographic programs.

Table 2.1. Summary of GC-MS methods used to characterize the fuels.

Fuel	Method
PP gasoline	30 m, 5 percent phenyl polydimethylsiloxane column with a coating thickness of 0.1 μm; 100:1 split injection via automatic sampler, temperature of injector = 200 °C at 55 kPa (8 psig) head pressure, injection volume = 1 μL, column temperature of 30 °C for 7 min, followed by temperature program at 15 °C/min to 150 °C; hold for 1 min; scan m/z from 33 to 200
PP diesel fuel	30 m, 5 percent phenyl polydimethylsiloxane column with a coating thickness of 0.1 μm; 70:1 split injection via automatic sampler, temperature of injector = 340 °C at 27.5 kPa (4 psig) head pressure, injection volume = 1 μL, column temperature of 30 °C for 10 min, followed by temperature program at 1 °C/min to 200 °C; 50 °C/min to 325 °C; hold for 2 min; scan m/z from 33 to 400

2.3. Results and discussion

Engineers are able to predict operational parameters (including engine starting ability, fuel system icing and vapor lock, fuel injection schedule, etc.) of complex liquid fuels from their characteristic distillation curves.[60, 61] ASTM D86 has traditionally been used for this purpose; however, we have found that the ADC method allows us to model the fluid with an equation of state as well as make these operational predictions. Throughout our analysis of the PP fuels, we found it useful to compare our measurements with previous ADC work on relevant conventionally-sourced fuels, both commercially available and research grade samples. In the remaining sections, we refer to six gasolines and four diesel fuels selected for comparison. A summary describing these fuels is presented in Table 2.2 and can be used as a reference throughout the remainder of this section.

Table 2.2. Summary of relevant previously measured fuels.

Gasolines	
91 AI SQ gasoline[56]	Premium summer quarter automotive gasoline formulated with no oxygenate additive and obtained from a commercial source; antiknock index = 91 (average of the research octane number (RON) and the motor octane number (MON)).
91 AI WQ gasoline[53]	Premium winter quarter automotive gasoline formulated with no oxygenate additive and obtained from a commercial supplier; antiknock index = 91.
91 AI gasoline used in dieseline mixtures[62]	An unleaded, unoxygenated gasoline obtained from a commercial source and not containing ethanol or other oxygenates such as ethers. This fuel had an antiknock index of 91, with the RON reported by the supplier as 97.
100LL avgas[44]	Low-lead (<0.65 g/L) commercial aviation gasoline for use in aircraft with piston engines; lean octane number = 100.
UL94 avgas[63]	Unleaded developmental aviation gasoline produced from conventional blending stocks, without dye or taggant; lean octane number = 94.
UL102 avgas[63]	Unleaded developmental aviation gasoline produced from cellulosic biomass, including switch grass and agricultural waste; lean octane number = 102.
Diesel fuels	
Ultra low sulfur diesel fuel (ULSD)[64]	Fuels for Advanced Combustion Engines (FACE) Diesel #9 Batch A, one of nine reference diesel fuels created and characterized by the Coordinating Research Council. This fuel, representative of current market diesel fuels, was selected in a previous study to guide surrogate mixture design.
ULSD used in dieseline mixtures[62]	This diesel fuel was obtained from a commercial distributor, free of oxygenate additives or cetane boosters. The fuel was a winter grade, low wax, ultra-low sulfur diesel fuel that incorporated a red dye (specifying off-road use), refined locally from petroleum from the Denver-Julesburg field; cetane number = 52.
ULSD certification fuel[64]	2007 #2 ULSD certification fuel from a commercial source, also used to inform the development of surrogates in previous work.
High aromatic diesel fuel (HAD)[65]	Type 2D grade fluid used for laboratory studies (that is, a noncommercial sample without taggant or dye). The aromatic content, measured with ASTM D5186, was 50 % by mass, including 4.8 % polycyclic aromatics.[66] Its cetane number, measured with ASTM D613, was 40.9 ± 0.8.[67]

2.3.1. Initial boiling temperatures

Initial boiling behavior of each fuel is presented in Table 2.3 as the average of three replicate measurements. The onset temperature is the temperature of the liquid at which bubble formation was first observed in the kettle. The vapor rise temperature, the temperature at which the vapor of the warm fluid moves into the distillation head, is considered the initial boiling temperature (IBT) of the liquid. Because vapor rise is characterized by a sharp increase in T_h, it is the least subjective and least uncertain of the initial temperatures. This data point is significant because it is the only point at which the temperature, pressure, and composition of the liquid are known, and because it can be modeled by an equation of state.[68, 69] The uncertainties in onset and vapor rise temperatures are approximately 3.0 °C and 0.3 °C respectively, based on repeated measurements and the calibration of the thermocouples.

The PP gasoline demonstrated initial boiling at a significantly higher temperature than the typical commercial gasolines with which we compared it. This behavior can be observed in Figure 2.1, where marks on the ordinate axis indicate each fuel's IBT. Initial boiling temperature and the low-temperature region of the distillation curve are important when evaluating the ease of starting and the potential for vapor lock, which can cause loss of power or complete stalling in the engine, especially in hot weather. In this case, the PP gasoline initially boiled 30 ºC higher than the closest conventional gasoline. A difference of this magnitude is significant and has the potential to affect engine performance with respect to ease of starting. As we would expect, the IBT is least similar to the winter quarter gasoline, which specifications require to possess higher volatility due to its use in low temperatures.

The reader may have noticed an apparent discrepancy between the initial boiling temperature of the PP gasoline (102.9 °C) and the starting temperature at which the gasoline

product was separated from the crude pyrolysis oil (35 °C). We attribute this difference in temperature to significant physical differences between the automated distillation system used to refine the crude pyrolysis oil and the ADC apparatus. In particular, using the ADC we measured the temperature in the boiling liquid, T_k; by contrast, the automated distillation system was measuring a vapor temperature with a probe positioned at the top of the distillation column, at least 90 cm away from the boiling liquid. As we know from monitoring T_h, the vapor temperature trails the boiling liquid temperature by at least a few degrees. This difference in measured temperatures was likely increased by the large physical distance (and implied temperature gradient) between the boiling liquid and the vapor temperature probe in the automated distillation system.

A comparison of initial boiling behavior of the PP diesel fuel is made in Figure 2.2 to other diesel fuels our laboratory has measured previously. We observed very good agreement between the IBTs of the PP diesel fuel and the experience base of conventional fuels. It falls within 8 °C of the IBT of the certification fuel provided by a commercial source.

Table 2.3. Summary of the initial boiling behavior of the two fuels presented as the average of three measurements. These temperatures have been adjusted to 101.325 kPa (1 atm) with the modified Sydney Young equation; the experimental atmospheric pressures are provided to allow recovery of the actual measured temperatures.

	PP gasoline	**PP diesel fuel**
Pressure (kPa)	83.3	83.5
Onset (°C)	89.0	195.0
Vapor rise / IBT (°C)	102.9	231.5

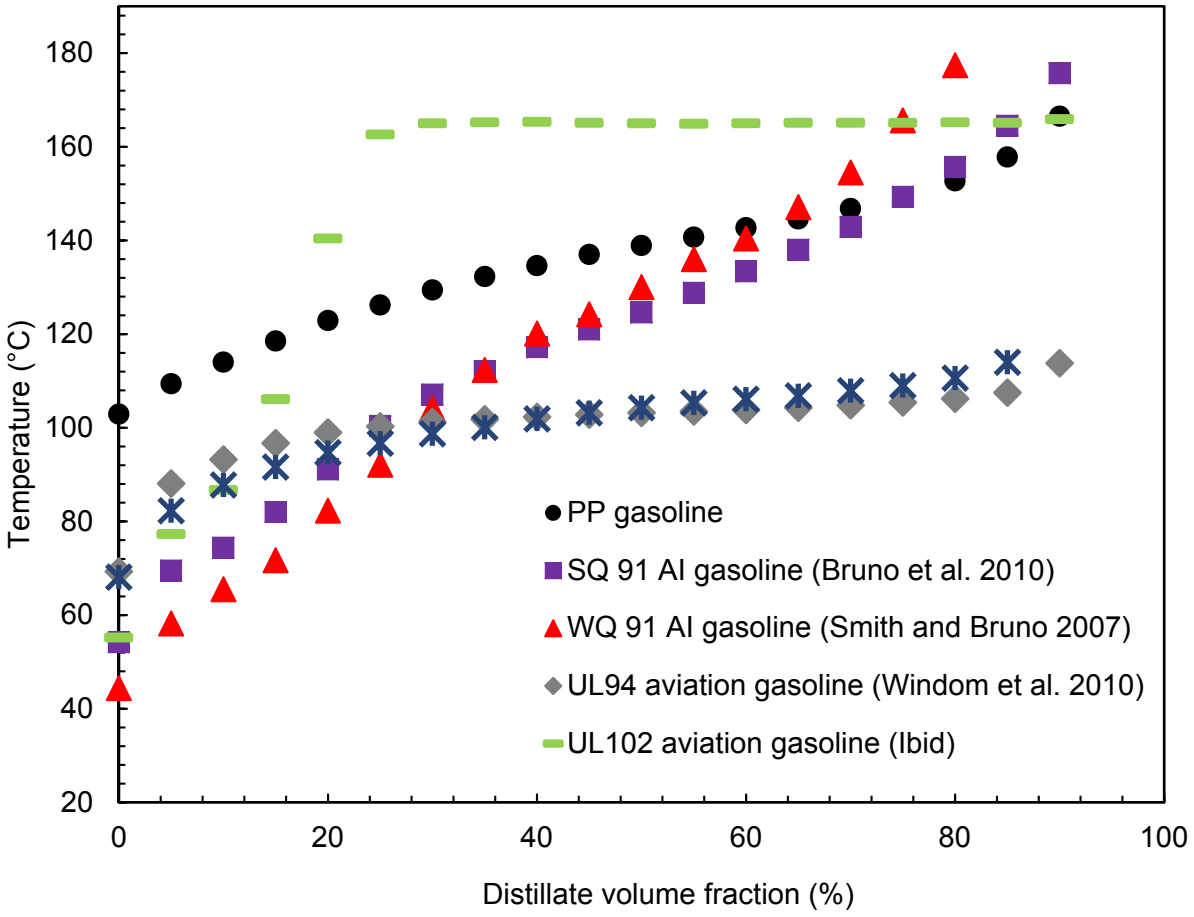

Figure 2.1. The distillation curve for PP gasoline overlaid with measurements of non-oxygenated conventional automobile gasoline and three types of aviation gasoline previously measured in our laboratory.[44, 56, 63] Marks on the vertical axis indicate each fluid's initial boiling temperature. Some error bars are hidden by the markers.

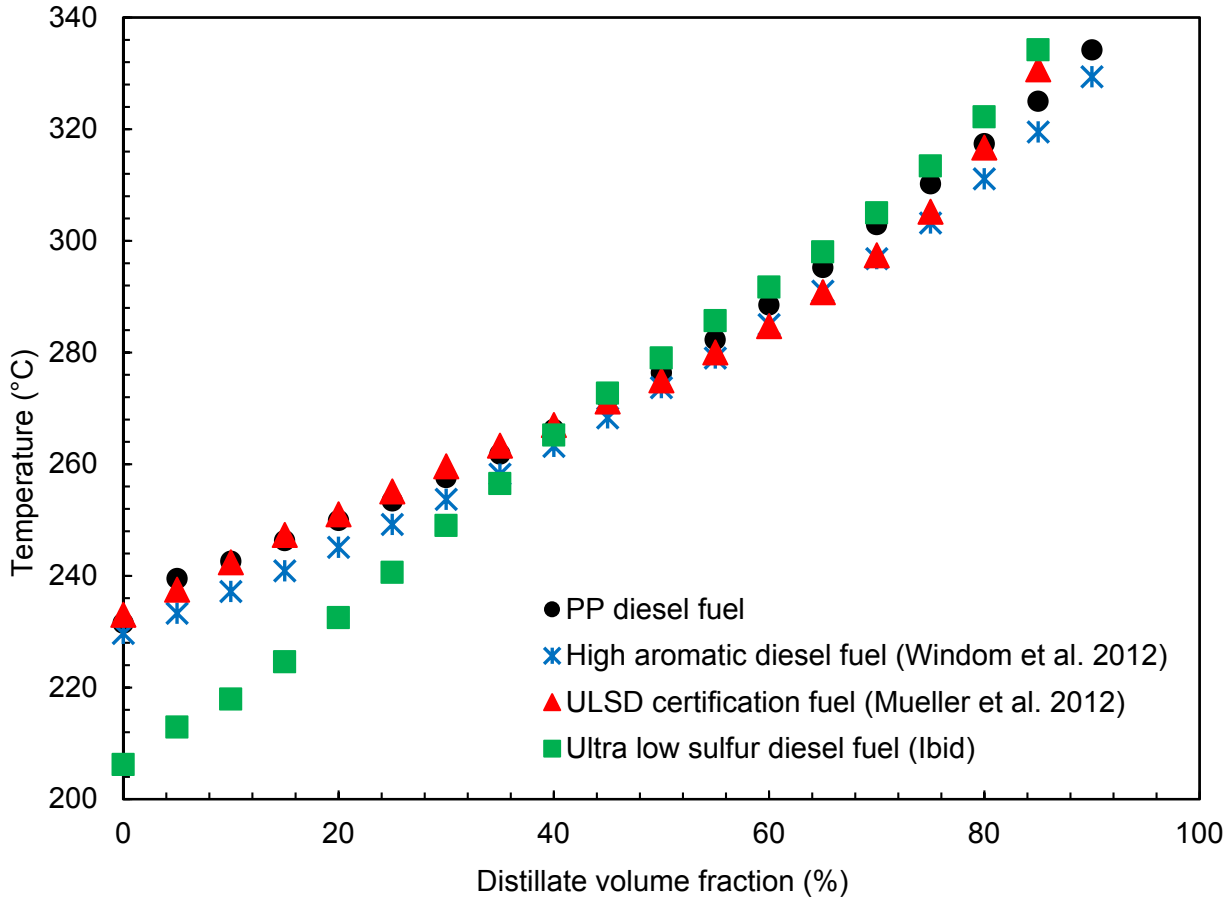

Figure 2.2. The distillation curve for PP diesel fuel, overlaid with measurements of several diesel fuels published previously.[64, 65] Marks on the vertical axis indicate each fluid's initial boiling temperature. Some error bars are hidden by the markers.

2.3.2. Distillation curves

Representative distillation curve data, presented as the average of three replicate measurements, are reported in Table 2.4. Based on the repeatability among measurements and the calibration of the thermocouples, the uncertainty in T_k over the distillation curve was determined to be 1 °C. Uncertainty in T_h was 2 °C. The uncertainty in the volume measurements used to determine DVF was 0.05 mL. T_h and T_k curves were compared for each distillation, and no azeotropic behavior was observed.

Table 2.4. Representative distillation curve data (given as the average of three distillation curves) for the PP fuels. These temperatures have been adjusted to 101.325 kPa (1 atm) with the modified Sydney Young equation; the experimental atmospheric pressures are provided to allow recovery of the actual measured temperatures.

	PP gasoline		**PP diesel fuel**	
Pressure	83.3 kPa		83.5 kPa	
DVF (%)	**T_k (°C)**	**T_h (°C)**	**T_k (°C)**	**T_h (°C)**
5	109.4	87.8	239.5	205.3
10	114.0	89.8	242.6	216.1
15	118.5	106.0	246.3	218.9
20	122.9	110.4	249.9	223.1
25	126.2	119.2	253.4	223.8
30	129.4	122.9	257.6	224.2
35	132.3	125.6	261.8	229.2
40	134.6	128.0	266.2	231.3
45	137.0	131.0	271.6	231.4
50	138.9	134.2	276.4	234.5
55	140.7	135.5	282.3	238.7
60	142.7	138.0	288.5	244.9
65	144.6	140.4	295.2	249.2
70	146.8	143.2	302.9	259.6
75	149.3	144.9	310.2	267.0
80	152.7	147.3	317.4	270.3
85	157.8	150.1	325.0	278.7
90	166.5	150.7	334.2	286.1

The T_k data are also presented graphically in Figures 2.1 and 2.2, where comparison is made to several conventional petroleum-sourced fuels currently in use in transportation applications (Table 2.2 provides a list). The distillation curve for PP gasoline is compared in

Figure 2.1 to two unoxygenated 91 AI conventional gasolines (labeled summer and winter quarter) and three aviation gasolines (Table 2.2). The boiling range of this fuel is smaller and shifted higher than its conventional automotive counterpart; as with IBT, this decreased volatility implies that ease of starting might be compromised when used in a spark ignition engine. Clearly the most disparate fuel in the figure is UL102, the developmental aviation gasoline produced from biomass; the sharp rise and rapid flattening is consistent with multiple high volatility components and few low volatility components present at appreciable concentration.

We were interested in comparing this gasoline with more conventional automotive fuels in use today and with the specifications governing fuels which are currently in use. Industry requires the use of the distillation standard ASTM D86 to measure a fuel's volatility and determine whether it meets specifications; however, we can draw some conclusions from the ADC metrology. Although we measured the distillation curve using the ADC, not D86, the head temperature (T_h) collected during the ADC is monitored from the same position in the distillation apparatus as the temperature measurement that is recorded in D86. ASTM D4814 is one industry standard specification that describes "various characteristics of automotive fuels for use over a wide range of operating conditions"; specifically, it mandates that fuels used in automotive spark ignition engines should not exceed two maximum temperature/DVF pairs as determined by ASTM D86. First, the fuel is not to exceed 70 °C at 10 % DVF, and second, it is not to exceed a maximum temperature of 121 °C at 50 % DVF.[70] Using T_h to approximate the D86 distillation curve, we find that $T_{h,10}$ = 89.8 ºC and $T_{h,50}$ = 134.2 ºC (from three replicate distillation measurements). Based on the distillation curve we measured, it is thus likely that this fuel may fail to meet the 10 % DVF and 50 % DVF volatility requirements in D4814.

There are several possible reasons why $T_{h,10}$ and $T_{h,50}$ fall so high above the limit, the most likely of which is that the composition of PP gasoline differs from that of conventional automotive gasoline. For example, the first drop (or the 0.025 % DVF) of the distillation of the PP gasoline is composed primarily of pentane, methyl pentane, and methyl pentenes, five- and six-carbon compounds. In a previous study of conventional automotive gasoline, we found butane and methyl butane in the 0.025 % DVF.[62] These C4 and C5 compounds are smaller, more volatile, and reflected in the lower IBT of conventional gasoline.

The shape of its distillation curve can indicate the level of complexity of a fuel with respect to both number of components and diversity in the moieties of these components. For example, the distillation curve for a pure substance is flat (that is, it has no slope) because its boiling point is a constant. As complexity is introduced to a fluid in the form of multiple components with different chemical properties, its distillation curve acquires slope and inflections. The PP diesel fuel is compared in Figure 2 to three other samples of conventional diesel fuel. This fuel showed promising agreement with all three conventional fuels in boiling range and distillation curve shape.

2.3.3. Distillate fraction composition and energy content

As stated in the previous section, individual fractions of condensed vapor were sampled during distillation and analyzed using GC-MS. Each pure component present with greater than 1 % abundance (determined by raw area count) in each volume fraction was identified through a combination of retention index matching and mass spectral analysis.[57, 58] As previous work has shown, the addition of a composition channel of data to the distillation curve enables quantitative thermochemical analysis of individual distillate fractions.[53, 71, 72] First, individual (pure) components of each distillate fraction are identified and their mole fraction contributions to the

mixture are measured. Then a composite net enthalpy of combustion, $-\Delta H_c$, is calculated based on the pure component enthalpies and their respective concentrations. We must be explicit in defining the enthalpy of combustion, since the water produced by the combustion reaction can be expressed as either liquid or vapor, depending on the relevant system and final state of the products. This choice is governed by the specific application, and it should be noted that all real-world systems will fall somewhere on a gradient between producing all vapor or all liquid water. The energy content applicable to these fuels and the systems in which they are used is the lower enthalpy of combustion (or net enthalpy or net heat). This enthalpy value is calculated assuming that water formed as a reaction product leaves the system as vapor, not liquid, and that the enthalpy of vaporization is not recovered by the system.

Net enthalpy of combustion was obtained from a reliable database for each pure component.[73] For components which lacked experimental data for $-\Delta H_c$, the Cardozo equivalent chain model was used to calculate its value.[73] This modeling approximation is one of the contributions to the uncertainty claimed in the composite enthalpy of combustion measurement.

Uncertainty in this calculation has been attributed to a number of sources, including (1) the decision to neglect enthalpy of mixing, (2) the uncertainty introduced by misidentification of a component, (3) the uncertainty in the measured and calibrated mole fraction, including that which is introduced by neglecting components present at levels below our chosen percent area cutoff, and (4) the uncertainty in the pure component enthalpy of combustion as tabulated in the database, especially when experimental data for the pure component enthalpy of combustion are unavailable and the Cardozo equivalent chain model must be used.[53, 71-73] On the basis of the uncertainty sources listed above and the samples being investigated, we assigned a 5 % uncertainty in the molar enthalpy calculations reported in this work.[62, 74, 75]

The molar enthalpy of combustion for both fuels (Table 2.5. and Figures 2.3-4) increases with distillate fraction because the concentration of heavier hydrocarbons increases as the distillation progresses to higher temperatures. As one might expect, the enthalpy of combustion overall is higher for the PP diesel fuel than for the PP gasoline. This, again, is attributable to the heavier hydrocarbon composition of the diesel fuel. Both fuels were similar in energy content to their conventional counterparts, as shown in Figures 2.3 and 2.4. Enthalpy of combustion presented as a function of mass or volume would be expected to show a less pronounced variation with DVF, as we have shown in prior work, but we did not have sufficient sample to make density measurements on the PP fluids to enable such a comparison.[65]

Table 2.5. The energy content or net enthalpy of combustion ($-\Delta H_c$) of the fuels as a function of distillate volume fraction and for the composite fuels.

DVF (%)	PP gasoline (kJ/mol)	PP diesel fuel (kJ/mol)
0.025	3277 ± 163	5147 ± 257
10	4001 ± 200	7642 ± 382
20	4537 ± 226	8229 ± 411
30	4776 ± 238	8302 ± 415
40	5189 ± 259	8651 ± 432
50	5412 ± 270	8914 ± 445
60	5620 ± 281	9326 ± 466
70	5702 ± 285	10009 ± 500
80	5825 ± 291	11125 ± 556
90	6084 ± 304	11829 ± 591
Composite	5368 ± 268	9228 ± 461

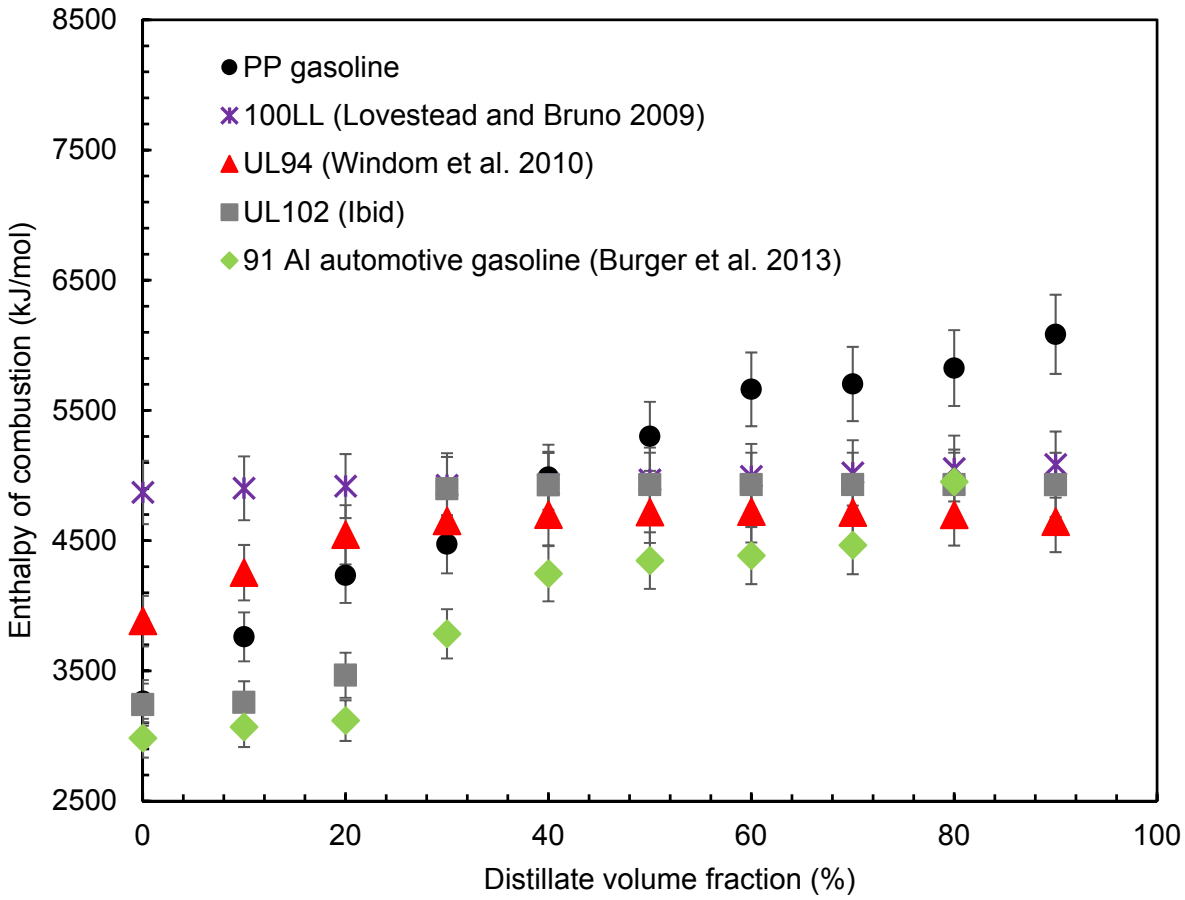

Figure 2.3. Energy content, presented as the composite net enthalpy of combustion on a molar basis, as a function of the DVF for the polypropylene gasoline. Several previously measured gasolines are also plotted for comparison.[44, 56, 62, 63] Values on the vertical axis represent the enthalpy content of the 0.025 % DVF.

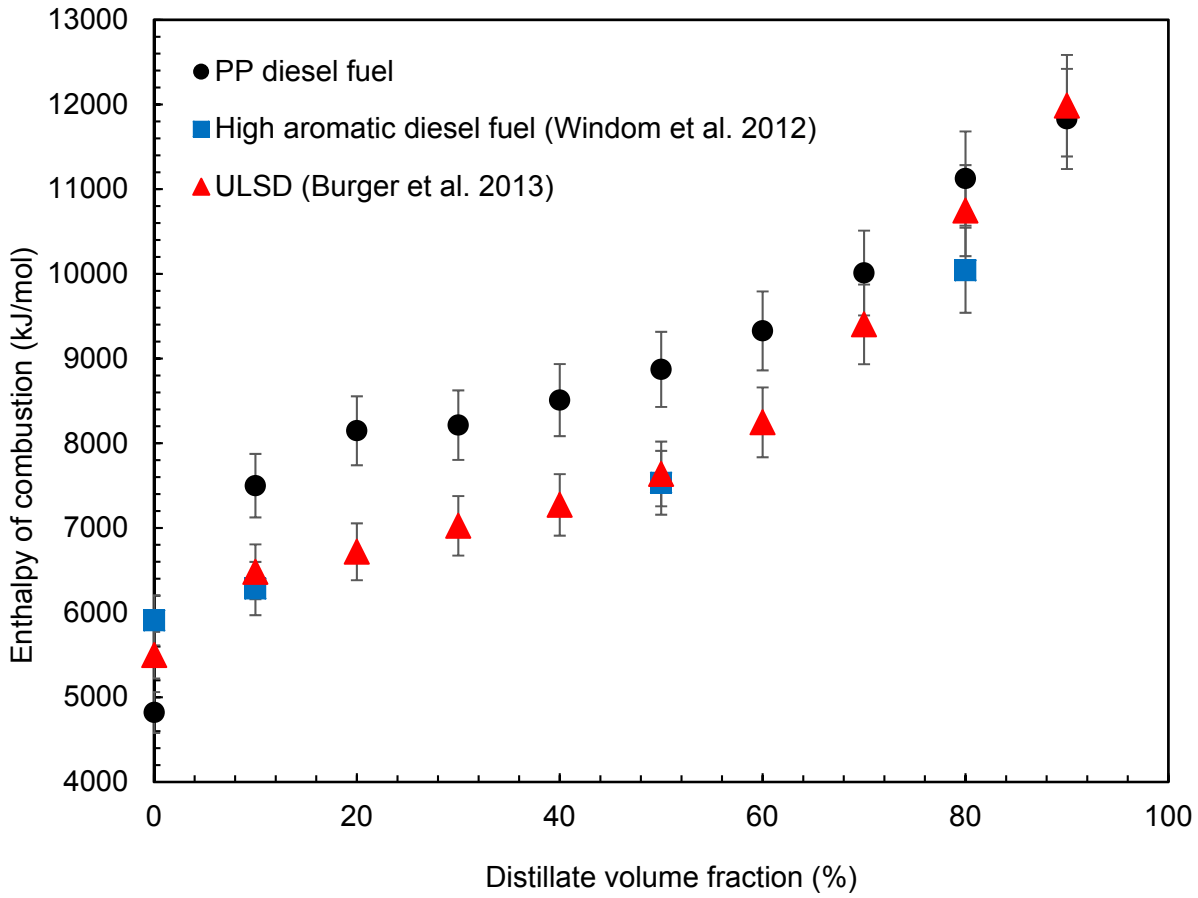

Figure 2.4. Energy content, presented as the composite net enthalpy of combustion on a molar basis, as a function of DVF for the polypropylene diesel fuel. Several previously measured diesel fuels are also plotted for comparison.[62, 65] Values on the vertical axis represent the enthalpy content of the 0.025 % DVF.

2.3.4. Hydrocarbon classification

In most reports of our prior work on fuel characterization with the ADC method, we have included a moiety family analysis as a function of DVF because it is important to visualize how the gross composition of a fuel changes as it vaporizes. We have primarily used a mass spectral fragmentation method based on ASTM D2789 (providing a volume % breakdown), and most recently we have used methods based on NMR spectrometry.[76] Many, if not most, fuel labs currently use MS to do this characterization, and this is also true of our previous in-house

measurements. Thus, the bulk of our historical experience is based on the mass spectral fragmentation approach; the limitations and uncertainties inherent in that approach are well understood. Among the limitations is that the mass spectral approach is strictly suited for low alkenic gasolines (although it has been used to characterize all kinds of fuels). We were therefore unable to use the mass spectral fragmentation approach on the PP fuels, since they are composed primarily of alkenes. For this reason, the hydrocarbon classifications presented in Figures 2.5 and 2.6 have been calculated by two different methods: our historical, experience-based trends were determined by the mass spectral fragmentation approach, while the entries for the PP fuels were determined by tabulating the identified pure components.

Figures 2.5 and 2.6 describe the hydrocarbon profiles of each fuel as they changed with DVF. Table S1 (found through the reference given at the beginning of this chapter) reports the hydrocarbon classification of the composite fuels. The analysis showed that conventional gasoline contains mostly monocyclic alkylbenzene compounds and alkanes of approximate carbon chain lengths 7 to 10, while the composition of the PP gasoline was primarily alkenes of carbon chain lengths 6 to 12.[62, 77] The slightly heavier composition of the PP gasoline is reflected in its distillation behavior compared to conventional gasoline.[56] The PP gasoline contained virtually no alkylbenzenes and fewer alkanes than conventional gasoline. These compositional differences likely affect the gasoline's fuel properties, e.g. density, and are a probable cause for the shallower distillation curve slope and narrower boiling range when compared to representative samples of conventional unoxygenated gasoline (Figure 2.1). We note that, although these PP fuels are primarily composed of alkenes, we have not included alkenes in the comparisons to conventional fuels in Figures 2.5 and 2.6. The specified method for quantifying

alkenes in fuels is not mass spectrometry; rather, it involves a separate fluorometric technique that was not performed on the conventional fuels in our past work.

The composition of the PP diesel fuel was weighted heavily towards alkenes of carbon chain lengths 7 to 23. Three out of ten distillate fractions of the PP diesel fuel contained a small fraction of heavy alcohols (isodecanol, isoundecanol, and isopentadecenol), composing less than 5 % in any one fraction. The diesel fuel contained significantly fewer alkylbenzene and alkane components than conventional diesel fuels that it was compared to.[62, 77] The plots shown in Figure 2.6 show little change in alkane or alkylbenzene composition with DVF.

The behavior of alkenes in fuels is known to be troublesome for several reasons: first, alkenes (in the form of fugitive vapors) are highly reactive in the atmosphere and rapidly contribute to ozone formation; second, alkenes may lead to the formation of engine deposits; finally, cetane number has been shown to be improved by the hydrogenation of unsaturated species, making alkenes relatively unfavorable in fuels used in compression-ignition engines.[78] The PP diesel fuel studied here was analyzed via derived cetane number (DCN) and was found to have a DCN of 35.5.[4] ASTM D975 requires a minimum cetane number of 40 for all grades of diesel fuel oils included in the standard; this PP diesel fuel falls short of specification.[79] Further thermophysical and fit-for-purpose property measurements are needed to better understand the effect of these compositional differences (with respect to conventional fuels) on other aspects of the fuels' behavior.

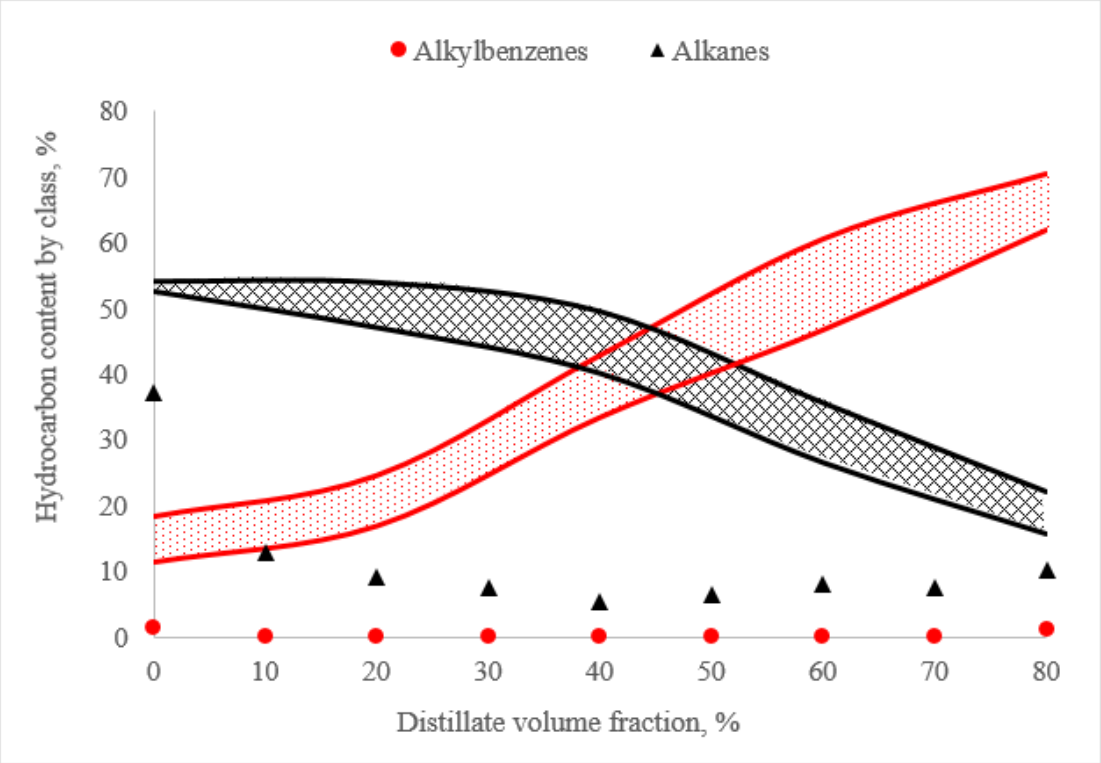

Figure 2.5. Selected hydrocarbon classes as a function of distillate fraction for the PP gasoline. Shaded bands of the same color are overlaid to indicate the typical range in hydrocarbon profile of a comparable conventional fuels measured previously.[62, 80] The remainder of the compounds in the PP gasoline were alkenes.

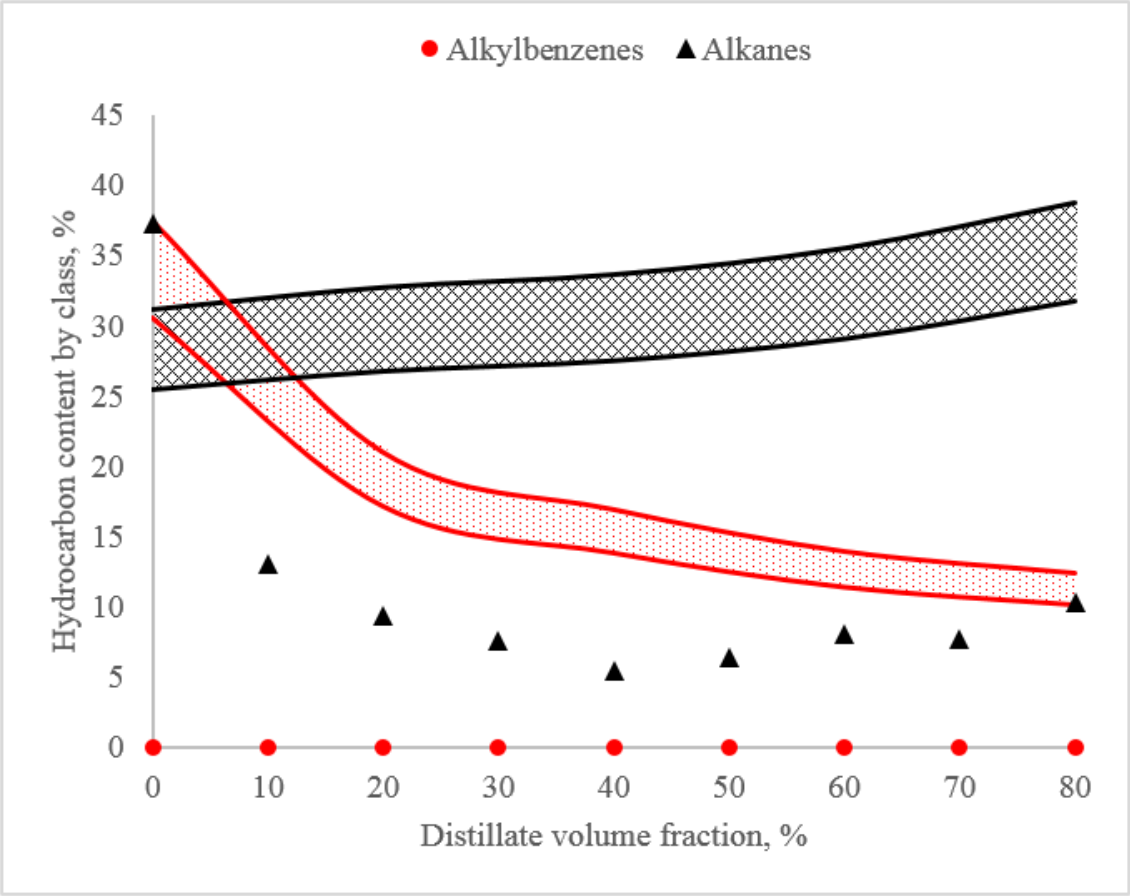

Figure 2.6. Selected hydrocarbon classes as a function of distillate fraction for the PP diesel fuel. Shaded bands of the same color are overlaid to indicate the typical range in hydrocarbon profile of comparable conventional fuels measured previously.[62, 81] The remainder of the compounds in the PP diesel fuel were alkenes.

2.4. Conclusion

The objective of this study was to characterize two alternative fuels produced by the pyrolysis of waste polypropylene corrugated advertisement plastic. We used the advanced distillation curve (ADC) method to understand their volatility profiles, composition and energy content. The resulting data matrix is important for (1) the consideration of these fuels for use in existing combustion engines, (2) future design of engines to run on these types of fuels, and (3) the associated development of models and equations of state to describe and predict the behavior

of these fuels and other alternative fuels. On the basis of our measurements, we conclude the following:

1. As expected, due to the exclusively hydrocarbon composition of the PP feedstock, the components of both fuels were almost entirely hydrocarbon compounds, with a small percentage of long-chain alcohols present in some distillate fractions of the PP diesel fuel. Both fuels were predominantly composed of alkenes.
2. The volatility profile of PP diesel fuel showed good agreement with diesel fuels currently in use in transportation applications. It might serve as a good blend stock.
3. Based on our ADC measurements, the PP gasoline would likely fail to meet the ASTM specifications regarding volatility for automotive spark ignition engine fuels. This fuel is potentially a candidate blend stock. Future generations of PP pyrolysis gasoline may also be made more similar to conventional gasoline by tuning the pyrolysis reaction with respect to temperature, pressure, and time; these variables all affect the composition of the resulting fluid.[82]
4. The molar enthalpy of combustion increases with distillate fraction as the concentration of heavier hydrocarbons increases in the later distillate fractions. The energy content of both PP fuels was similar to our experience base of conventional fuels.

2.5. References

4. Kunwar, B., Chandrasekaran, S. R., Moser, B. R., Deluhery, J., Kim, P., Rajagopalan, N., Sharma, B. K., Catalytic thermal cracking of postconsumer waste plastics to fuels: 2. Pilot-scale thermochemical conversion. *Energy & Fuels* 2017, *31* (3), 2705-2715.

9. *ASTM D86, Standard test method for distillation of petroleum products at atmospheric pressure*. ASTM International: West Conshohocken, PA, 2004.

39. Ott, L. S., Smith, B.L., Bruno, T.J., Composition-explicit distillation curves of mixtures of diesel fuel with biomass-derived glycol ester oxygenates: a fuel design tool for decreased particulate emissions. *Energy & Fuels* 2008, *22*, 2518-2526.

40. Bruno, T. J., Smith, B. L., Enthalpy of combustion of fuels as a function of distillate cut: application of an advanced distillation curve method. *Energy & Fuels* 2006, *20*, 2109-2116.

41. Smith, B. L., Bruno, T.J., Advanced distillation curve measurement with a model predictive temperature controller. *Int J Thermophys* 2006, *27*, 1419-1434.

42. Ott, L. S., Bruno, T.J., Corrosivity of fluids as a function of distillate cut: application of an advanced distillation curve method. *Energy & Fuels* 2007, *21*, 2778 - 2784.

43. Ott, L. S., Smith, B.L., Bruno, T.J., Advanced distillation curve measurement: application to a bio-derived crude oil prepared from swine manure. *Fuel* 2008, *87*, 3379-3387.

44. Lovestead, T. M., Bruno, T.J., Application of the advanced distillation curve method to aviation fuel avgas 100LL. *Energy & Fuels* 2009, *23*, 2176-2183.

45. Bruno, T. J., Ott, L.S., Smith, B.L., Lovestead, T.M., Complex fluid analysis with the advanced distillation curve approach. *Analytical Chemistry* 2010, *82*, 777-783.

46. Huber, M. L., Smith, B.L., Ott, L.S., Bruno, T.J., Surrogate mixture model for the thermophysical properties of synthetic aviation fuel S-8: Explicit application of the advanced distillation curve. *Energy & Fuels* 2008, *22*, 1104 - 1114.

47. Carpenter, D., Westover, T. L., Czernik, S., Jablonski, W., Biomass feedstocks for renewable fuel production: a review of the impacts of feedstock and pretreatment on the yield and product distribution of fast pyrolysis bio-oils and vapors. *Green Chemistry* 2014, *16* (2), 384-406.

48. Hsieh, P. Y., Bruno, T. J., Pressure-controlled advanced distillation curve analysis and rotational viscometry of swine manure pyrolysis oil. *Fuel* 2014, *132*, 1-6.

49. Gug, J., Cacciola, D., Sobkowicz, M. J., Processing and properties of a solid energy fuel from municipal solid waste (MSW) and recycled plastics. *Waste Manag* 2015, *35*, 283–292.

50. Subramanian, P., Plastics recycling and waste management in the US. *Resour Conserv Recycl* 2000, *28* (3), 253–263.

51. Wang, H., Wang, L., Shahbazi, A., Life cycle assessment of fast pyrolysis of municipal solid waste in North Carolina of USA. *Journal of Cleaner Production* 2015, *87*, 511-519.

52. Hadler, A. B., Ott, L. S., Bruno, T. J., Study of azeotropic mixtures with the advanced distillation curve approach. *Fluid Phase Equilibria* 2009, *281*, 49-59.

53. Smith, B. L., Bruno, T.J., Improvements in the measurement of distillation curves - part 3: Application to gasoline and gasoline + methanol mixtures. *Ind Eng Chem Res* 2007, *46*, 297-309.

54. Ott, L. S., Smith, B.L., Bruno, T.J., Experimental test of the Sydney Young equation for the presentation of distillation curves. *J Chem Thermodynam* 2008, *40*, 1352-1357.

55. Young, S., Correction of boiling points of liquids from observed to normal pressures. *Proc Chem Soc* 1902, *81*, 777.

56. Bruno, T. J., Wolk, A., Naydich, A., Composition-explicit distillation curves for mixtures of gasoline and diesel fuel with gamma-valerolactone. *Energy & Fuels* 2010, *24* (4), 2758-2767.

57. Bruno, T. J., Svoronos, P.D.N, *CRC Handbook of Basic Tables for Chemical Analysis, 3rd. ed*. Taylor and Francis CRC Press: Boca Raton, 2011.

58. NIST/EPA/NIH mass spectral library with search program. National Institute of Standards and Technology SRD Program, Ed. Gaithersburg, MD, 2014.

59. Haynes W. M. (editor), *CRC Handbook of Chemistry and Physics, 97th ed.* Taylor and Francis CRC Press: Boca Raton, FL, 2017.

60. Orbital Engine Company. *A literature review based assessment on the impacts of a 20% ethanol gasoline fuel blend on the Australian vehicle fleet*; 2002.

61. Orbital Engine Company. *Market barriers to the uptake of biofuels study: A testing based assessment to determine the impacts of a 20 % ethanol gasoline fuel blend on the Australian passenger fleet*; 2003.

62. Burger, J. L., Gough, R. V., Bruno, T. J., Characterization of dieseline with the advanced distillation curve method: hydrocarbon classification and enthalpy of combustion. *Energy & Fuels* 2013, *27*, 878 - 795.

63. Windom, B. C., Lovestead, T.M., Bruno, T.J., Application of the advanced distillation curve method to the development of unleaded aviation gasoline. *Energy & Fuels* 2010, *24*, 3275 - 3284.

64. Mueller, C. J., Canella, W. J., Bruno, T. J., Bunting, B., Dettman, H. D., Franz, J. A., Huber, M. L., Natarajan, M., Pitz, W. J., Ratcliff, M. A., Wright, K., Methodology for formulating diesel surrogate fuels with accurate compositional, ignition quality and volatility characteristics. *Energy & Fuels* 2012, *26*, 3284-3303.

65. Windom, B. C., Huber, M. L., Bruno, T. J., Lown, A. L., Lira, C. T., Measurements and modeling study on a high aromatic diesel fuel. *Energy & Fuels* 2012, *26*, 1787-1797.

66. *ASTM D5186, Standard test method for determination of the aromatic content and polynuclear aromatic content of diesel fuels and aviation turbine fuels by supercritical fluid chromatography*. ASTM International: West Conschoken, PA, 2009.

67. *ASTM D613, Standard test method for cetane number of diesel fuel*. ASTM International: West Conshohocken, PA, 2010.

68. Bruno, T. J., Smith, B.L., Evaluation of the physicochemical authenticity of aviation kerosene surrogate mixtures Part I: Analysis of volatility with the advanced distillation curve *Energy & Fuels* 2010, *24*, 4266-4276.

69. Bruno, T. J., Huber, M.L., Evaluation of the physicochemical authenticity of aviation kerosene surrogate mixtures Part II: Analysis and prediction of thermophysical properties. *Energy & Fuels* 2010, *24*, 4277-4284.

70. *ASTM D4814, Standard specification for automotive spark-ignition engine fuel*. ASTM International: West Conshohocken, PA, 2015.

71. Bruno, T. J., Method and apparatus for precision in-line sampling of distillate. *Sep Sci Technol* 2006, *41* (2), 309-314.

72. Smith, B. L., Bruno, T.J., Improvements in the measurement of distillation curves - part 4: Application to the aviation turbine fuel Jet-A. *Ind Eng Chem Res* 2007, *46*, 310-320.

73. Rowley, R. L., Wilding, W. V., Oscarson, J. L., Zundel, N. A., Marshall, T. L., Daubert, T. E., Danner, R. P., DIPPR data compilation of pure compound properties. Design Institute for Physical Properties AIChE, New York, 2004.

74. Bruno, T. J., Wolk, A., Naydich, A., Stabilization of biodiesel fuel at elevated temperature with hydrogen donors: evaluation with the advanced distillation curve method. *Energy & Fuels* 2009, *23*, 1015-1023.

75. Ott, L. S., Bruno, T.J., Variability of biodiesel fuel and comparison to petroleum-derived diesel fuel: application of a composition and enthalpy explicit distillation curve method. *Energy & Fuels* 2008, *22*, 2861-2868.

76. Burger, J. L., Widegren, J. A., Lovestead, T., M., Bruno, T. J., 1H and 13C NMR analysis of gas turbine fuels as applied to the advanced distillation curve method. *Energy & Fuels* 2015, *29* (8), 4874-4885.

77. Agency for Toxic Substances and Disease Registry, Toxicological Profiles. http://www.atsdr.cdc.gov/toxprofiles/.

78. de Klerk, A., *Fischer-Tropsch Refining*. Wiley-VCH: Weinheim, Germany, 2011.

79. *ASTM D975, Standard specification for diesel fuel oils*. ASTM International: West Conshohocken, PA, 2015.

80. Bruno, T. J., Wolk, A., Naydich, A., Composition-explicit distillation curves for mixtures of gasoline with four-carbon alcohols (butanols). *Energy & Fuels* 2009, *23*, 2295-2306.

81. Smith, B. L., Ott, L.S., Bruno, T.J., Composition-explicit distillation curves of diesel fuel with glycol ether and glycol ester oxygenates: a design tool for decreased particulate emissions. *Environ Sci Tech* 2008, *42* (20), 7682-7689.

82. Newalkar, G., Iisa, K., D'Amico, A. D., Sievers, C., Agrawal, P., Effect of temperature, pressure, and residence time on pyrolysis of pine in an entrained flow reactor. *Energy & Fuels* 2014, *28* (8), 5144-5157.

Chapter 3: Measuring the Distillation Curves of Non-Homogeneous Fluids: Method and Case Study of Two Pyrolysis Oils

Reprinted from Harries, M.E., McDonald, A.G., Bruno, T.J. Measuring the Distillation Curves of Non-Homogeneous Fluids: Method and Case Study of Two Pyrolysis Oils, Fuel *204, 24-27, 2017. doi: 10.1016/j.fuel.2017.04.066.*

3.1. Introduction

The distillation curve of a complex fluid is a measurement of the boiling temperature as a function of the volume fraction distilled. This measurement is critical to understanding the volatility of complex fluids and how fuels in particular behave in a refinery or an engine. This measurement of a fluid's volatility is also crucial to the understanding and modeling of fluid mixture thermophysical properties. The advanced distillation curve (ADC) method, developed at NIST, is a metrology for distillation curve measurement that provides a thermodynamically significant temperature measurement accompanied by a composition explicit data channel (composition measurement as a function of distillate volume fraction, DVF).[53, 72, 83, 84] It is an improvement to the traditionally used ASTM International D86 method.[9]

The ADC method was developed at NIST as a robust, data-rich distillation approach that has been described in depth in previous publications.[40-45] The ADC improves on the well-known D86 distillation method in the following ways: (1) a composition-explicit data channel for each distillate fraction (for both qualitative and quantitative analysis), (2) temperature measurements that are true thermodynamic state points that can be modeled with an equation of state, (3) temperature, volume and pressure measurements of low uncertainty suitable for equation of state development, (4) consistency with a century of historical data, (5) an assessment of the energy content of each distillate fraction, and (6) trace chemical analysis of each distillate fraction.

Sampling very small volumes of the distillate yields a composition-explicit data channel with nearly instantaneous composition measurements. Chemical analysis of the distillate fractions allows for some understanding of how the composition of the fluid varies with volume fraction and distillation temperature, even for complex fluids. This is critical when the fuel contains additives (such as cetane improvers, oxygenates or stabilizers) or unusual components (such as corrosives and manure sterols).[43, 74, 81, 85] The significant advantage offered by the ADC method is the ability to model the distillation curve with an equation of state.[9, 46] The ADC method also features a much lower uncertainty budget than is obtainable by D86.[53]

Importantly, this low uncertainty budget usually excludes consideration of sampling uncertainty, that is, how well an aliquot of fluid taken for ADC measurement represents the population material.[59] In previous fuel characterization studies using the ADC method, sampling uncertainty has been insignificant because the fluids measured were homogeneous, existing in a single, well mixed liquid phase. This is not always the case; indeed, unrefined pyrolysis fluids pose a particular challenge because the pyrolysis reaction can produce significant amounts of water. We encountered this challenge in the measurement of two crude pyrolysis oils, one made from ponderosa pine shavings and the other from dairy manure.

Numerous feedstocks are currently in use in pyrolysis reactors and gasifiers, including municipal refuse, various types of plastic, agricultural waste, and other biomass.[47] Our lab previously performed ADC characterization on a crude oil produced from pyrolysis of swine manure and on two liquid fuels refined from crude polyethylene pyrolysis oil.[43, 48] The appeal of alternative fuels sourced from waste is clear: the widespread use of waste feedstocks like the pine shavings and manure in this case would simultaneously reduce the need for fossil fuels and mitigate the load on landfills and pollution in the environment. For example, in 2006, livestock

in Canada alone produced over 180 million metric tons (1.8×10^{10} kg) of manure.[86] Although the fluids studied here were produced in a small, lab-scale reactor, a number of industrial scale plants exist in the United States for fuel production from the pyrolysis of waste.[87]

3.2. Material and methods

3.2.1. Crude pyrolysis oils

The crude pyrolysis fluids were produced from ponderosa pine saw-mill residues (< 5 mm) and dairy manure (dried and hammer milled; University of Idaho Dairy Farm) using a pilot scale auger pyrolysis unit (100 mm diameter, 450-500 ^{o}C, 20 kg h^{-1}) as described by Han et al.[5] The condensed fluids were stored frozen and then adjusted to room temperature before measurement. Both fluids were visibly non-homogeneous, having separated into two phases, one primarily aqueous and one organic, and vigorous attempts to adequately mix them were unsuccessful. The pine oil was dark in appearance and smelled like pinene. The manure oil was dark in appearance and had an objectionable odor with notes of cigarette butts and fresh asphalt. In both fluids, we observed phase separation into a light brown aqueous layer and a nearly black, sticky, more viscous organic layer. Both fluids showed a tendency to form a frothy top layer after mixing.

We attempted to mix the fluids by first placing them into one-gallon (nominal) uncoated steel paint cans. We added a handful of clean stainless steel nuts to each can to aid in agitation and mixed each can with a commercial paint shaker. This mixing operation was not effective at homogenizing the fluids. While we were loath to change the composition of the bulk fluids, we attempted chemical homogenization by adding a surfactant to a small aliquot. We conducted a test combining a small sample of organic phase from the manure oil with 1% (mass/mass)

cetyltrimethylammonium bromide (a cationic surfactant) dissolved in a roughly equal volume of water. We found that the surfactant did have a minor effect on promoting mixing; however, even with the application of heat to the oil-water-surfactant mixture, most of the organic material remained in a sticky layer separate from the water phase. Insufficient sample was available for testing additional surfactants or other means of homogenization. This led us to develop a curve offset method that can be applied to ADC measurements.

3.2.2. Advanced distillation curve

The ADC protocol has been described in detail in previous publications.[53, 72, 83, 84] The result of an ADC measurement is a temperature-volume-composition data matrix that includes two temperatures, the kettle temperature (T_k) and head temperature (T_h), and a composition analysis for each DVF. T_k is the thermodynamically consistent value characteristic of the remaining mixture in the kettle as distillation progresses. As in prior work on crude petroleum and pyrolysis oils, the temperatures we report have been adjusted to standard atmospheric pressure (101.325 kPa) using the modified Sydney Young equation in which the constant term was assigned a value of 0.000109 (corresponding to a hydrocarbon chain of 12).[54, 55, 84, 88, 89] We acknowledge that the composition of these fluids deviated significantly from dodecane, especially in the aqueous region of the distillation curve; however, applying the Sydney Young constant for water (0.000099) results in negligibly different (< 1 °C) corrected temperatures. Applying the Sydney Young constant for phenol (0.000107), sometimes used as a pyrolysis fluid model compound, results in < 0.2 °C differences in corrected temperatures. Taking all of this into consideration, we chose to continue using the constant value 0.000109, as it enables us to most directly compare the results to the distillation curves of relevant previously measured crude

oils for which the same constant was used.[88] For each of three replicate distillation curve measurements, a starting volume of 200 mL was measured by automatic pipette.

The uncertainty in our pressure measurements was 0.03 kPa, including uncertainty in the calibration with a corrected, fixed cistern mercury barometer. The uncertainty associated with temperature measurements was 1 °C, including uncertainty in calibrations with fixed point cells. The uncertainty in the volume measurements used to determine distillate volume fraction was 0.05 mL.

3.3. Results and discussion

3.3.1. Karl Fischer coulombic titrimetry

Because we observed an obvious separation between aqueous and organic phases, it was important to determine the water content of both crude pyrolysis oils. Each phase of the composite oils was measured separately, in triplicate, using the Karl Fischer coulometric titration method.[90] Samples were introduced by chromatographic syringe (5 μL for the aqueous phases and 2 μL for the organic phase). The organic fraction of manure oil was too viscous (even at elevated temperature) to introduce reproducibly to the titration cell, so we do not report a moisture value. As we suspected, the aqueous fraction of both oils contained more than 80% water by volume. Table 3.1 details the results. These measurements are consistent with our later findings using ADC.

Table 3.1. Water content (% volume) for each fraction of both crude pyrolysis oil. The manure oil's organic fraction was too viscous to make a measurement. The upper and lower values provided are based on expanded (k = 2) uncertainty.

	Pine oil	**Manure oil**
Aqueous fraction	82.1 % ± 1.6 %	83.1 % ± 1.6 %
Organic fraction	12.6 % ± 1.4 %	

3.3.2. Raw distillation curve results

The raw distillation curve data are presented in Figure 3.1 and Table S1 in Supplementary Information of the article cited at the beginning of the chapter. The fluids boiled near 100 °C (vaporization of the aqueous phase) for a significant portion of the total distillation volume before markedly increasing at the onset of vaporization of the organic constituents, the point we call the water-organic inflection. As the plots show, the amount of water varied significantly among replicates of the same fluid, which indicated that the fluids were not successfully homogenized. Had they been, the DVF of the water-organic inflection would have been repeatable. The high-boiling region after the water-organic inflection is due to the vaporization of the organic fraction.

It is important to note that the distillation temperatures of the low-boiling region were not perfectly constant and were also slightly elevated above the boiling temperature of pure water. This could indicate the presence of impurities in the aqueous phase, a phenomenon which we observed in previous analysis of liquors from an ethanol plant.[91] The impurities causing the elevated boiling temperatures could be either organic compounds that do mix easily with water (like acetic acid, the pyrolysis byproduct we observed in large quantities in samples from the pine oil's aqueous region) or simply compounds from the organic phase that have similar boiling points to water (like the 2-butenal present in the aqueous region of the pine oil). Indeed, the first

drop (0.025 % DVF) of both fluids contained light organic compounds insoluble in water, for example, toluene, ethylbenzene, and propane.

Each replicate distillation was conducted until a solid residue resembling bio char was observed in the boiling flask. At this point, no further distillation could occur. We observed smoke formation in the distillation head at high temperatures during distillations of both fluids, which also signified the end of the distillation and may be evidence of thermal cracking.

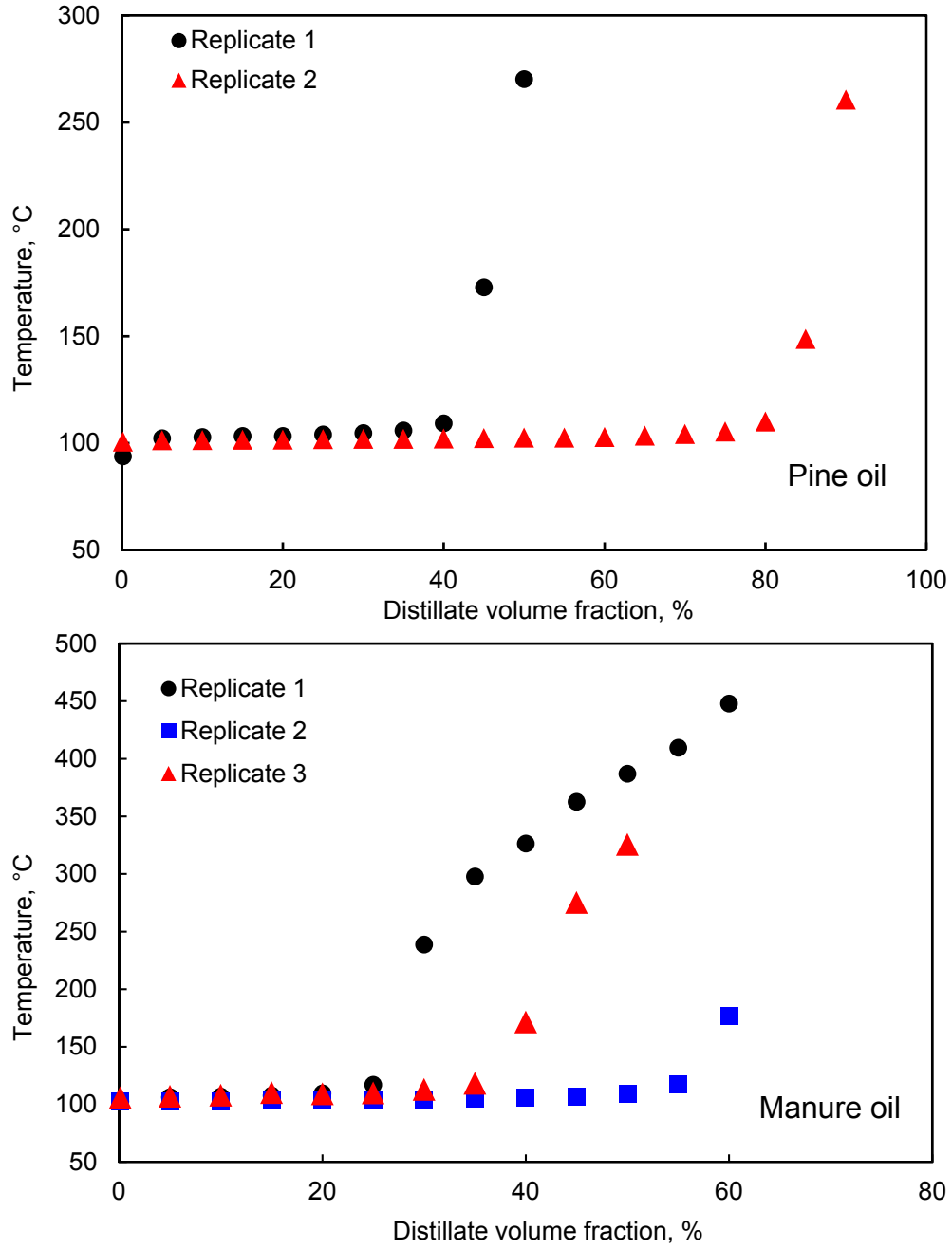

Figure 3.1. The raw distillation data (presented in terms of T_k) of pine oil (top) and manure oil (bottom) are overlaid to show the variability in the size of the low-boiling region. Data points at 0 % DVF represent the vapor rise or initial boiling temperature (IBT) of each replicate. Error bars are hidden behind the markers. A thermocouple failure during one pine oil distillation caused us to exclude that replicate, and limited sample prevented an additional measurement.

3.3.3. Offset procedure

Since the data showed that, sample to sample, we were not measuring the same mixture, we have attempted to correct for the water content variability by applying an offset at the water-organic inflection to the replicate distillations. Overlaid curves in Figure 3.2 show that, once this shift is applied, the characteristic distillation curve shape and boiling range for each fluid becomes apparent. Our method for conducting the offset was to select a water-organic inflection point on each curve such that the largest number of data points remained in the organic region while permitting the best agreement between replicates.

This manipulation imposes limitations on the analysis of the data; however, by applying the same procedure to previously measured ADC data, we are able to draw comparisons to another pyrolysis oil, made from swine manure, that also contained some water.[43, 48] Contrary to the present samples, the swine manure oil either existed as a single phase or as a stable emulsion, despite significant water content. As is typical for pyrolysis fluids made from biomass, the swine manure oil was composed of nitrogenated and oxygenated species as well as paraffins in the organic phase. In Table S3 found with the article referenced at the beginning of the chapter, it can be seen that the organic phase of the pine and manure oils had similar composition. Both fluids measured here were reasonably similar in boiling range to the swine manure pyrolysis oil. The offset pine and manure oil curves were also comparable in boiling range to previously measured two crude petroleum oils, one extracted from oil sands in Canada (T_k = 100-476 °C) and one North American crude oil from a Wyoming refinery (T_k = 74-392 °C).[88, 92] It is important to note that while the boiling ranges and component molecular weights of these oils are similar, the chemical composition of the pyrolysis fluids (Table S3) was significantly different from petroleum crude oils, which are overwhelmingly composed of hydrocarbons. The

pyrolysis fluids we report on would require extensive processing to resemble these petroleum crude oils in other respects important to their use as petroleum replacements or blend stocks.

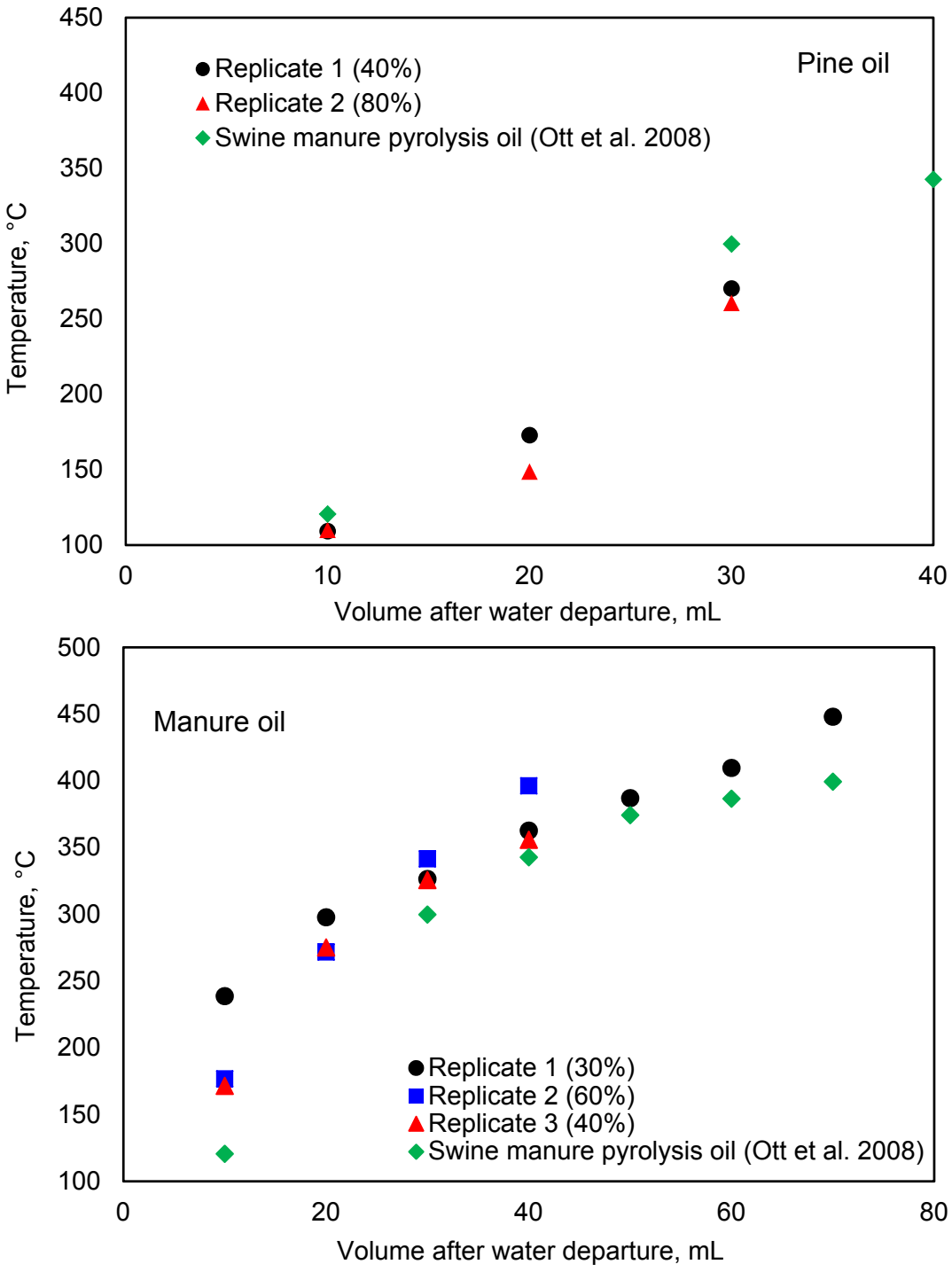

Figure 3.2. An offset has been applied to the horizontal axis of the distillation curves (the distillate volume) for pine oil (top) and manure oil (bottom) to account for the variability in the initial amount of water included in each replicate aliquot. The percentage in parentheses next to each legend entry represents the % DVF from the original measurements where the curves have now been offset to begin. We have compared the results to a previously-measured crude pyrolysis oil made from swine manure.[43]

3.3.4. Challenges and opportunities

Several difficulties arose during our data analysis, and we have considered ways to improve the procedure for measuring the distillation curves of non-homogeneous fluids in the future. First, the resolution on the horizontal (distillate volume) axis of the distillation curve was not fine enough to precisely pinpoint the starting temperature for the offset curves. In this context, resolution refers to the granularity or fineness of the temperature data grid (the number of and separation between temperature-volume pairs). Because the last of the water boiled off between recorded data points, there was a limit to the effectiveness of the offset procedure; for example, even after shifting there remained considerable difference among the replicates of manure oil at the 10 mL volume (Figure 3.2). The offset procedure could be made more precise by taking temperature measurements at 1 % DVF increments, especially in the transition zone between the low and high boiling regions. These additional data would make the distillation curve more continuous and allow for a more precise location of the water-organic inflection. Insufficient sample remained after these measurements were done to allow testing of this approach.

Second, in the future, the composition-explicit data channel provided by the ADC method could also be utilized to identify the correct offset. If samples were collected during every replicate distillation, an appropriate offset in composition space could be determined by requiring the composition, including water content (measured by Karl Fischer), of each DVF to be comparable among all the replicates within a given uncertainty. Importantly, the ADC is the only method that offers this ability to fix the distillation curve of a non-homogeneous mixture in the composition dimension.

Finally, a solution that might avoid the need for an offset at all is to use a membrane separation to remove most of the water prior to distillation without a major change to the composition of the organic fraction; some organics may be lost and some water would likely still be incorporated within the organic fraction. Again, sample availability prohibited a test of this method.

3.3.5. Fluid composition

In addition to the ADC measurement, we analyzed the composite (undistilled) organic fractions by gas chromatography coupled to mass spectrometry (GC-MS) for insight into their bulk composition. The GC-MS methods used are given in Table S2 in the Supporting Information of the article referenced at the beginning of this chapter. Table S3 summarizes the major components of the composite organic fractions, both of which were complex mixtures. Over 70 compounds were identified in the pine oil, and several of them were indicative of the feedstock, ponderosa pine shavings, used to make the oil. Substituted phenols such as creosol, catechol, and vanillin were abundant; the literature suggests that these represent the decomposition of lignin, the heterogeneous biopolymer that primarily composes plant material.[93] We also found a sugar derivative, levoglucosan, which may have formed from the depolymerization of cellulose and hemicellulose.[94] A heavier component consistent with the feedstock, dehydroabietic acid, was also present in the composite oil. Like the pine oil, the main peaks detected in the manure oil also included phenols. Notably, the organic fraction of the manure oil also contained long-chain nitriles, long-chain fatty acids, fatty acid methyl esters and thiols. The presence of oxygen and other heteroatoms in these fluids is typical for biomass pyrolysis, and removal of these species by further refining is an active area of research.[95]

3.4. Conclusion

The replicate distillation curves of two non-homogeneous crude pyrolysis fluids, made from pine shavings and dairy manure, were complicated by variable water content in each aliquot. We devised an approach to the data analysis to correct for the variability among the samples and elucidate a coherent distillation curve that can be compared to the experience base of previously measured crude oils. The water-organic inflection is the crucial data point driving the distillation curve offset procedure. The high-boiling regions of the distillation curves were comparable in temperature range and curve shape to a previously measured homogeneous crude pyrolysis oil. Finally, the composition of each fluid was determined; some components were indicative of the feedstock used in their production.

3.5. References

5. Han, Y., McIlroy, D. N., McDonald, A. G., Hydrodeoxygenation of pyrolysis oil for hydrocarbons production using nanosprings based catalysts. *J Anal Appl Pyrolysis* 2016, *117*, 94-105.

9. *ASTM D86, Standard test method for distillation of petroleum products at atmospheric pressure*. ASTM International: West Conshohocken, PA, 2004.

40. Bruno, T. J., Smith, B. L., Enthalpy of combustion of fuels as a function of distillate cut: application of an advanced distillation curve method. *Energy & Fuels* 2006, *20*, 2109-2116.

41. Smith, B. L., Bruno, T.J., Advanced distillation curve measurement with a model predictive temperature controller. *Int J Thermophys* 2006, *27*, 1419-1434.

42. Ott, L. S., Bruno, T.J., Corrosivity of fluids as a function of distillate cut: application of an advanced distillation curve method. *Energy & Fuels* 2007, *21*, 2778 - 2784.

43. Ott, L. S., Smith, B.L., Bruno, T.J., Advanced distillation curve measurement: application to a bio-derived crude oil prepared from swine manure. *Fuel* 2008, *87*, 3379-3387.

44. Lovestead, T. M., Bruno, T.J., Application of the advanced distillation curve method to aviation fuel avgas 100LL. *Energy & Fuels* 2009, *23*, 2176-2183.

45. Bruno, T. J., Ott, L.S., Smith, B.L., Lovestead, T.M., Complex fluid analysis with the advanced distillation curve approach. *Analytical Chemistry* 2010, *82*, 777-783.

46. Huber, M. L., Smith, B.L., Ott, L.S., Bruno, T.J., Surrogate mixture model for the thermophysical properties of synthetic aviation fuel S-8: Explicit application of the advanced distillation curve. *Energy & Fuels* 2008, *22*, 1104 - 1114.

47. Carpenter, D., Westover, T. L., Czernik, S., Jablonski, W., Biomass feedstocks for renewable fuel production: a review of the impacts of feedstock and pretreatment on the yield and product distribution of fast pyrolysis bio-oils and vapors. *Green Chemistry* 2014, *16* (2), 384-406.

48. Hsieh, P. Y., Bruno, T. J., Pressure-controlled advanced distillation curve analysis and rotational viscometry of swine manure pyrolysis oil. *Fuel* 2014, *132*, 1-6.

53. Smith, B. L., Bruno, T.J., Improvements in the measurement of distillation curves - part 3: Application to gasoline and gasoline + methanol mixtures. *Ind Eng Chem Res* 2007, *46*, 297-309.

54. Ott, L. S., Smith, B.L., Bruno, T.J., Experimental test of the Sydney Young equation for the presentation of distillation curves. *J Chem Thermodynam* 2008, *40*, 1352-1357.

55. Young, S., Correction of boiling points of liquids from observed to normal pressures. *Proc Chem Soc* 1902, *81*, 777.

59. Haynes W. M. (editor), *CRC Handbook of Chemistry and Physics, 97th ed.* Taylor and Francis CRC Press: Boca Raton, FL, 2017.

72. Smith, B. L., Bruno, T.J., Improvements in the measurement of distillation curves - part 4: Application to the aviation turbine fuel Jet-A. *Ind Eng Chem Res* 2007, *46*, 310-320.

74. Bruno, T. J., Wolk, A., Naydich, A., Stabilization of biodiesel fuel at elevated temperature with hydrogen donors: evaluation with the advanced distillation curve method. *Energy & Fuels* 2009, *23*, 1015-1023.

81. Smith, B. L., Ott, L.S., Bruno, T.J., Composition-explicit distillation curves of diesel fuel with glycol ether and glycol ester oxygenates: a design tool for decreased particulate emissions. *Environ Sci Tech* 2008, *42* (20), 7682-7689.

83. Bruno, T. J., Smith, B.L., Improvements in the measurement of distillation curves - part 2: Application to aerospace/aviation fuels RP-1 and S-8. *Ind Eng Chem Res* 2006, *45*, 4381-4388.

84. Bruno, T. J., Improvements in the measurement of distillation curves - part 1: A composition-explicit approach. *Ind Eng Chem Res* 2006, *45*, 4371-4380.

85. Burger, J. L., Gough, R. V., Lovestead, T., M., Bruno, T. J., Characterization of the effects of cetane number improvers on diesel fuel volatility by use of the advanced distillation curve method. *Energy & Fuels* 2014, *24*, 2437-2445.

86. Hofmann, N., A geographical profile of livestock manure production in Canada, 2006. *EnviroStats* 2008, *2* (4), 12-16.

87. Ocean Recovery Alliance. *Plastics-to-fuel project developer's guide*; American Chemistry Council: Los Angeles, 2015.

88. Ott, L. S., Smith, B.L., Bruno, T.J., Advanced distillation curve measurements for corrosive fluids: application to two crude oils. *Fuel* 2008, *87*, 3055-3064.

89. Young, S., *Fractional distillation*. Macmillan and Co., Ltd.: London, 1903.

90. *ASTM E1064, Standard test method for water in organic liquids by coulometric Karl Fischer titration*. ASTM International: West Conshohocken, PA, 2012.

91. Bruno, T. J., Wolk, A., Naydich, A., Analysis of fuel ethanol plant liquor with the composition explicit distillation curve approach. *Energy & Fuels* 2009, *23* (6), 3277-3284.

92. Hsieh, P. Y., Bruno, T. J., Measuring sulfur content and corrosivity of North American petroleum with the advanced distillation curve method. *Energy & Fuels* 2014, *28*, 1868-1883.

93. Lou, R., Wu, S., Lyu, G., Quantified monophenols in the bio-oil derived from lignin fast pyrolysis. *J Anal Appl Pyrol* 2015, *111*, 27-32.

94. Yu, Y., Chua, Y. W., Wu, H., Characterization of pyrolytic sugars in bio-oil produced from biomass fast pyrolysis. *Energy & Fuels* 2016, *30* (5), 4145-4149.

95. Elkasabi, Y., Chagas, B. M. E., Mullen, C. A., Boateng, A. A., Hydrocarbons from spirulina pyrolysis bio-oil using one-step hydrotreating and aqueous extraction of heteroatom compounds. *Energy & Fuels* 2016, *30* (6), 4925-4932.

Chapter 4: Phase Equilibria of Complex Fluid Mixtures: Modeling and Measurements with the Advanced Distillation Curve with Reflux

4.1. Introduction

Volatility is a two-phase property describing the tendency of a condensed-phase substance or mixture to partition to the gas phase. Like all physical properties, it is linked to chemical composition. The volatility of a pure substance is given by its vapor pressure at a particular temperature, while for a mixture it is provided by a distillation or boiling curve. For both the pure substances and mixtures, volatility is rigorously described by the relevant vapor-liquid equilibrium (VLE) and associated thermodynamics. On a practical level, the volatility of a mixture is useful not only as a property measurement, but also as an analytical tool because it is extremely sensitive to changes in chemical composition.

Vapor-liquid equilibrium (VLE) is a composition-explicit property of mixtures that describes their volatility; it quantifies how each component of that mixture is distributed in each phase. For simple (binary) mixtures, high quality, low uncertainty bubble point measurements are possible for a wide range of temperatures and pressures.[96] The most reliable methods used to make these precise measurements use an equilibrium VLE cell to which a well-known, constant composition mixture is introduced. These instruments precisely monitor temperature and pressure, changing one of these and measuring the other to collect bubble point data for that binary composition. The advantage of this method is very high-quality data; it avoids sampling the fluid and analyzing composition, which tends to introduce a great deal of uncertainty. One major drawback of measuring VLE using an equilibrium cell is that the measurements are extremely time consuming. The measurement of dew points requires a separate approach,

although some instrumentation is capable of measuring both. A great deal of binary data collected using equilibrium cells is available, and these data are vital to the development of binary interaction parameters and mixture models in general. The references provided here are only a small sample.[96-101] Models representing multicomponent mixtures are created using binary interactions between pairs of components, an estimation of the more complex interactions occurring in the mixture. Most of the fluids that are useful to us in real world applications (e.g. gasoline, diesel fuel, and other fuels), however, are far more complex than a binary, containing hundreds of components with varying chemical and physical properties. It has not been practical or popular to measure the vapor-liquid equilibrium of these fluids, although a handful of approaches were described in the 1980s.[102, 103] Still, data in the literature for these multicomponent mixtures are extremely limited, and thermodynamic models capable of predicting VLE for such mixtures are a major gap in this field of research. In fact, even a graphical representation of a multicomponent mixture's VLE across a range of state points does not exist. Some recent studies interested in the design of carbon capture and storage or enhanced oil recovery processes measured mixtures of crude oil and carbon dioxide; however, the authors treated oil as a single component, not the complex mixture that it is.[10, 11] This pseudo binary mixture is measurable without sampling composition. Those working in thermodynamic property measurement and modeling have commented on the absence of available VLE data for multicomponent mixtures, particularly measurements relevant to energy and fuels.[10, 102, 104] Addressing this gap, towards developing good models, requires well-resolved, low-uncertainty experimental measurements, or at least measurements for which the uncertainty is understood.

The ability to measure the VLE of mixtures such as fuels and develop high quality predictive models is important for several reasons. One major need for mixture VLE, which

concerns the research in this thesis, is in forensic science. The National Academy of Sciences in 2009 urged the forensics community to strive for increased rigor in their techniques; improving our knowledge of the thermophysical properties of fluid mixtures relevant to criminalistics is a crucial part of this effort because headspace (vapor) characterization methods are frequently used to analyze a condensed phase sample collected as evidence.[1] Headspace characterization is an approach to determining the composition of such a sample by collecting and analyzing the vapor that forms above and around the sample when it is placed in a closed volume and allowed to reach equilibrium.[105] It is ubiquitous in criminalistics and environmental analytical chemistry, including enforcement of regulations.[106-108] This type of analysis is desirable especially (1) in sampling situations that are unsafe (i.e. the detection of explosives or toxic compounds), (2) for dirty samples that would otherwise damage expensive instrumentation (e.g. fire debris analyzed by GC-MS), (3) when a sample must be collected from an otherwise inaccessible location (such as beneath the surface of the ground), or (4) to collect a representative sample over time, or of a large quantity where spot-checking methods are inadequate (as in testing for spoilage in an shipment of meat or poultry).[31, 34-36] Vapor sampling methods align with green chemistry principles by reducing or eliminating the solvent waste generated by the analysis compared to solvent extraction.

The difficulty shared among all headspace sampling methods is that the vapor phase is collected, but the composition of interest is the condensed phase artifact relevant to the applications discussed above. To obtain the desired measurement, one must know quantitatively how the composition of the two phases are related at equilibrium. That is, the ability to model and predict VLE is essential to bridge the gap between the composition of a sample's headspace, which is measured directly, with the composition of the condensed phase sample.

One common headspace sampling method used in arson investigation is the carbon strip method, wherein vapors from a sample of fire debris from the scene are passively collected onto an adsorbent carbon strip and analyzed for residual accelerant.[17] The interpretation of an arson fire debris headspace sample requires an additional consideration: the thermal weathering of ignitable liquids (IL) used to accelerate intentionally set fires. The residual IL found on fire debris has a different, weathered composition compared to the original, neat fuel before the fire started; this is one of the challenges presented in this area of forensic science. Because arson cases are among the most difficult for law enforcement to close, there are several groups working in the area of IL weathering prediction.[109-112] Although headspace analysis is the primary method by which this type of evidence is analyzed, current predictive methods do not address the need to connect the vapor measurement to the condensed phase evidence itself. To characterize a fuel's VLE with different degrees of weathering, towards rigorous fire debris headspace analysis, vapor-liquid equilibrium measurements across a range of increasing temperatures must be made. Understanding thermal weathering is also highly relevant to the study of the fate of fuels and other pollutants in the environment. This chapter presents an apparatus and method for collecting these data.

This method, which is called the advanced distillation curve with reflux or ADCR, is a modification of the advanced distillation curve (ADC), an existing approach to measuring the volatility of the same types of mixtures.[53, 72, 83, 84] The ADC is a method developed at the National Institute of Standards and Technology (NIST) for measuring a fluid's volatility as a function of the changing composition of the vapor phase across its distillation curve. The ADC measures distillation curves with very low uncertainty and corrects the shortcomings of the fuel distillation standard ASTM D86.[9] ASTM D86 distillations are plagued by systematic error, for

example, in its measurement of initial boiling temperature (IBT).[84, 113] Unlike ASTM D86, the ADC provides true thermodynamic state points, including IBT, and a volatility measurement that is physically meaningful and independent of situational variables like heating rate. ADC can therefore be applied to the development of equations of state describing the fundamental characteristics of fluids.[46, 53, 72, 83, 84, 114] The ADC has been used previously to measure the volatility of fuels and fuel mixtures with oxygenate additives made from both petroleum and alternative or renewable sources as well as surrogate mixtures designed to represent more complex fluids.[44, 48, 56, 68, 76, 115-120] ADC has also been used to model thermal weathering of fuels, an application that plays a role in the current work.[121, 122]

The classical ADC already collects three dimensions of the four required for a VLE measurement: temperature (T), pressure (P, which is constant and ambient), and the vapor composition (y). The reflux modification introduced in Section 4.2.2 allows for the collection of the liquid composition (x) and therefore the estimation of VLE. An advantage of building from such a well-used method is that a great deal of T-y data measured using classical ADC are already available in the literature.[40-46, 48, 53, 62, 63, 68, 72, 74, 76, 83-85, 88, 92, 114-120, 123-129] These existing data served as comparisons to data collected using the new ADCR apparatus.

To develop and demonstrate the ADCR concept, two hydrocarbon mixtures that represent fuels were chosen for initial measurements. The first, a binary mixture of *n*-decane (C10) and *n*-tetradecane (C14), was the simple mixture used in the early development of the ADC metrology.[84] The abundance of prior T-y data motivated this choice for exploratory ADCR work. To elucidate the complete two-phase region of the T-x-y diagram for the two-component mixture, starting mixtures with a variety of compositions were prepared. The second, three-component test mixture was selected to be more complex (in terms of number and heterogeneity

of components) and to represent a fuel, a category of fluids important to both forensics and the energy industry. This mixture, the Huber-Bruno (HB) surrogate, was developed in 2010 to represent the volatility of Jet-A with only three components.[69] The surrogate is composed (by mass) of 31 % *n*-dodecane, 38 % *n*-tetradecane, and 31 % 1,2,4-trimethylbenzene. There are no available experimental data measuring VLE among any of the pairs of components in either of these mixtures. Measurements of lighter hydrocarbons were used to inform the model used as a comparison to the present work.[98] The models referred to in the following sections are implemented in the NIST Reference Fluid Thermodynamic and Transport Properties Database (REFPROP)[130] that was used for all VLE calculations in this work.

4.2. Methods

4.2.1. Materials

The *n*-decane (C10), *n*-dodecane (C12), *n*-tetradecane (C14), and 1,2,4-trimethylbenzene (TMB) used to create the fluid mixtures were obtained commercially and tested for purity by use of gas chromatography. All were > 98 % pure and used as received. The mixtures were prepared gravimetrically as stock solutions. Because the stock solutions were of sufficient quantity to conduct several distillations over several days, the composition of the mixture was periodically by gas chromatography coupled to flame ionization detection (GC-FID) to ensure it had not changed over time. The initial volume used for the binary C10/C14 distillations was 200 mL; for the measurements of HB surrogate, it was 100 mL, a change which was motivated by a desire to conserve resources and minimize waste.

4.2.2. Apparatus

The classical ADC apparatus consists of a boiling flask (or kettle), distillation head, air-cooled condenser, sampling adapter for distillate collection, and a level-stabilized receiver for the measurement of distillate volume fraction (DVF). This is the pathway the fluid travels as it is distilled. While the distillation progresses, four variables are measured: the temperature of the boiling fluid (kettle temperature or T_k), the temperature of the vapor in the distillation head (head temperature or T_h), the DVF as it is collected in the receiver, and vapor composition obtained by sampling the condensate. More detailed descriptions of the apparatus and procedure for a classical ADC measurement are available in previous publications.[53, 72, 83, 84, 114]

Four measurands are necessary to describe a fluid's VLE: temperature, pressure, vapor composition, and liquid composition. As mentioned earlier, the classical ADC approach already includes the measurement of temperature (T_k, the temperature of the equilibrium state), pressure, and vapor composition but lacks a measurement of the composition of the liquid in the kettle as it changes with temperature. The challenge, however, in obtaining kettle composition is that a boiling liquid is in fact a two-phase fluid and cannot be reliably sampled. Any sample collected while the mixture in the kettle is boiling will not be representative of the bulk liquid phase and will be continuously variable due to the entrainment of irreproducible quantities of the vapor phase (bubbles) in the sampling device (usually a syringe).

The solution introduced by the ADCR apparatus is to impose a physical barrier between the vapor (which becomes the condensate collected in the receiver) and liquid (the raffinate which is left in the kettle) inside the apparatus once it reaches the target temperature (T_k) for a VLE measurement. The target T_k is selected by the experimenter; the fluid distills and collects in the receiver as in normal distillation until this temperature is reached. By separating the phases

when the liquid has achieved target T_k, the fluid in the kettle may be allowed to cool to sub-boiling temperature and resume a single phase before it is sampled, without any additional mixing or distillation confounding the result. The necessary physical separation is imposed by introducing a three-way valve with a switchable internal channel called the reflux junction.

The reflux junction is shown in Figure 4.1 and illustrated schematically in more detail in Figure 4.2. This switchable valve (made from a borosilicate glass standard taper joint) replaces the normal distillation head used in the classical ADC and has three branches spaced evenly about the valve body with 120 ° between them. When the ADCR is assembled, the bottom branch is connected to the middle neck of a 250 mL three-necked round bottom boiling flask. The other two necks of this flask are used for the placement of a thermocouple monitoring T_k and for liquid sampling through a septum cap. The left branch of the reflux junction is connected to the condenser, adapter, and receiver of the classical ADC apparatus. The right branch is connected to a vertically positioned reflux condenser. The top of the reflux condenser is capped with aluminum foil to minimize the escape of vapor when operating in reflux position. Escape of fugitive vapor is negligible; distillate has been observed traveling only a minimal distance up the reflux condenser before falling back into the kettle as liquid.

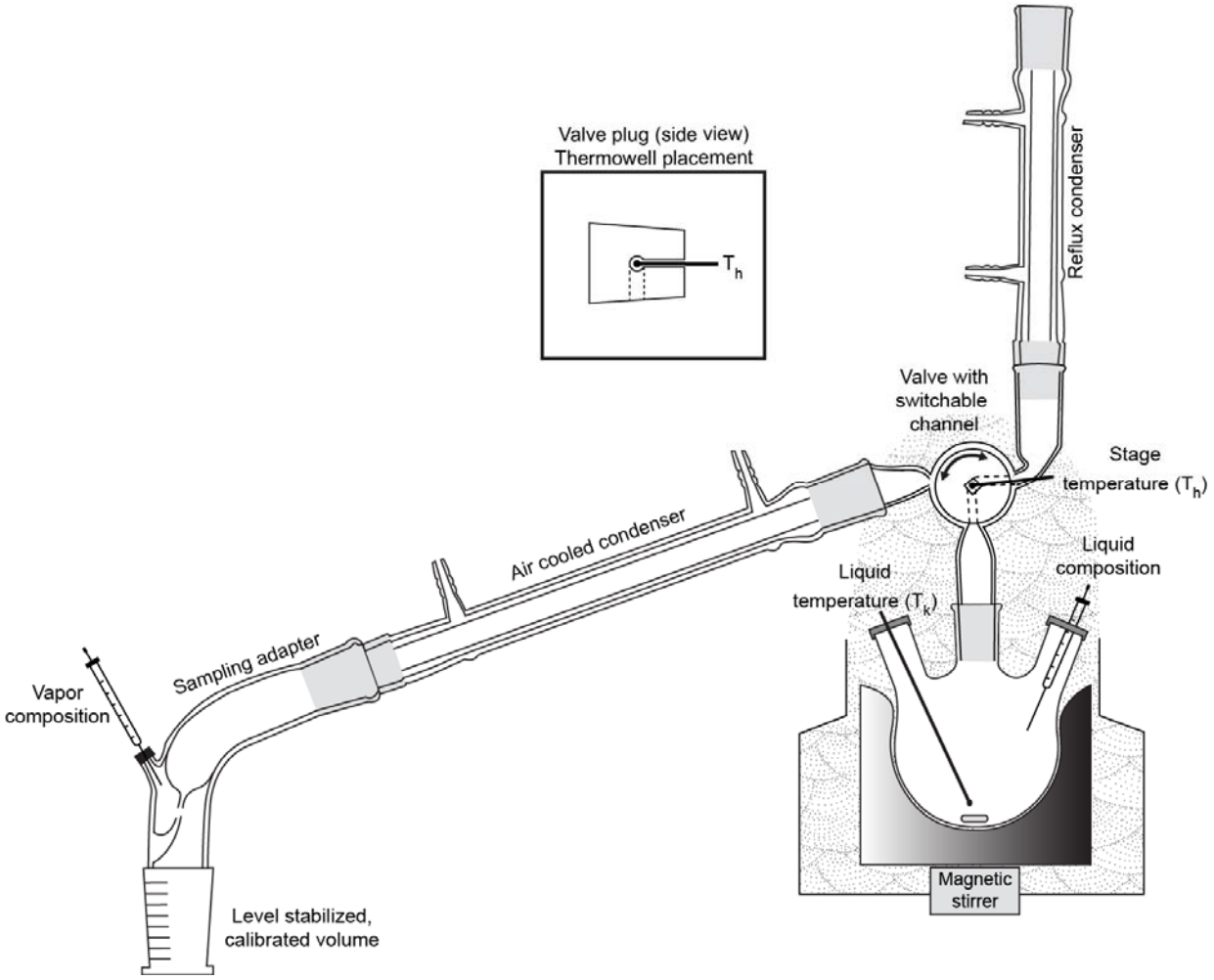

Figure 4.1. A schematic diagram of the ADCR apparatus, showing the junction that allows vapor to be routed to the condenser or reflux condenser.

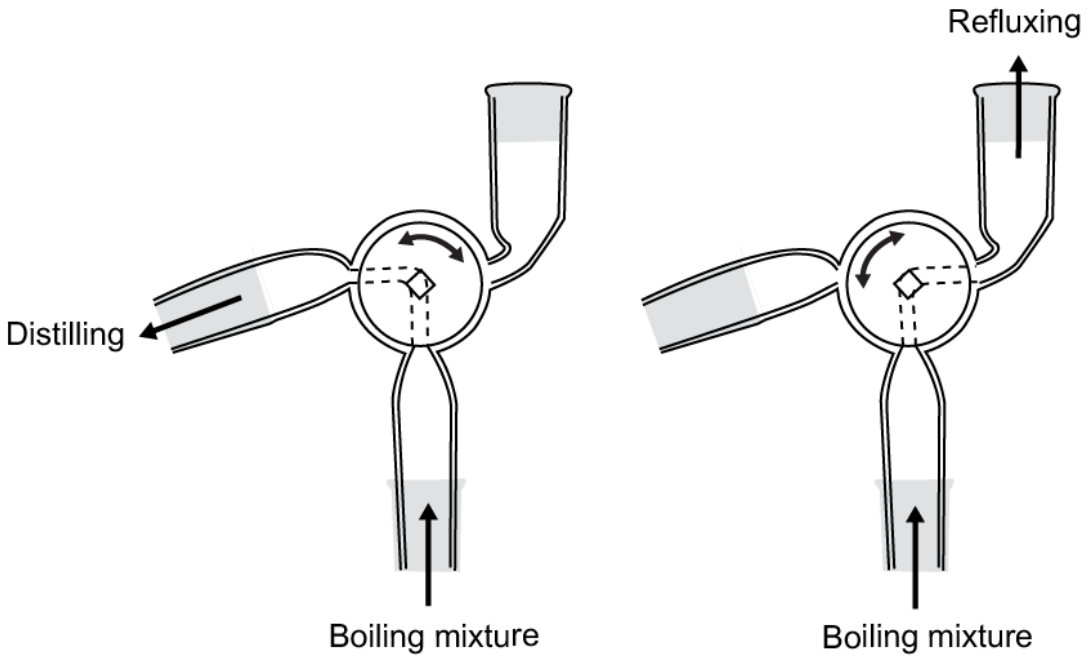

Figure 4.2. Schematics of the reflux junction in both operating modes. The junction is operated in distillation mode (left) until the boiling fluid reaches the target temperature (T_k) for which a composition measurement is desired. At this point, the plug is turned to reflux mode (right), preserving the composition of the liquid and permitting it to cool to sub-boiling before sampling.

A custom-made Teflon valve plug, also illustrated schematically in more detail in Figure 4.2, fits into the valve body to complete the reflux junction. This plug incorporates a cylindrical channel that aligns with two adjoining branches of the junction. There are two small round notches on the face of the plug to show where the openings of the channel are located so one can line them up to their desired position. The plug also has a square notch on its face. This notch is used along with a (3/8 inch nominal) socket driver to rotate the plug between operating modes.

A thermocouple well, drilled into the plug on axis, permits the measurement of the head temperature, T_h. Although during an ADCR measurement, T_k (the fluid temperature of the VLE data point) is used to decide when to stop the distillation, T_h is an important quantity to track for several reasons. First, this temperature is a useful diagnostic tool to ensure proper performance of the apparatus. Second, because T_h is part of the ADC measurement, recording it during the

ADCR as well allows more thorough comparison of results from the two methods. Finally, and most importantly, T_h represents the temperature of an equilibrium stage within the apparatus. The ADCR is not a perfectly simple distillation: the apparatus causes slight fractionation. Accounting for this experimental phenomenon in the corresponding mixture models requires assuming one theoretical plate, an equilibrium stage in the apparatus with temperature T_h located inside the Teflon plug, where rising vapor re-equilibrates and partially condenses. Acknowledging the role of T_h in an ADCR measurement is a crucial step in modeling and data interpretation.

4.2.3. Procedure

Each ADCR measurement is initiated by placing the necessary volume of the fluid mixture into the three-necked round bottom flask using an automatic pipette. The thermocouple submerged in the liquid must not be touching the flask or disturbed by the magnetic stir bar; the thermocouple in the vapor, inside the Teflon plug, must be centered and not touching the walls of the channel. The fluids measured in this work are not volatile enough to require cooling of the distillation or reflux condensers, but for lighter mixtures, both condensers should be chilled. The rate of distillation is controlled by a temperature program applied to the heating mantle that encloses the kettle.

At the start of a measurement, when normal distillation is desired, the channel inside the reflux junction is positioned to allow mass transfer along the path between the kettle and the volume receiver. The distillation is stopped at the target T_k by turning the valve plug from distillation mode to reflux mode (Figure 4.2) and ending the heating program. An aliquot from the sampling adapter is immediately collected for vapor phase composition. A sample of the condensed phase is collected from the kettle once it is cool. For the measurements presented

here, each small volume (~7 μL) sample was added to ~1 mL of a solvent and analyzed using GC-FID. Any method of chemical analysis could however be used to characterize the samples.

The uncertainty in kettle temperature in the ADCR apparatus is 2 °C; for the head temperature, it is 4 °C. Thermocouples were calibrated in an indium freezing point cell. The uncertainty in volume measurements is 1 mL. All uncertainty values presented in this chapter reflect expanded uncertainty calculated with a coverage factor k = 2 providing a 95% confidence interval.

4.2.4. Analytical methods

All samples in the present work were collected using a 10 μL glass barrel autosampler syringe and placed in autosampler vials containing *n*-octane as the solvent. All samples, analyzed using GC-FID, were run in triplicate and peak areas were averaged. Response factors (RFs) were periodically measured, and it was found that the instrument response to each compound was the same, permitting the direct use of area counts to determine mass fraction without calibration.

4.2.5. Theory

In previous work with the ADC, the distillation curve was modeled as a simple batch process where boiling vapor leaves the kettle at a constant flow rate and passes directly into a condenser without any reflux.[46, 69, 131, 132] The liquid is assumed to be at its bubble point and in equilibrium with the vapor phase. A mixture model based on Helmholtz form equations of state, as implemented in the NIST REFPROP computer program, was used to model the VLE of the fluids studied here.[130, 133, 134] Any model, including simpler equations of state such as the Peng-Robinson EOS, could also be used to model the VLE.[135] The Helmholtz models are generally more accurate but require high-quality experimental data to develop. These models were accessible, so Helmholtz models were chosen over the much simpler Peng-Robinson

formulations. If one does not have Helmholtz models, the Peng-Robinson model may be substituted; this may be useful for situations where one is interested in a fluid with limited property data, as it requires only the critical point and acentric factor to model a fluid.

The standard REFPROP computer program contains *n*-decane and *n*-dodecane, but does not contain *n*-tetradecane or 1,2,4-trimethylbenzene.[130] For *n*-tetradecane a REFPROP fluid file was used that was developed for work on jet fuel surrogate models that can be obtained from NIST.[131, 136] Similarly, a REFPROP fluid file for 1,2,4-trimethylbenzene was developed for a project on diesel fuels and also was obtained from NIST.[132, 136] For modelling VLE, the calculations can be very sensitive to the values of binary interaction parameters that are used. Due to lack of experimental data, the REFPROP program does not have values obtained from fitting experimental data for the binary pairs (*n*-decane/*n*-tetradecane, *n*-dodecane/*n*-tetradecane, *n*-dodecane/1,2,4-trimethylbenzene and *n*-tetradecane/1,2,4-trimethylbenzene) that are needed in this work. When experimental data are unavailable, the REFPROP program estimates the binary interaction parameters from an algorithm.[137] Since this algorithm was developed with one and two carbon hydrofluorocarbon refrigerants, it was not clear that it would perform well for the systems in this work that involve larger hydrocarbon molecules, so experimental initial boiling point data obtained in experiments described later were used to validate the binary interactions parameters. It was found that the estimation algorithm was adequate for *n*-alkane pairs, but it was necessary to fit experimental data for the pairs with 1,2,4-trimethylbenzene. The values of the binary interaction parameters γ_T and γ_V used in the Kunz-Wagner mixture model were determined to be γ_T =0.9968 and γ_V =1.0521 for *n*-tetradecane/1,2,4-trimethylbenzene and γ_T =0.9970 and γ_V =1.0345 for *n*-dodecane/1,2,4-trimethylbenzene.[133]

In the simplest distillation procedure, one first assumes there is a fixed amount of feed at a known pressure, and a known liquid composition, x_i. The bubble point temperature T_{bub1} and equilibrium vapor phase compositions y_i are then calculated with a mixture model. In this work, the REFPROP computer program is used to provide all VLE calculations. A constant number of moles n_i are next removed from the system, that are at the equilibrium vapor composition, y_i. A mass balance is then done to determine the new liquid composition left in the kettle and the remaining volume. The left panel of Figure 4.3 illustrates this process. This process is then repeated until 95% of all liquid in the kettle is gone, and a distillation curve is created by plotting the kettle temperature (the series of bubble point temperatures T_{bub1}) against the volume fraction collected in the receiver. In the original work it was found necessary to add a volumetric shift to enable the calculated curve to match the experimental curve.[46] This shift was entirely empirical and was explained as compensation for the fact that the actual distillation process involves dynamic holdup due to the volume of the glassware. In this work, the distillation is more realistically modeled by adding a single stage to account for reflux in an attempt to eliminate the need for an empirical shifting factor.

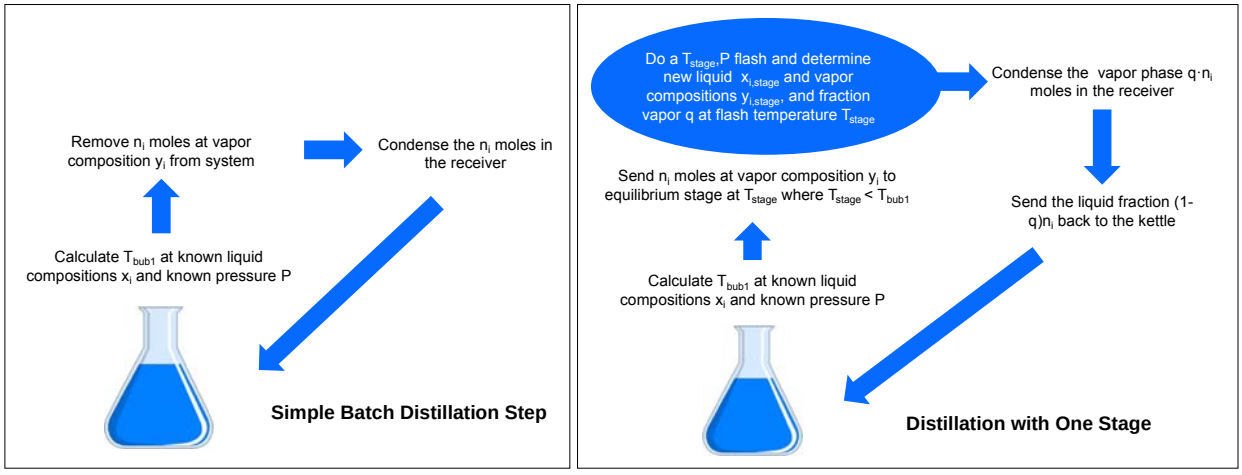

Figure 4.3. Illustration of a simple batch (no stage) distillation step (left) and a distillation step with one stage (right).

The revised calculation procedure incorporating a single stage is the following (illustrated in the right panel of Figure 3). First, initiate the distillation by calculating the bubble point temperature and equilibrium vapor composition given the liquid composition and the pressure. The bubble point temperature and equilibrium vapor phase compositions are then calculated with REFPROP. Instead of removing a constant number of moles from the system that are at the vapor composition, they are instead sent to an equilibrium stage operating at a temperature T_{stage} and the local pressure. A T, P flash is then performed that gives a new vapor composition $y_{i,stage}$ and a phase split (a liquid fraction and a vapor fraction). The vapor fraction with composition $y_{i,stage}$ and quantity q is sent to the receiver and condensed. The liquid fraction is returned to the kettle, and a mass balance is done to determine the new liquid composition in the kettle. This process is then repeated until 95% of the liquid in the kettle is gone.

The temperature of the stage, T_{stage}, is lower than the bubble point temperature T_{bub1}, but higher than the bubble point temperature of the vapor $y_{i,stage}$ (i.e. the bubble point if the vapor $y_{i,stage}$ is used as the composition for a bubble point calculation); call this temperature T_{bub2}. If the temperature in the head T_h is known, this is a reasonable choice for the stage temperature. If T_h is not known, it was found that, for the mixtures studied in this work, a reasonable approximation for T_h is $T_{stage}= 0.3T_{bub1}+0.7T_{bub2}$. This should not be taken as a rule; it may be different for mixtures of different compounds or with different apparatus. Experiments described later indicated that the addition of a single stage operating at the head temperature T_h to the distillation curve calculation reduced the need for an empirical shifting factor. A smaller and more realistic volumetric shift is still required; this is discussed in detail later, in Section 4.3.3. These findings indicate that reflux is occurring in the ADC process, and that the phenomenon can be modeled.

4.3. Results and discussion

All temperatures presented in this paper were measured at ambient pressure in Boulder, Colorado (about 83 kPa). The experimental pressures that correspond to the data sets are always provided. Temperatures have not been adjusted to 1 atm (101.325 kPa) as is conventional when reporting distillation curves measured by ADC or ASTM D86. The generally accepted method specified in ASTM D86 to correct observed temperatures for variations in atmospheric pressure is the modified Sydney Young (SY) equation.[9, 55, 89, 138] An experimental test of the SY equation (that also used the *n*-decane/*n*-tetradecane binary as the test mixture) found that it does not perform well to correct measured temperatures for simple mixtures.[54] Additionally, the Organisation for Economic Co-operation and Development (OECD) recommends applying the SY equation only in cases where the pressures differ by less than 5 kPa.[139] Therefore, the correction was not applied in this work in order to minimize any uncertainty introduced by such data manipulation.

4.3.1. Comparison to previous ADC measurements

Before the initiation of a comprehensive study of C10/C14 vapor-liquid equilibrium using ADCR, the modified apparatus was tested by distilling a 50/50 (mol/mol) mixture to ensure that the distillation curve measured by the classical ADC in Bruno 2006 was replicable.[84] The curves, which were measured in triplicate, showed consistent initial boiling temperatures, and temperatures in the late stages of the distillation (approaching 75 % DVF) were reproducible within 1.5 °C. The maximum difference between the curves was 4.8 °C, at 30 % DVF (Figure 4.4). These minor differences are attributable to the physical changes made to the classical ADC

to create the ADCR: the substitution of the three-way valve with Teflon plug for an ordinary distillation head.

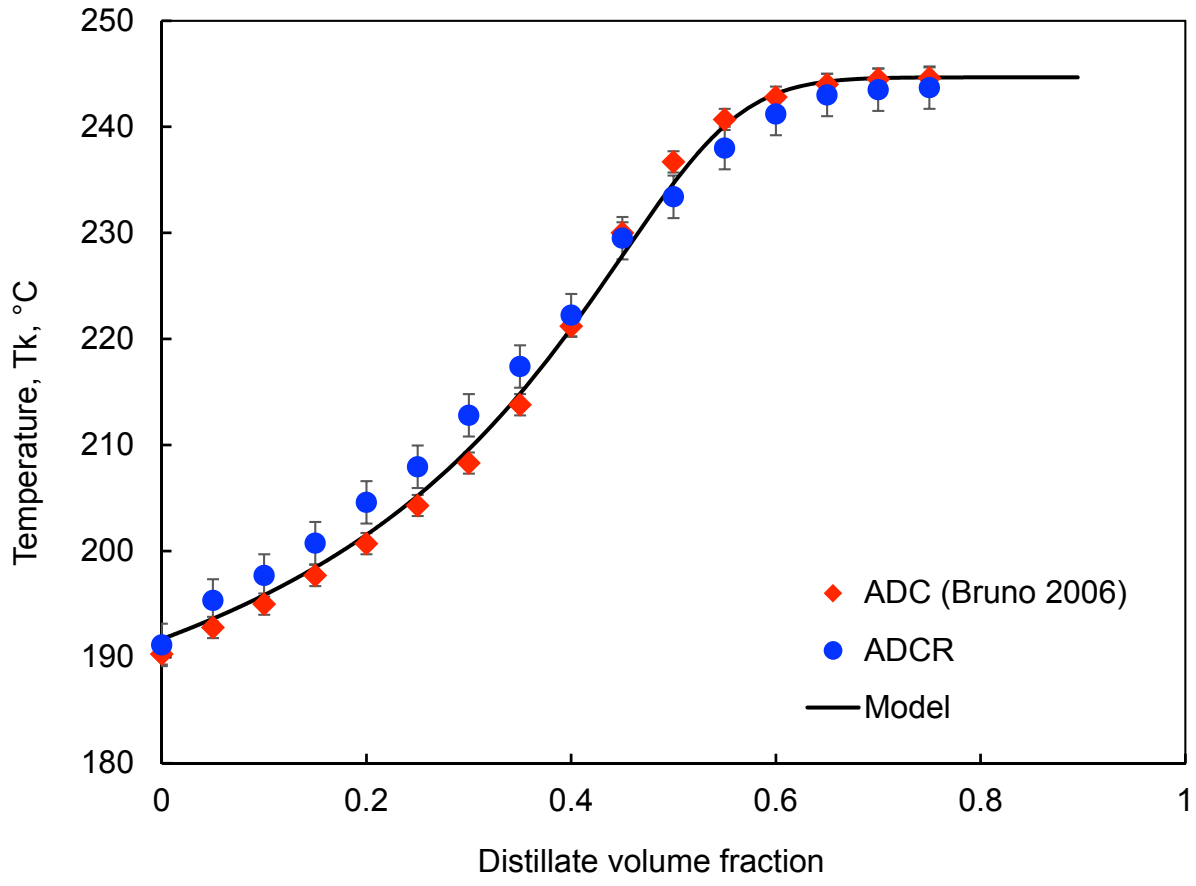

Figure 4.4. Distillation curve measurements of a 50/50 C10/C14 (mol/mol) mixture, conducted with the modified ADCR apparatus and compared to the original ADC data from 2006.[84] All temperatures were measured at atmospheric pressure in Boulder, CO, about 83 kPa, and were not corrected. The uncertainty of the Bruno 2006 kettle temperatures (T_k) is 1 °C. In some cases, error bars are smaller than the markers.

The same comparisons between ADCR measurements and previously published ADC data were made for the Huber-Bruno surrogate (Figure 4.5). Agreement among kettle temperatures for this mixture was good. The measured IBTs were identical. Measured temperatures were slightly higher in the ADCR measurements across the distillation curve. The

maximum difference between the measurements was 5.2 °C. These distillation curves were used to improve the binary interaction parameters for TMB with each of the alkanes.

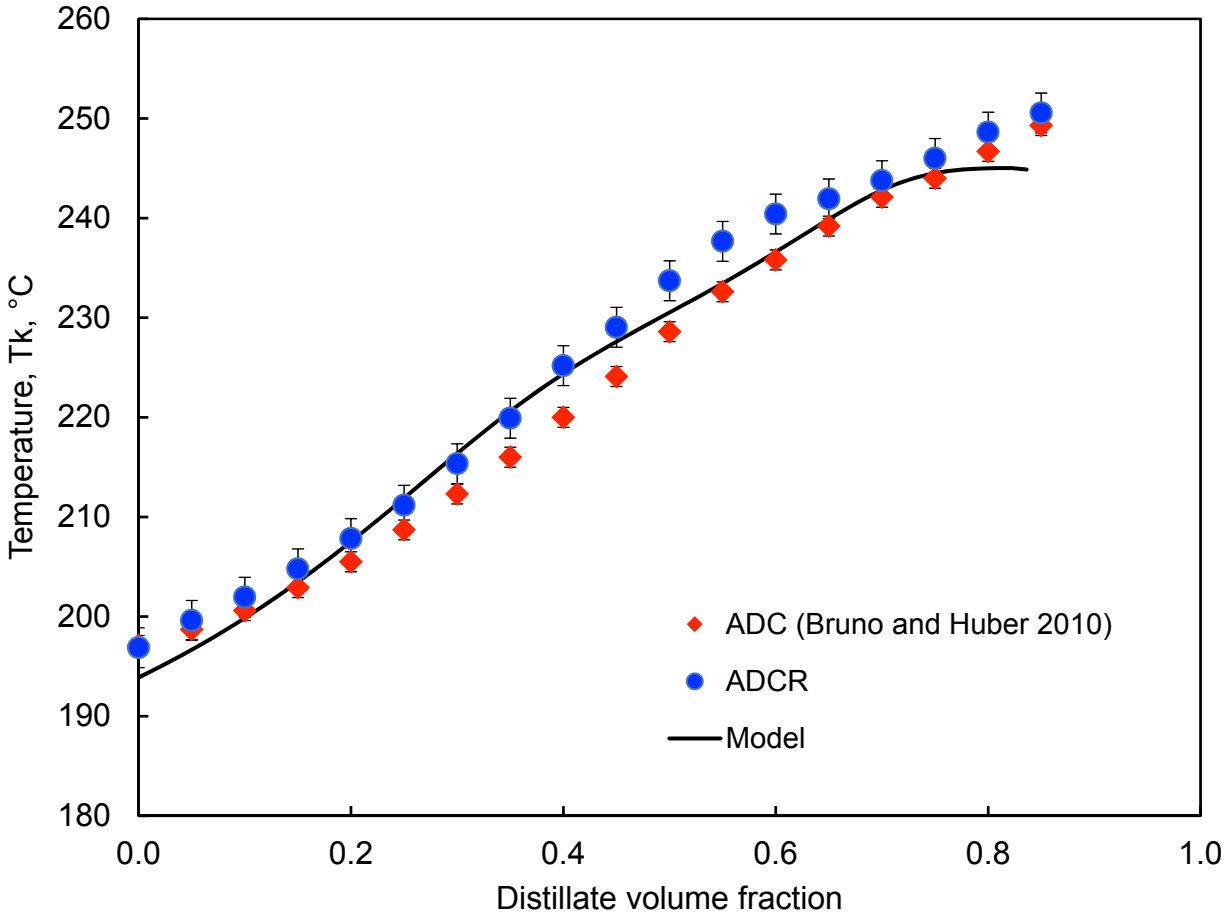

Figure 4.5. Comparison of kettle temperatures from a distillation of HB surrogate conducted with the modified ADCR apparatus to the original ADC data from 2010.[69] These curves were measured at atmospheric pressure in Boulder, CO, about 83 kPa. The uncertainty of the Bruno and Huber 2010 kettle temperatures (T_k) is 1 °C. In some cases, error bars are smaller than the markers.

From these experiments, it was concluded that distillation curves measured using the ADCR were consistent with previous ADC measurements. Head temperatures were also comparable, and both T_k and T_h were recorded throughout the remaining experiments.

4.3.2. Measurement and comparison to models

4.3.2.1. Decane/tetradecane binary

Figure 4.6 graphically presents the measurements made of the binary system *n*-decane/*n*-tetradecane and compares them to the model. VLE was measured at 13 target temperatures (T_k) chosen *a priori* to provide good resolution across the full two-phase region of the T-x-y diagram. Each data point represents the average of four individual measurements.

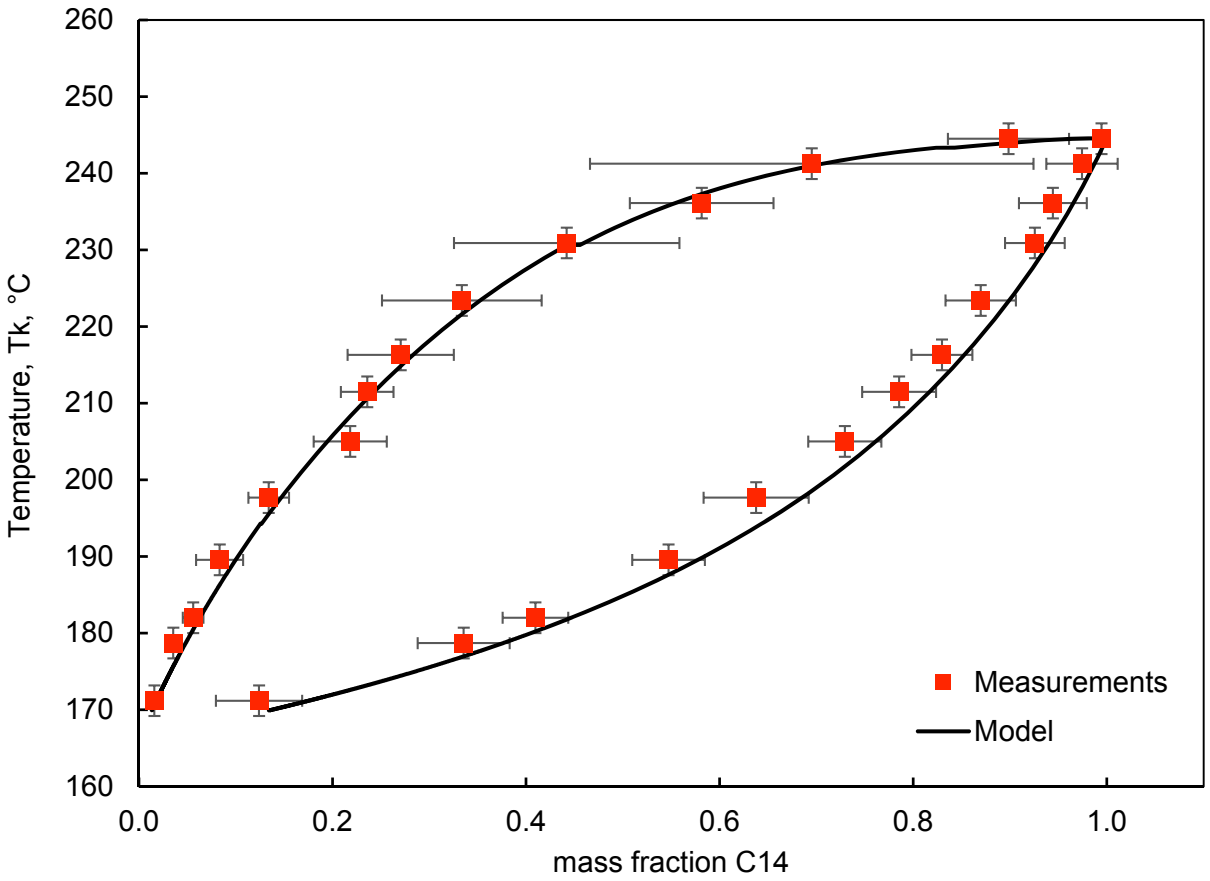

Figure 4.6. This T-x-y diagram for *n*-decane/*n*-tetradecane, plotted in terms of tetradecane mass fraction, describes the composition of each phase as a function of kettle temperature. The upper curve (dew curve) represents the vapor composition, and the lower curve (bubble curve) represents the liquid composition.

There was very good agreement between the measurements and model. The dew curve (upper curve, representing vapor composition) predicted by the model is faithfully produced by the experiments done with the ADCR method. At all temperatures, measured composition agrees with the model within experimental error. The shape and size of the two-phase region is similar in both cases. Of all the data, the most scatter was apparent among individual measurements of the vapor composition at temperatures between 223 and 245 °C. In this region of the T-y diagram, the vapor mass fraction of C14 is changing very rapidly with small changes in temperature. Put another way, the slope of the dew curve is very shallow at high temperatures. Although it is less pronounced, the same trend occurs along the bubble (lower) curve: the liquid composition measurements are more scattered at low temperatures, where this curve is shallowest and C14 concentration is changing rapidly with temperature. The error bars for liquid composition therefore broaden with decreasing temperature. In general, the repeatability of the liquid composition measurements was better than for the vapor phase. This is likely because the liquid remaining in the kettle is a larger population material from which to sample. The bulk of the liquid made its composition less sensitive to variability among independent measurements. It was therefore much more repeatable than vapor composition, the sample for which is collected from the smaller quantity of material in the sampling adapter. The vapor is also affected by more potential sources of variation among replicates than the liquid. The vapor must undergo the re-equilibration step and flow through the condenser before it reaches the sampling point, both processes which may affect the measured composition to some small degree.

Although the uncertainty in vapor composition is greater than the uncertainty in liquid composition, the model and measurements of the liquid do not agree as well as they do for vapor composition. The pattern of disagreement between the liquid composition measurements and

model predictions along the bubble curve suggests a possibly systematic error. Although in each case, the error bars on the measurements intersect the modeled curve, the model consistently predicts a greater concentration of C14 in the liquid than was measured at each temperature. If this error is truly systematic, either the model or the measurements must be wrong in some manner which pushes the two apart (or both are slightly wrong in opposite directions). The model could be inaccurate due to problems with the individual component equations of state or the binary interaction parameters in the mixture model. The assumptions made in modeling the equilibrium stage in the apparatus could be flawed, although including a stage in the model mostly affects the vapor composition and causes minimal change in the liquid composition compared to a model with no stage. If the model is reliable and instead there is some systematic error in the measurement of kettle composition that caused an undercalculation of C14, its source has not been identified. The sources of systematic error that have been considered would cause overcalculation of C14, moving the measurements down below the modeled bubble curve instead of above it. Several sources of error that were considered and discarded are discussed below.

First, before collecting the liquid sample, the magnetic stir bar is used to thoroughly mix the fluid remaining in the kettle. Any stratification that may occur because of differences in density were therefore eliminated. Next, the effect of any vapor condensate hang-up was considered (in the reflux condenser, inside the channel of the reflux junction, or coating the walls of the glassware); however, the effect, if it were significant, of such material being lost from the kettle would be an overcalculation of the C14 concentration. This held up condensed vapor would be enriched in C10, the more volatile component, causing the remaining kettle liquid to contain more C14, not less. Any effect of vapor forming in equilibrium above the kettle liquid (in

the headspace) would also cause an offset in the wrong direction. Finally, the error could be occurring in the temperature measurement due to a lag in thermocouple or readout response, but such a lag would have been reproduced in the initial comparison of the distillation curve with classical ADC measurements. This would shift the measurements to lower temperatures and again, below the model prediction—not above it, as is the case. Error in temperatures sensed by the thermocouples is prevented by regular calibration using an indium cell according to NIST protocol. Therefore, the minor disagreement between the modeled and measured bubble curves could not be definitively explained. The magnitude of the disagreement is small—smaller than the uncertainty in the measurements—but the source of a possibly systematic error should be discovered.

The expanded uncertainty in T_k (2 °C) and T_h (4 °C) is due to (1) the measured accuracy of the thermocouples, (2) calibration of the thermocouples, and (3) small variations in ambient pressure (±1.4 kPa) among replicates. To determine the effect of these pressure differences on temperature, the modified Sydney Young equation was used to shift the measured temperatures to the model's pressure, resulting in a maximum adjustment of 0.5 °C. Finally, since the data are averages representing multiple independent measurements, (4) small deviations in the actual T_ks about the target T_k (0.15 °C on average) were also considered. Uncertainty in composition measurements was determined based on (1) the effect that the uncertainty in temperature would have on composition (calculated using the model), (2) the effect of the (educated) assumption of a constant FID response to each compound, and (3) the repeatability of three replicate injections of each sample. Calculated uncertainties are presented alongside the measurements in Table 4.1.

Table 4.1. Measured values, their corresponding uncertainties, and modeled predictions of the binary mixture VLE by mass fraction are presented. x represents liquid composition and y represents vapor composition. Uncertainties (u) were calculated with a coverage factor k = 2.

		xC14 (liquid)				yC14 (vapor)			
T_k, °C	**P, kPa**	**Measured**	**u**	**Model**	**Model-Meas.**	**Measured**	**u**	**Model**	**Model-Meas.**
171.2	83.25	0.124	0.045	0.175	0.051	0.016	0.006	0.018	0.002
178.7	83.05	0.335	0.048	0.375	0.040	0.035	0.008	0.048	0.013
182.0	83.30	0.410	0.034	0.445	0.036	0.056	0.011	0.063	0.007
189.6	83.06	0.547	0.038	0.577	0.030	0.083	0.024	0.100	0.016
197.7	83.16	0.638	0.054	0.682	0.044	0.134	0.021	0.145	0.011
205.0	83.26	0.729	0.038	0.757	0.028	0.218	0.038	0.192	-0.027
211.5	82.97	0.785	0.038	0.814	0.029	0.236	0.027	0.240	0.004
216.3	83.47	0.830	0.031	0.852	0.023	0.270	0.055	0.282	0.012
223.4	83.36	0.870	0.036	0.896	0.027	0.334	0.082	0.348	0.014
230.9	82.90	0.926	0.031	0.939	0.013	0.442	0.116	0.455	0.013
236.1	83.43	0.944	0.035	0.964	0.019	0.581	0.074	0.545	-0.036
241.2	83.28	0.974	0.037	0.987	0.012	0.695	0.229	0.699	0.004
244.5	83.63	0.994	0.001	0.999	0.005	0.898	0.063	0.962	0.064
		xC10 (liquid)				**yC10 (vapor)**			
T_k, °C	**P, kPa**	**Measured**	**u**	**Model**	**Model-Meas.**	**Measured**	**u**	**Model**	**Model-Meas.**
171.2	83.25	0.876	0.061	0.825	-0.051	0.984	0.029	0.982	-0.002
178.7	83.05	0.665	0.057	0.625	-0.040	0.965	0.008	0.952	-0.013
182.0	83.30	0.590	0.040	0.555	-0.036	0.944	0.745	0.937	-0.007
189.6	83.06	0.453	0.039	0.423	-0.030	0.917	0.024	0.900	-0.016
197.7	83.16	0.362	0.049	0.318	-0.044	0.866	0.021	0.855	-0.011
205.0	83.26	0.271	0.029	0.243	-0.028	0.782	0.038	0.808	0.027
211.5	82.97	0.215	0.026	0.186	-0.029	0.764	0.027	0.760	-0.004
216.3	83.47	0.170	0.017	0.148	-0.023	0.730	0.055	0.718	-0.012
223.4	83.36	0.130	0.019	0.104	-0.027	0.666	0.082	0.652	-0.014
230.9	82.90	0.074	0.012	0.061	-0.013	0.558	0.116	0.545	-0.013
236.1	83.43	0.056	0.014	0.036	-0.019	0.419	0.074	0.455	0.036
241.2	83.28	0.026	0.014	0.013	-0.012	0.305	0.229	0.301	-0.004
244.5	83.63	0.006	0.001	0.001	0.005	0.102	0.063	0.038	0.064

4.3.2.2. Ternary Huber-Bruno surrogate

Triplicate ADCR measurements of the composition of the Huber-Bruno surrogate were conducted at each of five target temperatures evenly spaced across the distillation curve of the fluid. Figure 4.7 compares the measured values to the model.[69] The data are presented in Table 4.2 alongside model predictions.

There is excellent agreement between the HB surrogate model and the ADCR measurements. The areas of greatest deviation are in the vapor mass fraction of TMB and in the liquid mass fraction of the alkanes at high temperatures. It appears that the measured curves have slightly shallower slopes and slower changes in composition with changing temperature than predicted. The deviations do not appear systematic; instead, the model has a slightly greater slope; that is, it is changing more rapidly with temperature than was found in the measurements. The phenomenon is present in both phases but more pronounced in the vapor. This suggests that the assumptions made in modeling the equilibrium stage may be in slight disagreement with the reality of the measurements.

Figure 4.7 represents mass fractions of each component as stacked areas. For any given temperature along the x-axis, a vertical line can be drawn through both the lower (liquid composition) and upper (vapor composition) area plots. The length of the line segments inside each shaded area provide the mass fractions of each component present in each phase of the mixture at that temperature and pressure. By locating a measured composition of one phase on either the upper or lower stacked area plot, one can trace the vertical line at the corresponding temperature and use the figure to predict the composition of the other phase.

The sources of uncertainty in these measurements were the same as for the C10/C14 measurements in the previous section. Uncertainty in temperature remained 2 °C, and

uncertainties in composition measurements were calculated in the same way. Uncertainties in measured vapor composition were lower for this mixture than for the binary in the last section. As discussed, the high variability in some composition measurements was due to rapidly changing composition with small temperature changes in some parts of the binary T-x-y curve. Composition of this mixture changed more gradually with temperature, enabling the vapor samples to be repeated more easily and reducing the uncertainty in the average. Uncertainty values are presented alongside the data in Table 4.2.

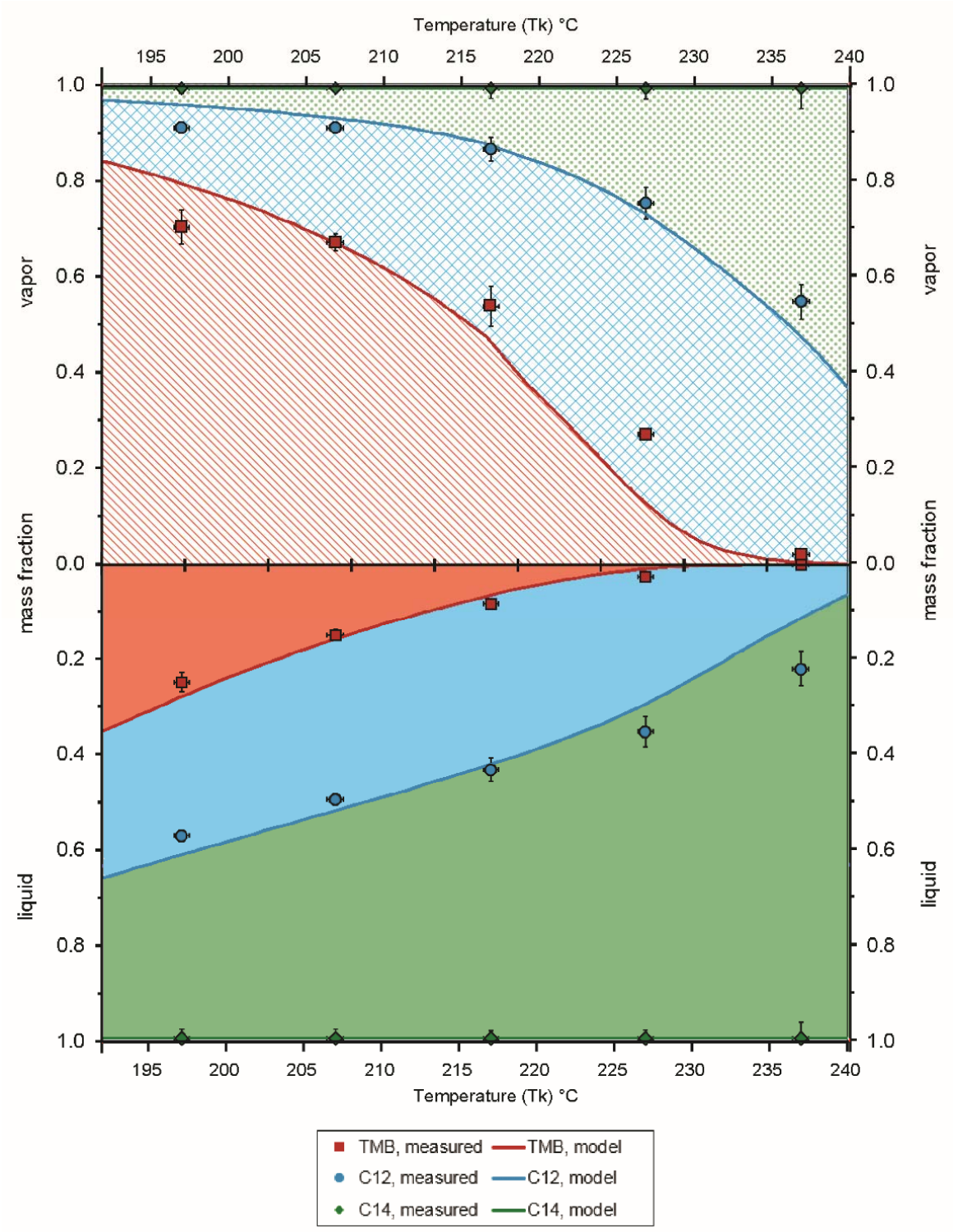

Figure 4.7. This T-x-y plot compares the Huber-Bruno model to measurements using ADCR. All measurements were made at ambient pressure, and the model is calculated at P = 83.18 kPa. Some error bars are hidden by the markers.

Table 4.2. Measured values, their corresponding uncertainties, and model predictions of the Huber-Bruno surrogate VLE by mass fraction are presented. x represents liquid composition and y represents vapor composition. Uncertainties were calculated with a coverage factor k = 2.

				xTMB				yTMB	
Tk, °C	**P, kPa**	**Measured**	**u**	**Model**	**Model-Meas**	**Measured**	**u**	**Model**	**Model-Meas**
197.1	82.91	0.250	0.020	0.282	0.032	0.708	0.036	0.797	0.089
207.0	82.86	0.150	0.012	0.166	0.017	0.676	0.018	0.675	-0.002
217.0	82.55	0.083	0.006	0.067	-0.016	0.542	0.042	0.478	-0.064
227.0	82.86	0.026	0.005	0.011	-0.014	0.272	0.011	0.123	-0.149
237.0	82.92	0.001	0.001	0.000	-0.001	0.020	0.005	0.003	-0.017
				xC12				**yC12**	
Tk, °C	**P, kPa**	**Measured**	**u**	**Model**	**Model-Meas**	**Measured**	**u**	**Model**	**Model-Meas**
197.1	82.91	0.324	0.012	0.332	0.009	0.209	0.012	0.168	-0.041
207.0	82.86	0.347	0.009	0.361	0.014	0.240	0.010	0.263	0.023
217.0	82.55	0.350	0.014	0.359	0.009	0.330	0.025	0.407	0.076
227.0	82.86	0.328	0.014	0.294	-0.035	0.486	0.032	0.609	0.123
237.0	82.92	0.221	0.016	0.126	-0.095	0.531	0.037	0.471	-0.060
				xC14				**yC14**	
Tk, °C	**P, kPa**	**Measured**	**u**	**Model**	**Model-Meas**	**Measured**	**u**	**Model**	**Model-Meas**
197.1	82.91	0.427	0.019	0.385	-0.041	0.083	0.011	0.035	-0.047
207.0	82.86	0.503	0.019	0.473	-0.031	0.083	0.003	0.063	-0.021
217.0	82.55	0.567	0.015	0.574	0.007	0.128	0.022	0.116	-0.012
227.0	82.86	0.646	0.018	0.695	0.049	0.241	0.023	0.268	0.027
237.0	82.92	0.778	0.034	0.874	0.096	0.449	0.043	0.526	0.077

4.3.3. Accounting for holdup

As discussed earlier, adding an equilibrium stage in the distillation model eliminated the need for the empirical shift that has been used to make previous measurements and models agree.[46] It is still reasonable, however, that a small volume adjustment would be necessary based on a physical and temporal delay in the ADCR apparatus, commonly called dynamic holdup. This delay exists between the instant a parcel of vapor leaves the kettle and the time it arrives at the adapter where the vapor is sampled for composition (Figure 4.1). This separation in time and distance implies that the vapor being sampled at the adapter originated from the kettle at a slightly earlier time and therefore a lower temperature. This delay is corrected for by adjusting the model-predicted temperatures corresponding to vapor phase composition. This correction only needs to be applied to the vapor phase.

The magnitude of the dynamic holdup correction depends on the volume of the ADCR glassware and the surface tension, density, and IBT of the fluid. Ferris and Rothamer presented an approach to determining dynamic holdup and calculated the appropriate adjustments for several mixtures; the offsets ranged from 1.4 to 7.2 % DVF.[113] They measured the same 50/50 (mol) C10/C14 mixture used in this work, and the correction they applied to that fluid was 3.6 % DVF.

The dynamic holdup offset is applied to a distillation curve (as in Ferris and Rothamer) in progress. The offset appropriate to a T-y curve is called the static holdup; this value is always less than the dynamic holdup. The amount of fluid held up between the kettle and receiver while a distillation is in progress and material is actively moving through the apparatus (dynamic holdup) is greater than that which remains after a distillation ceases and the intermediating material has time to finish traveling to the receiver (static holdup). The appropriate static and

dynamic holdup offsets were determined by empirically estimating the best fit while ensuring the value was realistic for the physical layout of the apparatus. These were applied to the models represented in Figures 4.4-4.7.

4.4. Conclusion

The phase equilibria for fluid mixtures with many components are not well characterized. Although binary fluids are commonly measured and the data used in the development of mixture models, most of the fluids of interest in real world applications contain many more than two components. One category of such fluids is fuels, which contain hundreds (gasoline) or thousands (diesel fuel) of components. Improving our ability to characterize the VLE of multicomponent fluids is important in part because of the prevalence of headspace analysis methods in forensic science and the need to improve the rigor of this field. The method used here is specifically designed to measure VLE for ignitable liquids at varying degrees of thermal weathering caused by fire in cases of arson, although ADCR could be applied to many fluids outside this category. Arson fire debris analysis is one common application of headspace methods and requires consideration of thermal weathering, which has been previously predicted using the ADC. The ADCR can measure vapor-liquid equilibrium of a multicomponent ignitable liquid across a range of temperatures as that liquid distills away. The resulting data supports the interpretation of arson fire debris headspace measurements, including the relationship between the weathered fire debris and the neat ignitable liquid. The same weathering processes are applicable to the study of the environmental fate of fuels that have contaminated a natural resource.

The advanced distillation curve with reflux (ADCR) metrology can be used to make measurements of vapor-liquid equilibrium and build T-x-y relationships that contribute to the development of models for thermally weathered fuels and their headspace composition. This approach is a modification of the ADC method for measuring a fluid's distillation curve as a function of its composition. The ADCR uses a three-way valve to physically separate the vapor and liquid phases, preserving the fluid's VLE at a desired temperature so that it may be measured. The ADCR method can measure the vapor-liquid equilibrium of fluid mixtures far more complex than the binaries conventionally studied using VLE equilibrium cells, and it dramatically reduces the amount of time required for data collection. This work also introduces the first visual representation of VLE data at multiple state points for a mixture of many components. Representations of this type of data did not preexist this work.

The ADCR method was demonstrated using two simple hydrocarbon mixtures: an *n*-decane/*n*-tetradecane binary and the three-component Huber-Bruno (HB) surrogate. Agreement between models and measurements was very good for both mixtures. More scatter in the vapor composition data was expected and observed in both cases. During this work, it was discovered that distillation models can be improved by adding an equilibrium stage, wherein a parcel of vapor leaving the kettle re-equilibrates at the head temperature. This reflects the fractionation occurring within the apparatus during the distillation and eliminates the need for an incompletely understood empirical factor applied in previous work. Measurements of the HB surrogate also helped optimize the binary interaction parameters used in the model for that mixture.

The ADCR will continue to be used to measure VLE for more complex fluids with the long-term goal of measuring common accelerants like gasoline. These mixtures contain hundreds of components or more, introducing a data analysis challenge. In future work, an initial approach

may be made by choosing a suite of marker compounds in these mixtures for which to measure VLE within the more complex mixture. The availability of good equations of state and mixture models is a limitation to the types and complexity of fluids that can currently be studied using this approach (although ADCR technology can measure any fluid). Such measurements would conversely contribute a great deal to the development and improvement of these models.

The ADCR measurements may also be directly connected with headspace characterization of arson fire debris; the HB surrogate is a logical accelerant for initial testing, because there are good-quality models and ADCR data for it. The VLE data should predict the thermal weathering observed on the debris as well as infer the composition of the condensed phase debris from measurement of the headspace. Experiments like this would explore the utility of ADCR measurements for the interpretation of headspace characterization data.

These proof-of-concept experiments indicate that the ADCR is capable of measuring mixtures of increasing complexity, although of course data analysis will present a challenge with the addition of components. The unavailability of reliable equations of state and mixing parameters for many fluids is a limitation to this work, but a more granular set of measurements (that is, high resolution in the temperature dimension) could circumvent the need for model comparisons as well as contribute to the development of models.

4.5. References

1. National Research Council, *Strengthening Forensic Science in the United States: A Path Forward*. The National Academies Press: Washington, DC, 2009.

9. *ASTM D86, Standard test method for distillation of petroleum products at atmospheric pressure*. ASTM International: West Conshohocken, PA, 2004.

10. Al Ghafri, S. Z., Maitland, G. C., Trusler, J. P. M., Experimental and modeling study of the phase behavior of synthetic crude oil+CO2. *Fluid Phase Equilibria* 2014, *365*, 20-40.

11. Turek, E. A., Metcalfs, R. S., Yarborough, L., Robinson, R. L., Jr., Phase Equilibria in CO2 - Multicomponent Hydrocarbon Systems: Experimental Data and an Improved Prediction Technique. *Society of Petroleum Engineers Journal* 1984, *24* (3).

17. Zhang, C.-Y., Zhang, Q., Zhong, C.-H., Guo, M.-Q., Analysis of volatile compounds responsible for kiwifruit aroma by desiccated headspace gas chromatography–mass spectrometry. *Journal of Chromatography A* 2016, *1440*, 255-259.

31. Lovestead, T. M., Bruno, T. J., Trace headspace sampling for quantitative analysis of explosives with cryoadsorption on short alumina porous layer open tubular columns. *Analytical Chemistry* 2010, *82*, 5621-5627.

34. Lovestead, T. M., Bruno, T. J., Detecting gravesoil with headspace analysis with adsorption on short porous layer open tubular (PLOT) columns. *Forens Sci Int* 2011, *204*, 156-161.

35. Nichols, J. E., Harries, M. E., Lovestead, T. M., Bruno, T. J., Analysis of arson fire debris by low temperature dynamic headspace adsorption porous layer open tubular columns. *Journal of Chromatography A* 2014, *1334*, 126-138.

36. Lovestead, T. M., Bruno, T. J., Detection of poultry spoilage markers from headspace analysis with cryoadsorption on a short alumina PLOT column. *Food Chem* 2010, *121*, 1274-1282.

40. Bruno, T. J., Smith, B. L., Enthalpy of combustion of fuels as a function of distillate cut: application of an advanced distillation curve method. *Energy & Fuels* 2006, *20*, 2109-2116.

41. Smith, B. L., Bruno, T.J., Advanced distillation curve measurement with a model predictive temperature controller. *Int J Thermophys* 2006, *27*, 1419-1434.

42. Ott, L. S., Bruno, T.J., Corrosivity of fluids as a function of distillate cut: application of an advanced distillation curve method. *Energy & Fuels* 2007, *21*, 2778 - 2784.

43. Ott, L. S., Smith, B.L., Bruno, T.J., Advanced distillation curve measurement: application to a bio-derived crude oil prepared from swine manure. *Fuel* 2008, *87*, 3379-3387.

44. Lovestead, T. M., Bruno, T.J., Application of the advanced distillation curve method to aviation fuel avgas 100LL. *Energy & Fuels* 2009, *23*, 2176-2183.

45. Bruno, T. J., Ott, L.S., Smith, B.L., Lovestead, T.M., Complex fluid analysis with the advanced distillation curve approach. *Analytical Chemistry* 2010, *82*, 777-783.

46. Huber, M. L., Smith, B.L., Ott, L.S., Bruno, T.J., Surrogate mixture model for the thermophysical properties of synthetic aviation fuel S-8: Explicit application of the advanced distillation curve. *Energy & Fuels* 2008, *22*, 1104 - 1114.

48. Hsieh, P. Y., Bruno, T. J., Pressure-controlled advanced distillation curve analysis and rotational viscometry of swine manure pyrolysis oil. *Fuel* 2014, *132*, 1-6.

53. Smith, B. L., Bruno, T.J., Improvements in the measurement of distillation curves - part 3: Application to gasoline and gasoline + methanol mixtures. *Ind Eng Chem Res* 2007, *46*, 297-309.

54. Ott, L. S., Smith, B.L., Bruno, T.J., Experimental test of the Sydney Young equation for the presentation of distillation curves. *J Chem Thermodynam* 2008, *40*, 1352-1357.

55. Young, S., Correction of boiling points of liquids from observed to normal pressures. *Proc Chem Soc* 1902, *81*, 777.

56. Bruno, T. J., Wolk, A., Naydich, A., Composition-explicit distillation curves for mixtures of gasoline and diesel fuel with gamma-valerolactone. *Energy & Fuels* 2010, *24* (4), 2758-2767.

62. Burger, J. L., Gough, R. V., Bruno, T. J., Characterization of dieseline with the advanced distillation curve method: hydrocarbon classification and enthalpy of combustion. *Energy & Fuels* 2013, *27*, 878 - 795.

63. Windom, B. C., Lovestead, T.M., Bruno, T.J., Application of the advanced distillation curve method to the development of unleaded aviation gasoline. *Energy & Fuels* 2010, *24*, 3275 - 3284.

68. Bruno, T. J., Smith, B.L., Evaluation of the physicochemical authenticity of aviation kerosene surrogate mixtures Part I: Analysis of volatility with the advanced distillation curve *Energy & Fuels* 2010, *24*, 4266-4276.

69. Bruno, T. J., Huber, M.L., Evaluation of the physicochemical authenticity of aviation kerosene surrogate mixtures Part II: Analysis and prediction of thermophysical properties. *Energy & Fuels* 2010, *24*, 4277-4284.

72. Smith, B. L., Bruno, T.J., Improvements in the measurement of distillation curves - part 4: Application to the aviation turbine fuel Jet-A. *Ind Eng Chem Res* 2007, *46*, 310-320.

74. Bruno, T. J., Wolk, A., Naydich, A., Stabilization of biodiesel fuel at elevated temperature with hydrogen donors: evaluation with the advanced distillation curve method. *Energy & Fuels* 2009, *23*, 1015-1023.

76. Burger, J. L., Widegren, J. A., Lovestead, T., M., Bruno, T. J., 1H and 13C NMR analysis of gas turbine fuels as applied to the advanced distillation curve method. *Energy & Fuels* 2015, *29* (8), 4874-4885.

83. Bruno, T. J., Smith, B.L., Improvements in the measurement of distillation curves - part 2: Application to aerospace/aviation fuels RP-1 and S-8. *Ind Eng Chem Res* 2006, *45*, 4381-4388.

84. Bruno, T. J., Improvements in the measurement of distillation curves - part 1: A composition-explicit approach. *Ind Eng Chem Res* 2006, *45*, 4371-4380.

85. Burger, J. L., Gough, R. V., Lovestead, T., M., Bruno, T. J., Characterization of the effects of cetane number improvers on diesel fuel volatility by use of the advanced distillation curve method. *Energy & Fuels* 2014, *24*, 2437-2445.

88. Ott, L. S., Smith, B.L., Bruno, T.J., Advanced distillation curve measurements for corrosive fluids: application to two crude oils. *Fuel* 2008, *87*, 3055-3064.

89. Young, S., *Fractional distillation*. Macmillan and Co., Ltd.: London, 1903.

92. Hsieh, P. Y., Bruno, T. J., Measuring sulfur content and corrosivity of North American petroleum with the advanced distillation curve method. *Energy & Fuels* 2014, *28*, 1868-1883.

96. Outcalt, S. L., Lee, B.-C., A small-volume apparatus for the measurement of phase equilibria. *J Res Natl Inst Stand Technol* 2004, *109*, 525-531.

97. Mansfield, E., Bell, I. H., Outcalt, S. L., Bubble-point measurements of n-propane + n-decane binary mixtures with comparisons of binary mixture interaction parameters for linear alkanes. *J Chem Eng Data* 2016, *61*, 2573-2579.

98. Dejoz, A., González-Alfaro, V., Miguel, P. J., Vázquez, M. I., Isobaric Vapor−Liquid Equilibria for Binary Systems Composed of Octane, Decane, and Dodecane at 20 kPa. *Journal of Chemical & Engineering Data* 1996, *41* (1), 93-96.

99. Ma, X.-B., Liu, X.-G., Li, Z.-H., Xu, G.-H., Vapor–liquid equilibria for the ternary system methanol + dimethyl carbonate + dimethyl oxalate and constituent binary systems at different temperatures. *Fluid Phase Equilibria* 2004, *221* (1), 51-56.

100. Outcalt, S. L., Lemmon, E. W., Bubble-point measurements of eight binary mixtures for organic Rankine cycle applications. *Journal of Chemical & Engineering Data* 2013, *58* (6), 1853-1860.

101. Muhammad, F., Oliveira, M. B., Pignat, P., Jaubert, J.-N., Pinho, S. P., Coniglio, L., Phase equilibrium data and modeling of ethylic biodiesel, with application to a non-edible vegetable oil. *Fuel* 2017, *203*, 633-641.

102. Matthews, M. A., Li, F., Towler, B. F., Bell, D. A., Vapor liquid equilibrium measurements with semi-continuous mixtures. *Fluid Phase Equilibria* 1995, *111*, 101-111.

103. Angelos, C. P., Bhagwat, S.V., Matthews, M.A., Measurement and modeling of phase equilibria with synthetic multicomponent mixtures. *Fluid Phase Equilibria* 1992, *72*, 182-209.

104. Li, H., Jakobsen, J. P., Wilhelmsen, Ø., Yan, J., PVTxy properties of CO2 mixtures relevant for CO2 capture, transport and storage: Review of available experimental data and theoretical models. *Applied Energy* 2011, *88* (11), 3567-3579.

105. Ioffe, B. V., Vittenburg, A.G., Manatov, I.A., *Head-Space Analysis and Related Methods in Gas Chromatography*. Wiley-Interscience: 1984.

106. Ghasemi, E., Sillanpaa, M., Optimization of headspace solid phase microextraction based on nano-structured ZnO combined with gas chromatography-mass spectrometry for preconcentration and determination of ultra-traces of chlorobenzenes in environmental samples. *Talanta* 2014, *130*, 322-327.

107. Higashikawa, F. S., Cayuela, M. L., Roig, A., Silva, C. A., Sánchez-Monedero, M. A., Matrix effect on the performance of headspace solid phase microextraction method for the analysis of target volatile organic compounds (VOCs) in environmental samples. *Chemosphere* 2013, *93* (10), 2311-2318.

108. Lorenzo, N., Wan, T., Harper, R. J., Hsu, Y.-L., Chow, M., Rose, S., Furton, K. G., Laboratory and field experiments used to identify Canis lupus var. familiaris active odor signature chemicals from drugs, explosives, and humans. *Analytical and Bioanalytical Chemistry* 2003, *376* (8), 1212-1224.

109. National Center for Forensic Science University of Central Florida, Ignitable Liquids Reference Collection Database. http://ilrc.ucf.edu/.

110. Birks, H. L., Cochran, A. R., Williams, T. J., Jackson, G., The surprising effect of temperature on the weathering of gasoline. *Forensic Chemistry* 2017, *4*, 32-40.

111. Martín-Alberca, C., Ortega-Ojeda, F., García-Ruiz, C., *Analytical tools for the analysis of fire debris. A review: 2008-2015*, Vol. 928, 2016.

112. Baerncopf, J. M., McGuffin, V. L., Smith, R. W., Association of ignitable liquid residues to neat ignitable liquids in the presence of matrix interferences using chemometric procedures. *Journal of Forensic Sciences* 2011, *56* (1), 70-81.

113. Ferris, A. M., Rothamer, D. A., Methodology for the experimental measurement of vapor–liquid equilibrium distillation curves using a modified ASTM D86 setup. *Fuel* 2016, *182*, 467-479.

114. Windom, B. C., Bruno, T.J., Improvements in the measurement of distillation curves-part 5: Reduced pressure distillation curve method. *Ind Eng Chem Res* 2011, *50*, 1115-1126.

115. Anitescu, G., Bruno, T. J., Biodiesel fuels from supercritical fluid processing: quality evaluation with the advanced distillation curve method and cetane numbers. *Energy & Fuels* 2012, *26*, 5256-5264.

116. Burger, J., Harries, M., Bruno, T. J., Characterization of four diesel fuel surrogates by the advanced distillation curve method. *Energy & Fuels* 2016, *30* (4), 2813–2820.

117. Burger, J. L., Bruno, T. J., Application of the advanced distillation curve method to the variability of jet fuels. *Energy & Fuels* 2012, *26*, 3661-3671.

118. Hsieh, P. Y., Abel, K., Bruno, T. J., Analysis of marine diesel fuel with the advanced distillation curve method. *Energy & Fuels* 2013, *27*, 804-810.

119. Lovestead, T. M., Windom, B.C., Riggs, J.R., Nickell, C, Bruno, T.J., Assessment of the compositional variability of RP-1 and RP-2 with the advanced distillation curve approach. *Energy & Fuels* 2010, *24*, 5611-5623.

120. Windom, B. C., Bruno, T. J., Application of pressure-controlled advanced distillation curve analysis: virgin and waste oils. *Ind Eng Chem Res* 2013, *52*, 327-337.

121. Bruno, T. J., Allen, S., Weathering patterns of ignitable liquids with the advanced distillation curve method. *J Res Nat Inst Stds Tech (US)* 2012, *117*, 29-51.

122. Bruno, T. J., Lovestead, T. M., Huber, M. L., Prediction and preliminary standardization of fire debris analysis constituents with the advanced distillation curve method. *J Forensic Sci* 2011, *56*, S191 - S202.

123. Bruno, T. J., Ott, L.S., Lovestead, T.M., Huber, M.L., Relating complex fluid composition and thermophysical properties with the advanced distillation curve approach. *Chemical Eng Tech* 2010, *33* (3), 363-376.

124. Bruno, T. J., Abel, K., Riggs, J. R., Comparison of JP-8 and JP-8+100 with the advanced distillation curve approach. *Energy & Fuels* 2012, *26*, 5843 - 5850.

125. Burger, J. L., Schneider, N., Bruno, T. J., Application of the advanced distillation curve method to fuels for advanced combustion gasoline engines. *Energy & Fuels* 2015, *29*, 4227 - 4235.

126. Harries, M., Sharma, B. K., Bruno, T. J., Application of the advanced distillation curve method for the characterization of two alternative transportation fuels prepared from the pyrolysis of polyethylene bags. *Energy & Fuels* 2016, *30*, 9671-9678.

127. Lovestead, T. M., Bruno, T.J., Comparison of the hypersonic vehicle fuel JP-7 to the rocket propellants RP-1 and RP-2 with the advanced distillation curve method. *Energy & Fuels* 2009, *23* (7), 3637-3644.

128. Lovestead, T. M., Windom, B.C., Bruno, T.J., Investigating the unique properties of Cuphea derived biodiesel fuel with the advanced distillation curve method. *Energy & Fuels* 2010, *24*, 3665-3675.

129. Windom, B. C., Bruno, T. J., Pressure controlled advanced distillation curve analysis of biodiesel fuels: assessment of thermal decomposition. *Energy & Fuels* 2012, *26*, 2407 - 2415.

130. Lemmon, E. W., McLinden, M.O., Huber, M.L., REFPROP, Reference fluid thermodynamic and transport properties, NIST Standard Reference Database 23, V9.1. National Institute of Standards and Technology, Gaithersburg, MD: 2013.

131. Huber, M. L., Lemmon, E.W., Bruno, T.J., Surrogate mixture models for the thermophysical properties of aviation fuel Jet-A. *Energy & Fuels* 2010, *24*, 3565-3571.

132. Mueller, C. J., Cannella, W. J., Bays, J. T., Bruno, T. J., DeFabio, K., Dettman, H. D., Gieleciak, R. M., Huber, M. L., Kweon, C.-B., McConnell, S. S., Pitz, W. J., Ratcliff, M. A., Diesel surrogate fuels for engine testing and chemical-kinetic modeling: Compositions and properties. *Energy & Fuels* 2016, *30* (2), 1445-1461.

133. Kunz, O., Klimeck, R., Wagner, W., Jaesche, M., The GERG-2004 Wide-Range Reference Equation of State for Natural Gases and Other Mixtures; GERG Technical Monograph Fortschr.-Ber. VDI; VDI-Verlag:Dusseldorf, Germany. 2007.

134. Lemmon, E. W., Jacobsen, J. T., A generalized thermodynamic model for the thermodynamic properties of mixtures. *Int J Thermophys* 1999, *20* (3), 825-835.

135. Peng, D.-Y., Robinson, D. B., A new two-constant equation of state. *Ind Eng Chem Fundam* 1976, *15* (1), 59-64.

136. Personal communication to M. Harries from M.L. Huber, NIST, Boulder, CO. 2016.

137. Lemmon, E. W., McLinden, M. O., *Method for estimating mixture equation of state parameters*. Proc Thermophysical Properties and Transfer Processes of New Refrigerants Conference, Paderborn, Germany, International Institute of Refrigeration: Paderborn, Germany, 2001; pp 23-30.

138. Young, S., *Distillation principles and processes*. Macmillan and Co., Ltd.: London, 1922.

139. Organisation for Economic Co-operation and Development, *OECD Guideline for the testing of chemicals, No. 103, boiling point*. Paris, France, 1995.

Chapter 5: Field Portable Low Temperature Porous Layer Open Tubular Cryoadsorption Headspace Sampling and Analysis: Applications

Reprinted from Harries, M., Bukovsky-Reyes, S., Bruno, T. J. Field Portable Low Temperature Porous Layer Open Tubular Cryoadsorption Headspace Sampling and Analysis Part II: Applications. J. Chromatogr. A. *1429, 72-78. 2015. doi: 10.1016/j.chroma.2015.12.014.*

5.1. Introduction

This chapter is reprinted from Part II of a two-part series on field portable porous layer open tubular cryoadsorption (PLOT-cryo). Part I describes the apparatus and sampling method.[37] We anticipate the utility of the field portable approach in a multitude of applications, for example, environmental and criminalistic sampling situations. This might include sampling pollution due to illegal dumping, leaks in fracking wells and service tanks, the location of clandestine graves, the detection of food spoilage, and arson fire debris investigation. In previous work, we have applied the laboratory-based PLOT-cryo approach to several of these applications.[31, 34-36]

The field portable method and apparatus was applied to the vapor analysis of coumarin, 2,4,6-trinitrotoluene (2-methyl-1,3,5-trinitrobenzene, TNT), aviation turbine fuel, and naphthalene. These samples are four of the benchmark analytes used in previous work to evaluate the performance of PLOT-cryo.[37, 80] Use of these compounds and mixtures, the behavior of which in the vapor phase is well understood, enabled us to test the portable apparatus with a variety of test beds and matrices and to compare the results to those previously obtained with the laboratory-based PLOT-cryo approach.

Finally, we explored the sensitivity limits of the portable PLOT-cryo unit when applied to diesel fuel, a complex mixture of common concern for environmental reasons. This was done on two matrices: glass beads and soil.

5.2. Methods and results

For context and clarity, the experimental details are combined with the results in the following sections.

5.2.1. Materials

For all analyses presented in this paper, we used PLOT capillary wafers comprised of single or multiple alumina coated PLOT capillaries for vapor collection. During each experiment, the capillary wafer was cooled during vapor collection and heated during elution. The test beds were sampled at ambient room temperature. The borosilicate glass beads were obtained from a commercial supplier, and were typical chromatographic glass beads. For the work on coumarin and TNT, nominal 1 mm beads were used (which measured 1.2 ± 0.05 mm). For the work on diesel fuel, a 50/50 (vol/vol) mixture of 1- and 2 mm nominal beads were used. The 1 mm nominal beads were of the same diameter as those used for the coumarin and TNT; the 2 mm nominal beads measured 1.8 ± 0.2 mm. The soil used in the work on diesel fuel was clay soil collected locally on the NIST Boulder campus and air-dried in our lab for three years. The soil was then size-selected for particles between 1.7 and 2.0 mm in diameter using standard testing sieves (nominal grating numbers 10 and 12). This prepared soil was then used in the manner described in Section 5.2.4. The specifics on each solute will be presented later in the discussion of the results.

Spectroscopic-grade acetone was used as the solvent for all capillary elutions. The acetone was analyzed in our lab using established GC-MS protocols.[57] We chose this solvent because it is an effective eluent when paired with alumina coated capillaries, and for the safety of the researchers, especially student workers. The capillaries were eluted with acetone into crimp-cap autosampler vials and analyzed using gas chromatography coupled with either single-quadrupole mass spectrometry (GC-MS) or tandem quadrupole - time of flight mass spectrometry (GC-QTOF) operated in single MS mode with high mass resolution.

5.2.2. Initial studies: Coumarin and TNT

As with the laboratory implementation of PLOT-cryo, the first demonstrations of the field portable PLOT-cryo vapor sampling apparatus were done with coumarin dispersed on glass beads and TNT dispersed on glass beads.[80] The sample test beds for these solutes were 20 mL scintillation vials equipped with plastic caps, into which two small holes (an inlet and an outlet, both of which were 3.2 mm, 0.125 in) were drilled. Such test beds have been used and described previously.[80] In this work, approximately 50 mg of solid coumarin and solid TNT were solvent dispersed (in acetone) separately on approximately 5 g of 2 mm glass beads. Subsequent to deposition, the solvent was slowly evaporated in a vacuum desiccator. The vapor collection from the vials of these compounds was done with the field portable PLOT-cryo apparatus described fully in Part I.[56] Multiple experiments were conducted to demonstrate both the hand piece and the standoff module and probe, in combination with both the single and multiple capillary wafers. For a typical test, vapor collection proceeded for 3 minutes with the sample at laboratory ambient temperature (23 ± 1 °C), while the PLOT capillary was chilled to -20 ± 5 ºC. Chilling was done with the cold air vortex tube on the portable apparatus. Following solute collection, the PLOT wafers were then heated to 80 ± 5 ºC with the hot air vortex tube. Once warmed, the wafer

was eluted with 1.5 mL of acetone for each vapor collection trial, and the resulting solutions were analyzed by gas chromatography with (single quadrupole) mass spectrometry (GC-MS).

For coumarin, the following GC-MS method was used: 30 m, 5 percent phenyl polydimethylsiloxane column, coating thickness of 0.1 μm; splitless injection via automatic sampler, temperature of injector = 325 °C at 55 kPa (8 psi) constant head pressure; injection volume = 3 μL, column temperature of 55 °C for 0.75 min, followed by a temperature program at 99 °C/min to 80 °C, then 35 °C/min to 275 °C; scan m/z from 35 to 350, SIM m/z = 89, 90, 118, 146. For TNT, the following method was used with the same column: splitless injection via automatic sampler, temperature of injector = 275 °C at 83 kPa (12 psi) head pressure; injection volume = 3 μL, column temperature of 60 °C for 1 min, followed by a temperature program at 80 °C/min to 170 °C, then 35 °C/min to 290 °C; scan m/z from 35 to 550, SIM m/z = 89, 134, 180, 210.[57, 140] The scan mode allows more facile library matching for identification (where the libraries themselves contain scan-mode data), while the SIM mode is more sensitive and especially useful for a definitive go or no-go that the compound was detected in the vapor.

All the experiments were successful in identifying the target compounds with the single and multiple capillary wafers, in the standoff module and with the handpiece; for brevity we will discuss the results obtained using a multiple capillary wafer and the standoff module. Typical sample chromatograms are provided in Figure 5.1(a-d). The target analyte was easily detected with excellent signal-to-noise ratios in both scan and SIM modes. The recovery obtained by use of the multiple capillary wafer and the standoff probe was as good as that achieved in the laboratory. Earlier, for example, we determined that we could detect and quantitate TNT in the vapor above a substrate with 0.064 μg/g TNT (repeatability of 10% COV) on the glass bead matrix.[31] The major differences in this work (as reflected in Figure 5.1(a-d)) as compared with

the earlier laboratory work (also done with vials as the test beds) are the collection speeds and the fact that all collections are done with the sample at ambient temperature. The much higher flow rate (with no loss of surface contact) provided by the multiple capillary wafer makes faster collection possible. This is in sharp contrast with the early laboratory work in which the coumarin samples were collected at 1 mL/min for 60 min at a sample temperature of 110 °C, and TNT was collected at 1 mL/min for 120 min at a sample temperature of 125 °C. Furthermore, the collection of TNT vapor was conducted at near ambient temperature (30 °C); in the previous work, collection at this temperature at 1 mL/min required 4000 min (nearly 3 days) with a single capillary.[141] The long collection times required in the earlier measurements caused the decomposition and discoloration of the dispersed TNT. Discoloration is nearly always noted with this solute when it is exposed for sampling for more than a few minutes. No such discoloration was noted in this work; the vapor collection was completed rapidly enough to avoid this commonly observed color change.

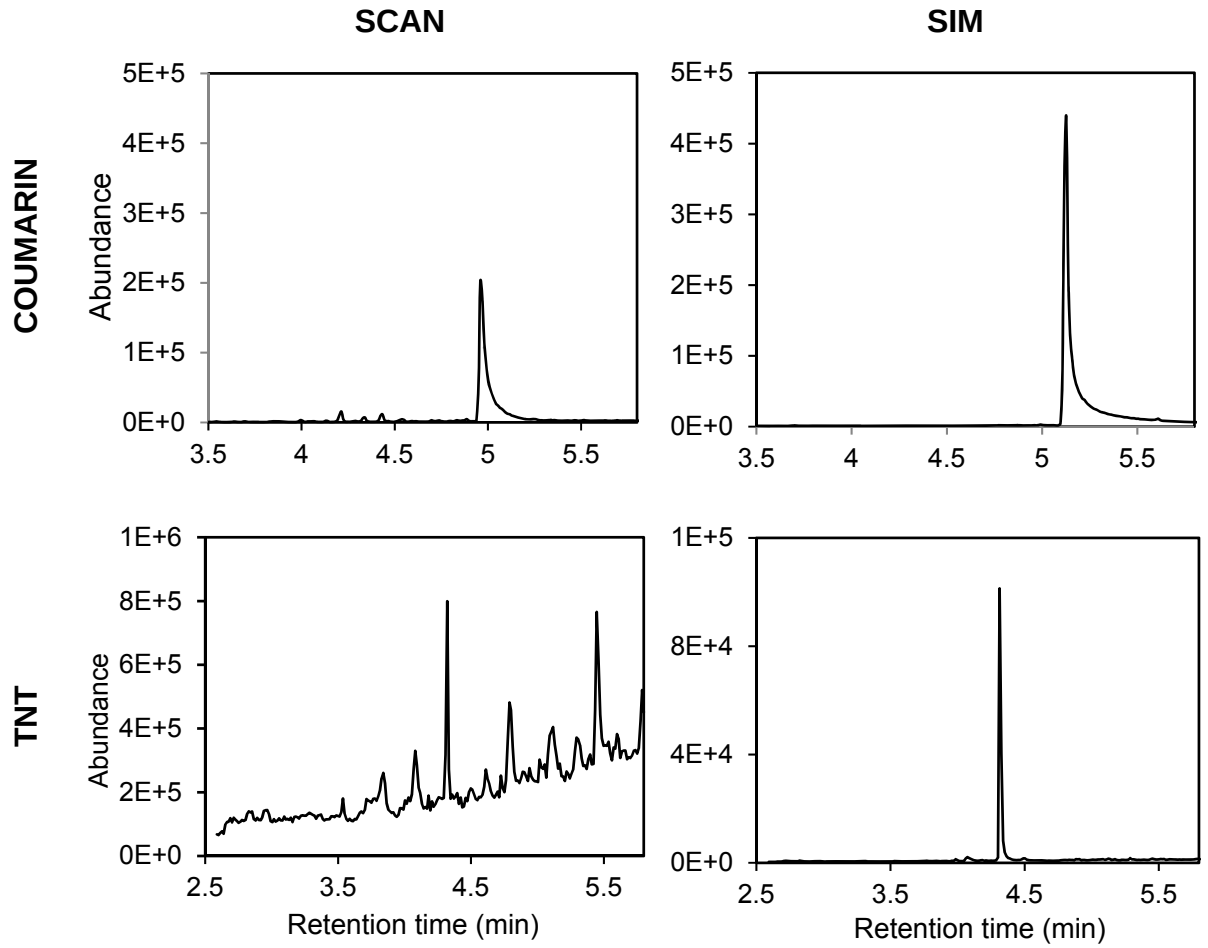

Figure 5.1. Gas chromatograms showing typical analyses for vapor samples collected by use of the multiple capillary wafer from solutes dispersed on glass beads in scintillation vials, collected for 3 min. Panel (a) is for coumarin in scan mode, panel (b) is for coumarin in SIM mode; panel (c) is for TNT in scan mode and panel (d) is for TNT in SIM mode. Conditions are described in the text. The abundance is presented in arbitrary units.

5.2.3. Aviation turbine kerosene

Because the multiple capillary wafer is especially suited for larger sample volumes, 118 mL (4 oz) paint cans were also used as test beds. These provided samples of a larger size to better simulate field conditions. As with the vials, two small holes (an inlet and an outlet, both of which were 3.2 mm, 0.125 in) were drilled in the lid of the paint cans. The solutes tested with this approach have included aviation turbine kerosene (JP-5, a specially formulated low volatility gas turbine kerosene used extensively on aircraft carriers), crude oil and a selection of natural

essential oils. In each case, one drop of fluid was placed in the paint can, and the lid affixed. After about 1 hour of equilibration time, the standoff probe was inserted into one of the holes, and vapor was collected for 30 s by use of the multiple capillary wafer. Collection was done with the sample at laboratory ambient temperature (23 ± 1 °C), while the capillary wafer was chilled to -20 ± 5 ºC. The PLOT wafer was then heated to 80 ± 5 ºC and eluted with 1.5 mL of acetone for each vapor collection trial. For brevity in this article, only the results for JP-5 are presented. JP-5 is a well-characterized fuel, the vapor phase of which was previously studied using the advanced distillation curve method.[117]

For JP-5, the following GC-MS method was used to analyze the eluted sample: 30 m, 5 percent phenyl polydimethylsiloxane column with a coating thickness of 0.1 μm; splitless injection via automatic sampler, temperature of injector = 325 °C at 83 kPa (12 psi) head pressure, injection volume = 2 μL, column temperature of 50 °C for 2 min, followed by temperature program at 10 °C/min to 150 °C, then 60 °C/min to 325 °C; hold for 1 min; scan m/z from 15 to 550, SIM m/z = 51, 55, 56, 57, 65, 71, 77, 84, 85, 91, 96, 99, 105, 106, 109, 112, 113, 114, 115, 116, 117, 118, 119, 121, 124, 128, 131, 142, 156, 169, 183, 198, 212, 226, and 240. The large number of ions used for the kerosene reflects the very complex chromatogram typically obtained for such fluids. The chromatograms are shown in Figure 5.2a-b. While the SIM chromatogram is simpler, the use of fewer ions spread over the m/z range does not provide a sensitivity enhancement; however, the noise is reduced. The chromatogram of the collected headspace allows a reliable identification of the sample on the basis of the composition. Indeed, it is possible to readily distinguish the sample as a relatively low volatility aviation turbine kerosene from the chromatogram by comparison with known samples.[117]

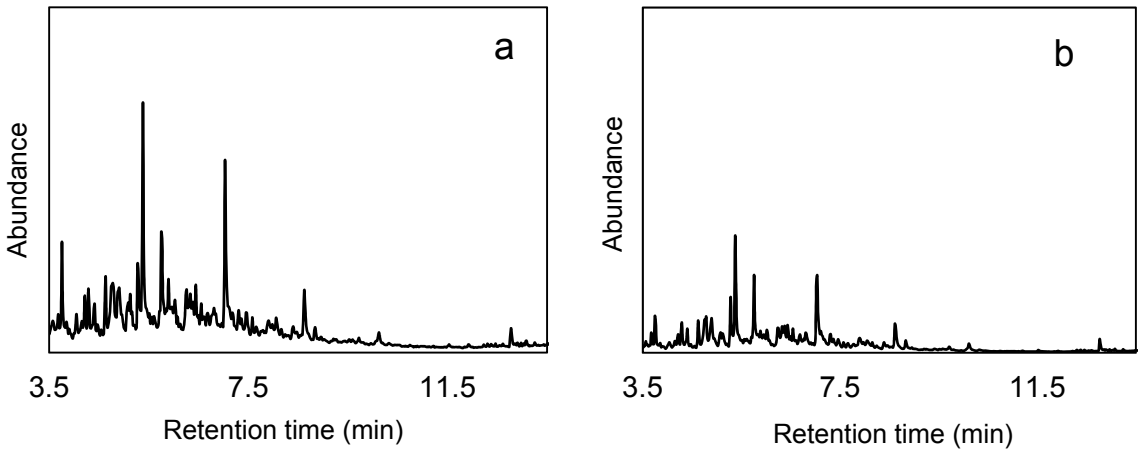

Figure 5.2. Gas chromatograms showing typical analyses for vapor samples produced at ambient temperature from one drop of JP-5 (low volatility gas turbine kerosene) in a 118 mL (4 oz) paint can, collected for 30 s. Panel (a) shows results from scan mode, panel (b) shows results from SIM. Conditions are described in the text.

5.2.4. Naphthalene

The utility of the multiple capillary wafer in rapid sampling for solutes dispersed in even larger volumes was illustrated by use of a solute diffuser (similar to a scent or odorant diffuser) to distribute solute in a closed environment or chamber. The solute diffuser was made from one of the aforementioned 118 mL cans, prepared by drilling a circular pattern of 0.3175 cm (0.125 in) holes in the lid. Then 50 mg of naphthalene was placed into the can and the lid firmly affixed. This can was placed in a hard sided valise (40 X 20 X 20 cm, 16 X 8 X 8 in) into the side of which a small hole was drilled. The diffuser was allowed to equilibrate inside the valise for 4 h at ambient temperature (23 °C with a variation of 1 °C). One can approximate the concentration of naphthalene in the vapor phase in the valise based on the partial pressure of naphthalene. Assuming that air and naphthalene behave as ideal gases, at equilibrium approximately 9.5 X 10^{-5} mol of vapor will be present, resulting in a concentration of 0.07 % (mass/mass). Note that this is an upper bound subject to the efficiency of the solute diffuser; the actual concentration is likely lower due to incomplete equilibration, which was not measured in this work. The vapor

inside of the valise was then sampled by use of the standoff probe and multiple capillary wafer that was chilled to -10 ± 5 ºC. In these tests, sampling was allowed to proceed for 3 s. The wafers were then heated to 60 ± 5 ºC and eluted with 1.5 mL of acetone.

The eluted naphthalene sample was analyzed by mass spectrometry with the following method: 30 m, 5 percent phenyl polydimethylsiloxane column with a coating thickness of 0.1 μm; splitless injection via automatic sampler, temperature of injector = 275 °C at 83 kPa (12 psi) head pressure, injection volume = 1 μL, column temperature of 50 °C for 2 min, followed by temperature program at 60 °C/min to 100 °C, then 20 °C/min to 175 °C; hold for 1 min; scan m/z from 33 to 330, SIM m/z = 125. The chromatogram measured in scan mode is provided in Figure 5.3a, while the SIM is provided in 5.3b. In both chromatograms, the naphthalene elutes at approximately 6 min. In scan mode, the mass spectrum allows easy identification via a library search (although the early part of the chromatogram shows the noise of an incompletely cleaned multiple capillary wafer). The SIM trace is striking in that it shows an intense peak in response to the target compound; the fact that it is the result of only a 3 s collection demonstrates the practical utility of the multiple capillary wafer. Indeed, even shorter sampling times are possible for field applications. We do not report shorter collection times here because of difficulty in measuring such shorter collection times reliably. The ability to rapidly sample the vapor and efficiently desorb solute for analysis makes the approach well suited to sampling large volumes.

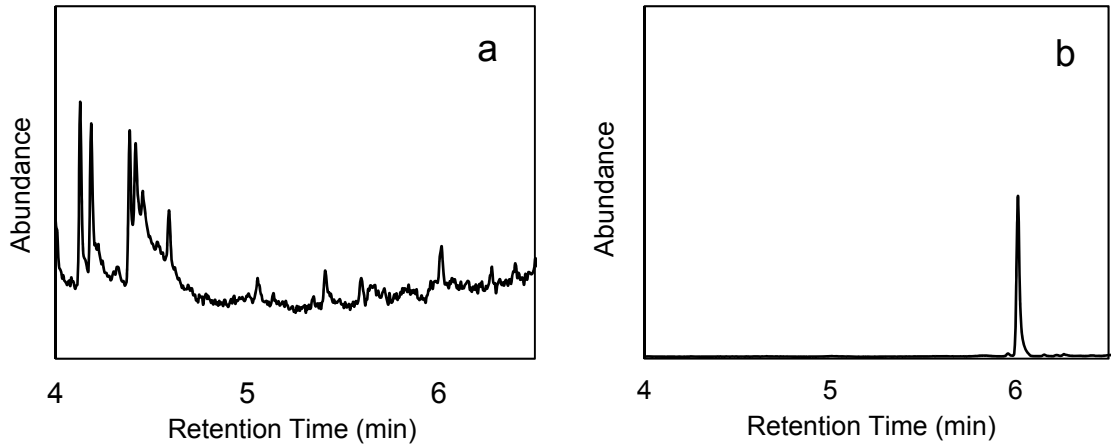

Figure 5.3. Gas chromatograms showing analyses for vapor samples of 50 mg naphthalene produced inside of a diffuser that was placed in a small valise. Panel (a) shows results from scan mode, and panel (b) shows results from SIM. Naphthalene's retention time is about 6 minutes. Vertical scale is the same to indicate the success of SIM in isolating the peak.

5.2.5. Diesel fuel on soil

For this demonstration of one environmental application of the field portable apparatus, a typical diesel fuel was spiked onto clay soil described in Section 5.2.1. The diesel fuel was a commercial winter-grade, low-wax, ultralow-sulfur formulation that was refined from petroleum of the Denver-Julesburg field, and incorporated with a red dye indicating off road use. This lower-aromatic fuel typically has a cetane number between 51 and 52. This fluid was stored at 7 ^{o}C to preserve any volatile components, and no phase separation was observed. The fluid was chosen in part because it has been well-characterized in previous work.[65] One drop of this diesel fuel was dissolved in a scintillation vial of acetone. In the 118 mL paint can test bed, we prepared clay soil mixtures spiked with the diesel fuel/acetone mixture to obtain samples with concentrations 40 ppm, 8.7 ppm, and 4 ppm (mass/mass). To obtain the lower-concentration samples, we serially diluted the appropriate mass of spiked soil into clean soil. Samples were mixed well in gas-tight earthen jars on a rolling mill for 1 hour.

The vapor collection from the cans was done using the portable unit's standoff module. We modified the paint can test bed by addition of a wire mesh screen, attached to the lid of the can on the inside of the can. This shielded the standoff probe from direct contact with the soil, as this would contaminate the vapor analysis. The sample collection temperature was ambient (22 ± 3 ^{o}C). The multiple capillary wafer was cooled and maintained at -10 ± 5 ^{o}C during collection. Collection was allowed to proceed for 10 minutes; subsequently the wafer was heated (to 60 ± 5 ^{o}C) and eluted with 1.5 mL acetone.

Analysis of the eluted samples was done by GC-MS as described earlier. The following program was used: 30 m, 5 percent phenyl methyl siloxane column with a coating thickness of 0.25 μm; splitless injection via automatic sampler; temperature of injector = 325 °C at 10 psi head pressure; injection volume = 3 μL, column temperature of 33 °C for 1 min, followed by temperature program at 70 °C/min to 80 °C, then 35 °C/min to 170 °C; hold for 2 min; SIM m/z = 41, 42, 43, 44, 53, 55, 56, 57, 58, 67, 69, 70, 71, 81, 82, 83, 84, 85, 97, 98, 99, 113, and 142. Diesel fuel contains hundreds of components, and during early experiments, we identified one high-abundance component in the vapor phase, *n*-decane, that could serve as a sentinel compound indicating the presence of diesel fuel on soil. An example chromatogram measured in SIM mode is provided in Figure 5.4.

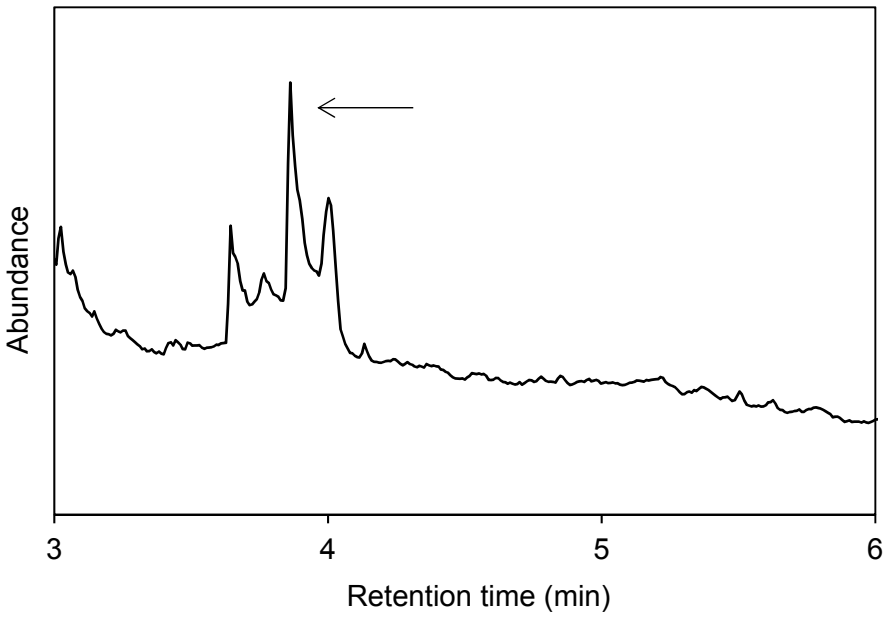

Figure 5.4. A sample chromatogram in SIM mode showing the results of sampling a paint can containing a 4 ppm mixture of diesel fuel and clay soil. An arrow points to the n-decane peak (RT = 3.9 min). Conditions are described in the text.

Increasingly dilute preparations of diesel fuel on soil were analyzed until the detection limit, 4 ppm (mass/mass), was determined by assessment of the n-decane signal relative to noise. We selected a minimum acceptable signal-to-noise ratio of 3:1.

This analysis was challenging because of the high degree of complexity in the diesel fuel mixture. Even utilizing SIM mode, the ions of interest for *n*-decane were shared by other hydrocarbon compounds that neighbored or co-eluted with the *n*-decane peak. We identified the unit-mass resolution of the single quadrupole MS as a limitation in this work. In the following section, we apply an accepted detection limit determination method using the more sensitive QTOF mass spectrometer.

5.2.6. Sensitivity assessment: Diesel fuel on glass beads

It was of interest to us to determine at what level the portable apparatus is effective at detecting a typical analyte when GC-MS was used. We used the EPA standard, Appendix B to Part 136, Definition and Procedure for the Determination of the Method Detection Limit, for the determination of the method detection limit.[142] This guidance was developed specifically to be sensitive to matrix, instrument, and analyst effects, and captures the uncertainty inherent in sample collection, processing, and analysis. We chose the EPA standard because it enabled us to include the real-world sources of variability inherent with this type of portable method applied to complex mixtures. In the guideline, the method detection limit (MDL) is calculated in terms of signal units (in our case, area counts under the mass spectral peak) by multiplying the sample standard deviation (s) of at least seven samples of the same concentration and preparation(s) by the Student's t-value for the corresponding degrees of freedom (t_{n-1}) and desired confidence level (α). We selected alpha = 0.05 for this calculation.

$$MDL = s * t_{n-1, 0.05}$$

For this assessment of its sensitivity, we selected diesel fuel on glass beads as the test analyte. We chose a spike level of 1 ppm (mass/mass) diesel fuel for our replicate preparation based on preliminary experiments exploring the method's sensitivity at varying levels. We employed a laboratory preparation using the same diesel fuel described in Section 5.2.5; however, in these experiments this fluid was spiked onto a matrix of a 50/50 (vol/vol) mixture of 1 and 2 mm (nominal) borosilicate glass beads in the 118 mL paint can test bed. Preparations of the diesel fuel and glass beads (1 ppm by mass) were prepared in clean paint cans by serial dilution. Higher concentration samples were prepared (40 ± 10 ppm) by placing drops of diesel fuel into cans filled with glass beads (270 ± 30 g). The lids were affixed, and the sealed cans

were mixed on a rolling mill for 45 minutes to ensure thorough distribution of the solute. Solvent dispersion was not used in these experiments. Subsequently, sixteen replicate mixtures (1 ± 0.0365 ppm) were prepared by placing the appropriate amounts (20 ± 10 g) of the higher-concentration spiked samples into additional cans with clean glass beads (260 ± 30 g) to achieve the desired final concentration. The cans were sealed and mixed as above and sampled using the field portable apparatus the same day.

The vapor collection from each can was carried out at ambient temperature using the standoff module with the wafer cooled to -10 °C (± 5 °C). Collection was allowed to proceed for 10 minutes for these tests. This is longer than what might be desirable for field use; however, we chose this sampling time as a benchmark of optimized performance. After vapor collection, the wafer was then heated to 60 °C (± 5 °C) and eluted with 1.5 mL acetone.

Contamination is a concern whenever analyzing samples near the detection limit of a method. Frequent rinsing and careful handling of the entire apparatus was required to minimize residual contamination from previous runs. We tested the components of the apparatus regularly for cleanliness and ran daily matrix blanks on the glass beads to establish background signal and ensure there was no carryover.

Eluted samples were analyzed using GC-QTOF mass spectrometry. Time-of-flight (TOF) mass analyzers are capable of very high resolution and mass accuracy and are therefore powerful tools in the identification of unknown components. Our instrument maintained sub-ppm mass accuracy and resolution of about 7000 in our m/z range of interest during these measurements, which enabled us to identify components assignable to diesel fuel to their unequivocal chemical formulas, given only their parent ion mass-to-charge ratio. We note that although our instrument is capable of tandem MS/MS, for these measurements, the quadrupole was operated in full

transmission mode, and the collision cell was not in use. The following method was used: 30 m, 5 percent phenyldimethylsiloxane column with a coating thickness of 0.25 µm; pulsed split injection (15:1; 25 psi pulse) via automatic sampler; temperature of injector = 300 °C at 8 psi head pressure; injection volume = 1 µL, column temperature of 50 °C for 1 min, followed by temperature program at 20 °C/min to 120 °C, then 50 °C/min to 280 °C; hold for 2 min; emission current = 35 mA; scan m/z from 50 to 300; 200 ms/scan. Each eluted sample was run in triplicate and the responses averaged.

We used the same single-compound approach as in Section 5.3.5; however, in this experiment we identified a compound eluting around 4.9 min, with the chemical formula C_9H_{12}, as the sentinel indicating the presence of diesel fuel. We found this component to be much more abundant than *n*-decane in the headspace of these samples; therefore, we replaced *n*-decane (used in the previous section) as the sentinel compound for the calculation of the method detection limit. Differences between the matrices of soil and glass beads is one probable reason for this difference in abundance in the vapor. Using the high mass accuracy of the QTOF described above, we determined that only hydrocarbon compounds with this chemical formula could yield the parent ion mass 120.0939 kg/kmol (120.0939 amu). Diesel fuel contains several components with this chemical formula, and through retention time matching and analysis of the fragmentation pattern, we identified the compound as 1,2,4-trimethylbenzene (TMB). TMB is an appropriate marker to use when analyzing diesel fuel for several reasons. Because of its aromaticity and relatively high volatility, TMB is present in high concentrations in the headspace. It is also one of the more carefully-regulated chemicals present with high abundance in diesel fuel, which demonstrates the applicability of this technology in regulatory situations. TMB is regulated for occupational exposure by the National Institute for Occupational Safety

and Health (with a threshold limit value, TLV, of 25 ppm), the American Conference of Governmental Industrial Hygienists (25 ppm), and the US Environmental Protection Agency (45 ppm).[143-145] Additionally, current EPA Superfund protocols for site inspections are limited to sample collection at the surface of the suspected polluted area.[146] One of the advantages of the field portable PLOT-cryo apparatus is that, with the standoff probe attachment, chemical information can be safely and effectively derived from areas well beneath the soil's surface. One of our goals in performing the method detection limit calculation was to confirm that the portable PLOT-cryo method performs with sufficient sensitivity to be applied in these types of regulatory situations.

For each of the sixteen 1 ppm replicates, we generated extracted ion chromatograms for the exact masses 105.0767 and 120.0939 (mass accuracy 200 ppm). An example of these is shown in Figure 5.5. The 120.0939 m/z ion was used to confirm the identity of the peak. We used the signal generated by the 105.0767 m/z ion in our MDL calculations because it was the more abundant fragment.

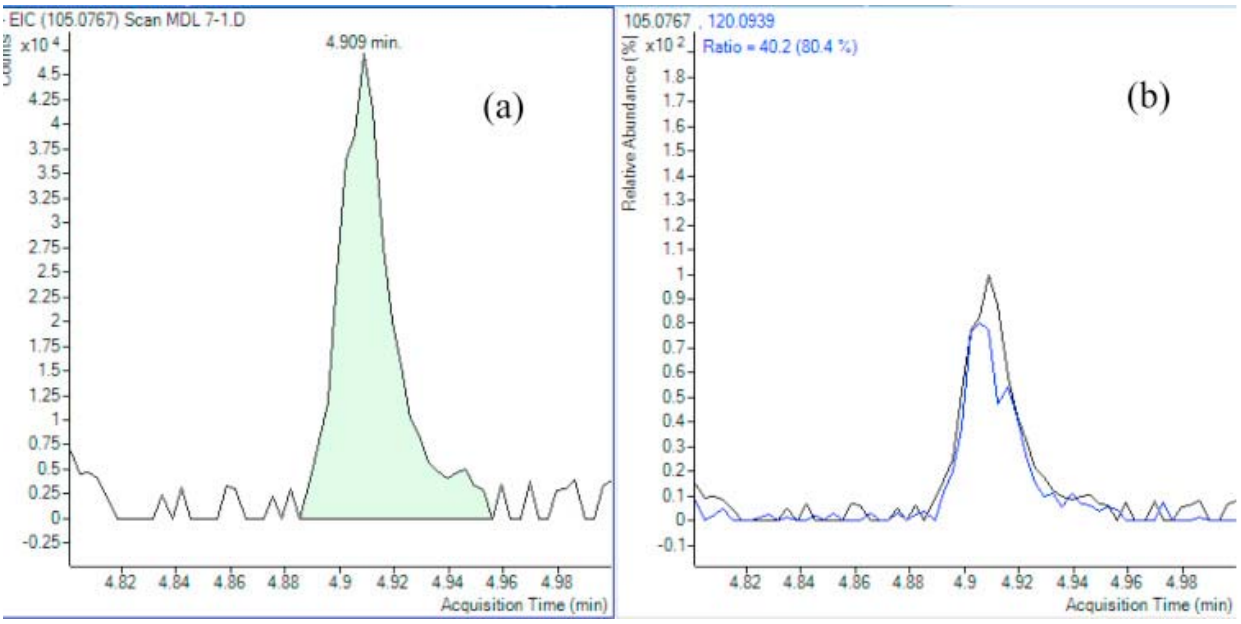

Figure 5.5. Sample extracted ion chromatograms show the results of vapor samples of 1 ppm diesel fuel on a matrix of glass beads. Panel (a) depicts the 1,2,4-trimethylbenzene base peak used to generate area counts (105.0767 amu, 200 ppm mass accuracy). Panel (b) displays the parent ion (120.0939 amu ± 200 ppm mass accuracy) peak overlaid with the supporting peak. The presence of both ions within an allowed relative abundance verified the identity of TMB.

The sample standard deviation for the sixteen 1 ppm replicates was 15194 arbitrary units (AU). The appropriate Student's t-value for 15 degrees of freedom, with a confidence interval of 95%, is 2.131. The calculated MDL was 32378 AU. This represents the area count or signal threshold above which diesel fuel contamination can be detected 95% of the time. The MDL reported here is strictly applicable to diesel fuel spiked on a matrix of glass beads, sampled with the field portable apparatus, eluted with 1.5 mL of solvent, and analyzed using the GC-QTOF method described above. We did not attempt quantitation based on instrument response; however, based on the mean signal obtained from the 1 ppm replicates (53997 AU), the signal detection limit we obtained corresponds to an MDL below 1 ppm.

We observed a great deal of variation in the signal for replicates of the same concentration, evidenced by the sample standard deviation. Even for samples collected at much

higher concentrations during preliminary experiments, we were unable to satisfactorily calibrate the signal and quantitate the sentinel compound. This variation was in part a result of sampling uncertainty between separately-prepared 1 ppm samples.

Another likely source of this variation is the sampling flow rate. We did not monitor the suction flow rate during collection for every sample, but during routine checks, we observed rates varying between 55 and 72 mL/min (a decrease from 180 mL/min observed with the newly fabricated unit discussed in Part I).[37] The high variability in flow rate for the field portable apparatus can be ascribed to two major sources. First, there is a great deal of variability in the suction (vacuum) that is generated by the laboratory compressed air. While the flow of compressed air to the vacuum generator is controlled by a valve, the pressure of the "house air" is not controlled at the portable unit. Variations in the pressure and flow rate occur as a result of intermittent and random compressed air usage elsewhere in the building. Clearly, under such circumstances, the pressure is not controlled as precisely as the electronic pressure control inlets used in the laboratory implementation of PLOT-cryo, for example. The compressed air source is used in the operation of both the heating and cooling vortex tubes as well as the suction, further adding to the variability in the proportion of compressed air pressure available to the vacuum generator. The second major factor in variability is flow rate impedance caused by the matrix geometry. Because the standoff probe is positioned beneath the surface of the matrix during sample collection, the suction may cause matrix particles (in this case glass beads) to become lodged against the probe and thus partially impede flow rate. This can occur randomly, and is a vagary of any matrix (glass bead, soil, etc.)

A third major source of variation among samples is the unknown local vapor concentration in the test beds. The condensed-phase solute concentration on the glass beads was

nominally 1 ppm (± 0.037 ppm); however, differences in pressure, temperature, humidity, and solute distribution could affect the vapor concentration a great deal. It is also worth noting that, especially at such a low concentration, depletion of the analyte likely occurred both locally, in the matrix around the standoff probe, and in the whole volume of the test bed, which could affect the amount of solute in the vapor collected. Without addressing these issues, we cannot calibrate the method for quantitative measurements. This is not a serious disadvantage, however, since matrix variability will be present in nearly any field sampling scenario, and it was important for us to capture as much of this variability as possible. We are confident that our calculated MDL, 32378 AU, corresponds to a limit in terms of concentration of below 1 ppm, given that the mean response to our 1 ppm spiked samples was 53997 AU. Future work will address control and monitoring of the flow rate and apply the method to known vapor concentrations to help attribute this variation to potential sources.

5.3. Conclusion

This work explored the applicability of the novel portable PLOT-cryo approach, discussed in Part I, to several benchmark analytes and a typical environmental situation. Our goals were to (1) confirm that the approach can effectively and reliably detect compounds present in the headspace above a condensed sample, and (2) calculate the method detection limit for a prototype complex sample, namely diesel fuel at a known concentration on a matrix of glass beads. We draw the following conclusions from this study:

(1) The field portable apparatus allowed for the successful collection and detection of the compounds in these experiments. We observed reliable results with samples maintained at ambient temperature and samples that were heated to promote mass transfer to the

headspace. The method allowed for very short collection times (as low as 3 s), enabled by the high flow rate through the multiple capillary wafer.

(2) Limit of detection was determined qualitatively by observing the chromatographic response to 4 ppm diesel/soil when using a single quadrupole mass spectrometer. The MDL calculated for analyses done with QTOF was 32378 AU, the equivalent to a concentration below 1 ppm. The QTOF provided a significantly lower MDL than the single quadrupole instrument. By leveraging the high-mass-accuracy extracted ion counts achievable with QTOF detection, the sensitivity of the portable unit was increased. According to the National Institute for Occupational Safety and Health, the acceptable exposure limit for trimethylbenzene is 25 ppm.[145] We expect, therefore, that the portable PLOT-cryo apparatus would reliably detect the conditions deemed problematic by federal regulations.

(3) We encountered issues with variability and contamination, especially when working at low concentrations, near the MDL. We attribute the increase in variability relative to some of the results previously obtained with the laboratory PLOT-cryo apparatus to three major factors. These factors are inconsistency in the vacuum generator's source of compressed air, potential flow rate impedance due to matrix geometry, and local depletion of the solute around the probe. It should be noted that the matrix of glass beads, or a pure sample dispersed in an enclosed test bed, represents the least variable, "best" case. In real-world forensic or environmental samples, matrix effects and moisture levels would likely further increase variability.

(4) Quantitation has been successfully demonstrated with the lab-based PLOT-cryo approach in past work, but has not been achieved with the portable unit.[80] The laboratory

apparatus achieves a better detection limit and lower variability than the portable unit, which we expected, given the challenges inherent in field sampling. Future development will focus on ways to improve performance. Studying samples with known vapor concentrations may yield more information about the precise sources of variability in sampling.

5.4. References

31. Lovestead, T. M., Bruno, T. J., Trace headspace sampling for quantitative analysis of explosives with cryoadsorption on short alumina porous layer open tubular columns. *Analytical Chemistry* 2010, *82*, 5621-5627.

34. Lovestead, T. M., Bruno, T. J., Detecting gravesoil with headspace analysis with adsorption on short porous layer open tubular (PLOT) columns. *Forens Sci Int* 2011, *204*, 156-161.

35. Nichols, J. E., Harries, M. E., Lovestead, T. M., Bruno, T. J., Analysis of arson fire debris by low temperature dynamic headspace adsorption porous layer open tubular columns. *Journal of Chromatography A* 2014, *1334*, 126-138.

36. Lovestead, T. M., Bruno, T. J., Detection of poultry spoilage markers from headspace analysis with cryoadsorption on a short alumina PLOT column. *Food Chem* 2010, *121*, 1274-1282.

37. Bruno, T. J., Field portable low temperature porous layer open tubular cryoadsorption headspace sampling and analysis Part I: Instrumentation. *Journal of Chromatography A* 2016, *1429*, 65-71.

56. Bruno, T. J., Wolk, A., Naydich, A., Composition-explicit distillation curves for mixtures of gasoline and diesel fuel with gamma-valerolactone. *Energy & Fuels* 2010, *24* (4), 2758-2767.

57. Bruno, T. J., Svoronos, P.D.N, *CRC Handbook of Basic Tables for Chemical Analysis, 3rd. ed*. Taylor and Francis CRC Press: Boca Raton, 2011.

65. Windom, B. C., Huber, M. L., Bruno, T. J., Lown, A. L., Lira, C. T., Measurements and modeling study on a high aromatic diesel fuel. *Energy & Fuels* 2012, *26*, 1787-1797.

80. Bruno, T. J., Wolk, A., Naydich, A., Composition-explicit distillation curves for mixtures of gasoline with four-carbon alcohols (butanols). *Energy & Fuels* 2009, *23*, 2295-2306.

117. Burger, J. L., Bruno, T. J., Application of the advanced distillation curve method to the variability of jet fuels. *Energy & Fuels* 2012, *26*, 3661-3671.

140. Bruno, T. J., Svoronos, P.D.N., *CRC Handbook of Fundamental Spectroscopic Correlation Charts*. Taylor and Francis CRC Press: Boca Raton, 2006.

141. Bruno, T. J., Simple, quantitative headspace analysis by cryoadsorption on a short alumina PLOT column. *J Chromatogr Sci* 2009, *47*, 5069-5074.

142. United States Code of Federal Regulations, Title 40: Protection of Environment, Part 136 – Guidelines establishing test procedures for the analyses of pollutants, Appendix B to Part 136 – definition and procedure for the determination of Method Detection Limit. 1999.

143. National Advisory Committee for Acute Exposure Guideline Levels for Hazardous Substances, Acute Exposure Guideline Levels (AEGLs) for 1,3,5-trimethylbenzene, 1,2,4-trimethylbenzene, 1,2,3-trimethylbenzene. US Environmental Protection Agency, Washington, DC, 2007.

144. American Conference of Governmental Industrial Hygienists, Trimethyl benzene isomers. In *Documentation of the Threshold Limit Values and Biological Exposure Indices*, Cincinnati, OH, 2002.

145. National Institute for Occupational Safety and Health, NIOSH recommendations for occupational safety and health: Compendium of policy documents and statements. US Department of Health and Human Services, Cincinnati, OH, 1992.

146. Office of Emergency and Remedial Response, Guidance for Performing Site Inspections Under CERCLA. US Environmental Protection Agency, Washington, DC, 1992.

Chapter 6: Field Demonstration of Portable Headspace Sampling in a Simulated Cargo Container

6.1. Introduction

Approximately 90 % of international trade passes through seaports inside shipping containers.[147] This high volume of freight must be inspected by importing countries and international bodies to address illegal activity. In 2006, the United States Congress passed the Security and Accountability For Every Port Act (SAFE Port Act), comprised of a number of programs to increase security at both domestic and foreign ports that participate in international trade with the United States.[148] One of these programs, the Container Security Initiative, empowers the US Department of Homeland Security to screen shipping containers that are either departing for the United States from a foreign port or arriving at a US domestic port. Customs and Border Patrol (CBP) conducts the screenings of roughly 4 % of containers.[149] Lawmakers have pushed for 100 % screening in recent years, and legislation has been introduced twice, but not passed, to require CBP to do so.[149-151] According to the Congressional Budget Office, the funding, manpower, and technology required for 100 % screening would be prohibitively enormous using the current screening methods.[149] New, low-cost approaches to improving transportation infrastructure security and enforcing the lawfulness of commerce are thus appealing to supplement the screening procedures currently in place. Many countries maintain screening programs, and an international effort, Programme Global Shield, was created in 2010 as a partnership of the World Customs Organization, INTERPOL, and the United Nations Office on Drugs and Crime, to support these goals.

Law enforcement organizations like CBP inspect containers involved in international trade for explosive devices, including nuclear material. Transportation infrastructure is a frequently discussed target for terrorism, and bombings make up 64 % of terrorist attacks on transportation infrastructure.[152, 153] In addition to these national security risks, law enforcement is interested in screening for human trafficking, illicit drugs and their precursors, other illegal activity, and general safety. An example of the last is a vehicle in a shipping container with a ruptured fuel tank, an event which could generate an explosive mixture in the closed environment of the container.

Current practice for cargo screening consists of random sampling and physical searches, inspection of provenance documents, x-ray or gamma-ray radiography, and sniffer dogs. Radiation detectors are used to locate nuclear materials.[154] These tools used together can be effective in detecting illicit materials, but they also have some disadvantages. Physical searches could be dangerous to the inspector and are time consuming—as is radiography. Dogs are incredibly sensitive to the compounds they are trained to identify and have been very successful when deployed for explosive and drug screening; however, they require expensive training and expert human partners, can only detect the compounds used in training, and their low duty cycle is a major limitation.[155]

Ideally, a method should be developed that removes the human and canine component of chemical screening of cargo. Vapor sampling could supplement, and offer a safer alternative to, the law enforcement tools currently in practice. These methods can be non-destructive, minimally intrusive, rapid, and safer for the inspector than physical inspection of container interiors. Vapor sampling consists of collecting a quantity of air from inside a container and analyzing its chemical composition. The sample can be introduced directly to an analytical

instrument or first preconcentrated on an adsorbent trap. Vapor sampling directly into an instrument without the use of a trap is advantageous for real-time measurements; however, preconcentration on a sorbent trap is often necessary to obtain enough analyte for a signal to be detected. Chemical analysis of vapor can provide the analyst with a complete chemical characterization of the container. Both vapor sampling devices and the corresponding analytical equipment can be made portable for an application such as cargo screening.

There are opportunities for vapor sampling methods to make a difference in this area, and there is future demand for the technology. CBP reports to Congress have included chemical detectors in its Inspection and Detection Technology Multi-Year Investment and Management Plan. In 2016, the agency projected a need for 137 vapor/chemical detectors by 2021.[156] The potential benefit to national security is one reason why the development of portable vapor sampling systems is an active area of research, including field-deployable methods to automate the analysis of results. Other fields which are exploring portable technology include environmental monitoring and the aroma analysis of beverages.[13, 23, 157] The most familiar portable vapor sampling device is the Breathalyzer used to detect alcohol intoxication in the field.

The portable vapor sampling device demonstrated in this work is based on a new technology, developed at NIST, called porous layer open tubular cryoadsorption (PLOT-cryo), which uses a capillary column coated with an adsorbent phase (alumina in this case) and chilled to subzero temperatures as a trap to preconcentrate analytes present in the collected vapor. PLOT-cryo can be coupled with any analytical method, such as gas chromatography (GC), mass spectrometry (MS), and nuclear magnetic resonance (NMR). Over the last 10 years, this approach has been applied to samples including explosives, arson fire debris, cannabis, and

natural gas.[30, 31, 33-36] In order to further expand the use of PLOT-cryo and address field applications of the method, the portable PLOT-cryo instrument was recently developed and tested under lab conditions.[37, 38] This current work deployed portable PLOT-cryo into the field as a tool for cargo screening with a series of four experiments. The set of experiments investigated the detection of naphthalene, explosive-related compounds, decomposition products, and gasoline, inside a test bed designed to simulate a shipping container.

6.2. Methods

6.2.1. Materials

Pure test compounds, solvents used in GC analyses, and gasoline were purchased from commercial sources and used as received. Diffusers were made from either clean, commercially obtained 8 oz nominal steel paint cans or 4 mL borosilicate glass vials.

6.2.2. Experimental setup

A shipping container was simulated by adapting a surplus United States Army communications bunker ("bunker" hereafter) for this field demonstration of portable PLOT-cryo. It was repurposed from another location at the NIST laboratory site, where it was in disuse, and moved to a parking space outside the laboratory building where it became a test bed for these experiments. Figure 6.1 shows photographs of the bunker setup. The bunker interior dimensions were 1.91 m wide by 1.86 m high by 3.85 m deep. After adjusting for the other elements inside the bunker (e.g. HVAC duct) which occupied some of its volume, the total volume was determined to be 13.6 m^3 ± 0.31 m^3. Holes in the walls of the bunker, including vents and incidental holes and gaps incurred due to age, were sealed using gaffer's tape, epoxy, and pop riveting as well as possible. Even given these repairs, airtightness could not be reasonably

expected. Shipping containers undergoing screening in a real scenario would also not be perfectly sealed. All commercial containers are designed with air vents, so the existence of leaks in the bunker were an advantage that added realism to the testing.

Figure 6.1. Photographs of the bunker are presented. (a) Exterior front and side of the bunker. (b) Open hatch on the front wall. (c) Bunker interior. (d) Side view of the bunker; one of the walls into which sampling ports were drilled.

Because air vents were not built into the bunker through which to sample the vapor, using a power drill, five (0.125" diameter nominal) ports in each side of the bunker were made to enable introduction of the sampling probe to the inside of the container. Two rows of ports located at the bottom, middle, and top of the bunker wall were made at 1/3 and 1/2 the full length of the bunker, as shown in Figure 6.2. A heavy steel rail prevented drilling the bottom port halfway down the bunker wall, resulting in five total ports on either side. These multiple sampling locations were used to explore whether the location of vapor collection affects the results. Some research has shown that sampling vapor from different locations on a shipping container affects the aerodynamics within.[19] The volume was not intentionally mixed, and vapor concentrations of the compounds were not spatially constant inside the bunker. Real cargo containers are not mixed and likely do not exhibit even distribution of vapor, either, so this aspect of the experimental setup was another factor making these tests resemble a real-world situation. A factor affecting the environment inside a shipping container which was absent from these experiments was the cargo itself and its distribution inside the volume.

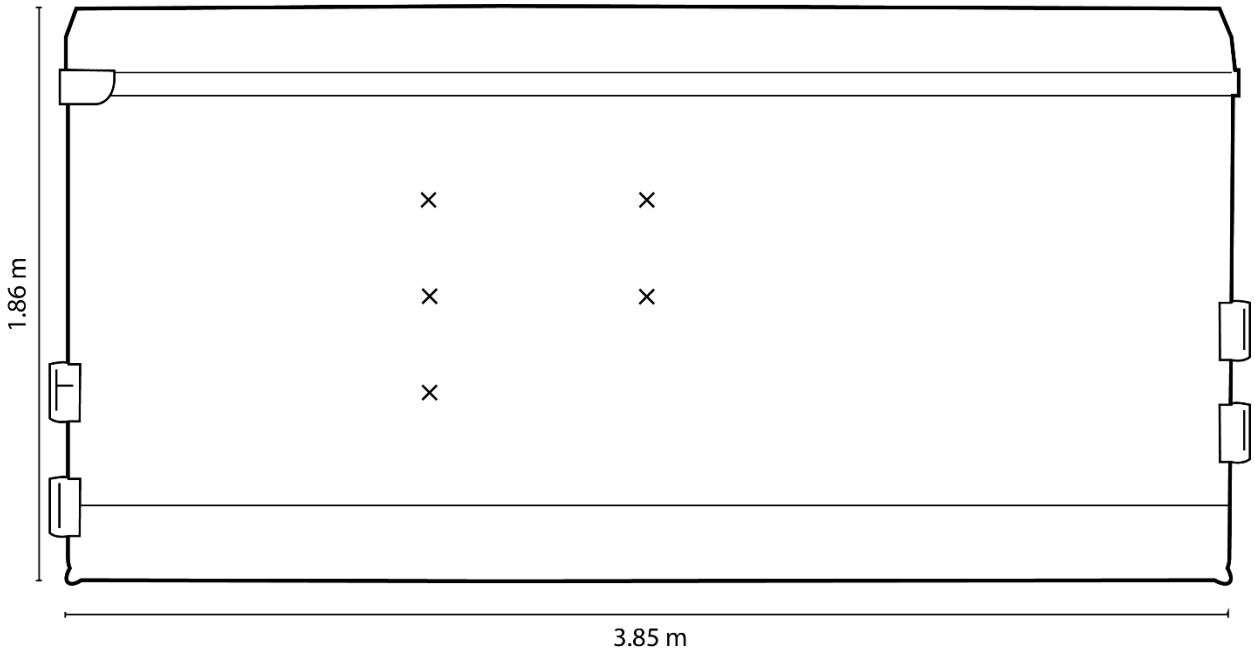

Figure 6.2. Locations of the ports used for sampling in the bunker are marked with an x on this schematic side view of the bunker.

Because the bunker was outside and exposed to the elements and variable weather, many experimental variables which are controlled in a laboratory setting were left up to nature: the temperatures inside and outside the bunker, atmospheric pressure, relative humidity, contamination inside the bunker, and diffusion of analyte vapor through the volume. The uncontrolled variables were recorded whenever possible.

6.2.3. Sampling protocol

Operation of the portable PLOT-cryo unit has been described in detail in previous work and in Chapter 5 of this thesis.[37, 38] The device, which is powered by compressed air, is housed in an aluminum briefcase which contains three major components: the unit's operating platform, which controls temperature and sample collection, the insulated standoff module containing a multicapillary PLOT trap, and the probe used to access vapor inside the volume of interest. Multicapillary PLOT traps typically are composed of six individual PLOT capillaries cast into an

epoxy or silicone monolith with connections to inlet and outlet fittings. The multicapillary trap has also been referred to as the wafer, and these terms are interchangeable. To prepare for use, a compressed air line is connected to the operating platform through a quick connect fitting. Compressed air operates the entire unit, providing (1) suction to pull vapor from the bunker and through the multicapillary trap, and (2) hot and cold air for temperature control of the standoff module. Because compressed air is used instead of electricity, the device is safe to use in sampling situations where flammable material may be present, for example, the gasoline experiment done here. There was no spark or ignition source in the portable unit or the bunker.

In preparation for a vapor sample collection, cold air from the operating platform is applied to chill the module and multicapillary trap to temperatures below 0 °C (to promote adsorption of volatile analytes). The probe is attached to the standoff module opposite the suction and inserted into the space to be sampled. When suction is switched on, sample collection begins and vapor pulled from the bunker passes over the cold multicapillary trap, where analyte is captured. The sample must then be released from the trap for analysis. To desorb the multicapillary trap, it is heated to about 60 °C (to promote desorption of analytes) and eluted with 1 mL of solvent into an autosampler vial for analysis. The sample in liquid form can be analyzed by any analytical method(s), in this case, gas chromatography-mass spectrometry (GC-MS). Once the sample is solvent desorbed, the multicapillary trap can be reactivated and reused by heating the module while purging with air. Desorption and reactivation of the multicapillary traps can be done in the lab or in the field.

To set up each experiment, known quantities of the analytes were placed in individual diffusers made from either steel cans (8 ounces nominal) with perforated lids or 4 mL borosilicate glass vials. The diffusers were placed in the center of the bunker floor. Individual

vapor samplings occurred between 24 hours and several weeks after the sample introduction. After each experiment, the diffusers were removed and weighed to determine the fraction that vaporized during the experiment. Before starting a new experiment, removal was attempted of any residual analyte from the previous experiment by airing out the bunker with the door open and a fan to circulate fresh outdoor air. Bunker "blank" samples were then collected in between sets of experiments; analytes from previous experiments was sometimes observed remaining inside, but this was easily detected and disregarded.

For quality control, the multicapillaries were periodically tested for contamination. The only compounds prone to carryover were heavier solvents used for desorption in prior work. Solvent choice depends on the analyte of interest, and in some previous studies with portable PLOT-cryo, tetradecane was used to desorb analytes. The source of tetradecane found in any of the samples was therefore known and considered an artifact. It did not interfere with the analysis of the compounds used in the bunker.

Each experiment tested a range of sample collection times – the only completely controlled sampling variable – to determine the approximate time needed to detect the test compounds. For each individual vapor collection, the following parameters were recorded: port used, ambient outdoor temperature, temperature inside the bunker, temperature inside the module containing the multicapillary trap, ambient relative humidity, and ambient pressure. Temperatures were measured using thermocouples with an uncertainty of 1 °C. Relative humidity data were taken from a monitoring station at the National Center for Atmospheric Research (NCAR) 1.1 miles away. Ambient pressure was measured with an electronic barometer with an uncertainty of 0.03 kPa. Samples were desorbed with acetone and characterized by gas

chromatography-mass spectrometry (GC-MS) operating in both scan and selective ion monitoring (SIM) modes.

6.2.4. Background signal

Before embarking on this series of experiments, the vapor contents of the bunker itself, in the absence of any test compounds, were analyzed to establish a baseline. The bunker had its own musty, slightly sweet smell, which suggested an interesting vapor composition. Analysis revealed a mixture of compounds, dominated by C6-C12 unsaturated ketones with and without rings. These are probably the byproducts of degradation of polyurethane foam insulation exposed to years of weathering. This type of insulation, which was used in the era when the bunker was likely made, was observed sandwiched between the aluminum walls of the bunker. It was a light yellow color consistent with the discoloration of polyurethane foam exposed to heat over time.

The background compounds were at times detected more strongly than the analytes used in the experiments. This may have interfered with the collection of target analyte or caused chemical reactions to happen, changing the composition of the vapor in the bunker, but these potential complications are beyond the scope of the current experiments and may be investigated in the future.

6.3. Results and discussion

Results from four experiments are presented, which tested the following compounds: naphthalene, explosive-related compounds, protein decomposition-related compounds, and gasoline. Vapor pressures of the test compounds ranged widely from 4934.8 Pa (dimethyl disulfide) to 0.5 Pa (diethyl phthalate), calculated at 30 °C and ambient Boulder pressure (83

kPa). All vapor pressures and concentrations provided here and in the following subsections were determined using the Antoine equation and the ideal gas law.[158-160] Because the bunker was not well sealed or well mixed, the calculated concentrations represent an upper limit only.

6.3.1. Naphthalene

The first analyte tested in the bunker was naphthalene, because it was used in the development of PLOT-cryo and subsequently as a test compound to indicate that the instrumentation is working correctly. In fact, naphthalene was the first analyte tested with portable PLOT-cryo. In that earlier work, a diffuser containing 50 mg of naphthalene was placed inside a valise with a volume of 1.68×10^{-2} m^3 (resulting in a saturated vapor concentration approximately 1234 mg/m^3). The analyte was detected in a 3 second collection time using the portable unit.[38] Incidentally, the valise was previously the largest volume tested with portable PLOT-cryo; the volume of the bunker surpasses it by almost three orders of magnitude.

For the bunker experiment, a diffuser containing 0.53 g of naphthalene was placed on the floor in the center of the bunker, and vapor was allowed to develop for 24 hours before the first vapor collection. The calculated vapor concentration was 39 mg/m^3, assuming full vaporization of the analyte. The naphthalene had not been fully vaporized when the experiment concluded after 21 days; in fact, the analyte had gained 0.03 g, which can be attributed to humidity and water vapor permeating the sample. The lack of mass change indicated that real vapor concentrations in the bunker were much lower than 39 mg/m^3, and this number is provided only to indicate that the concentration was not greater.

Two samples were taken on each of two separate days, two days apart, for a total of four samples. The bunker temperatures on the first day were 33 and 42 °C. The relative humidity was 26 %. Naphthalene was detected in 30 seconds under these conditions. An example result is

shown in Figure 6.3. On the second day, the weather was rainy with 91 % RH. The bunker temperature was 17 °C for both samples. A 30 second sample did not detect naphthalene under these conditions. An extended two minute collection time successfully detected naphthalene.

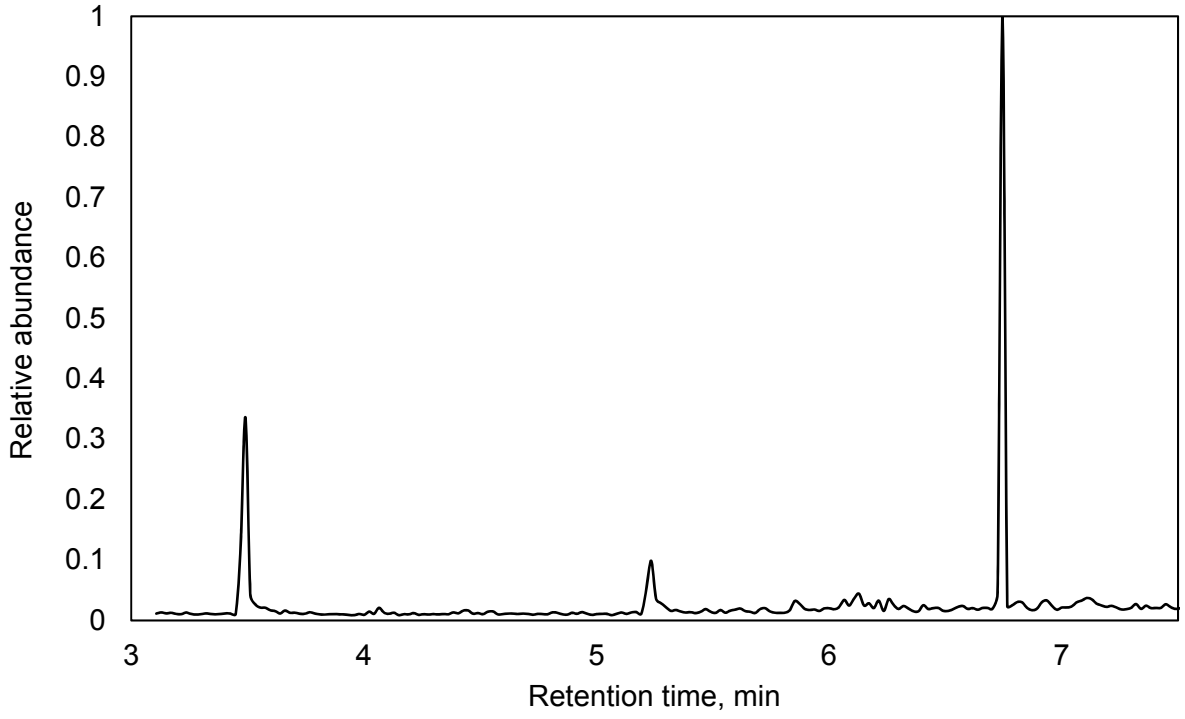

Figure 6.3. This background subtracted, representative SIM chromatogram is the result of a 30 s collection with portable PLOT-cryo. Naphthalene is the peak at 5.2 min. The two other peaks are constituents of the bunker background signal.

6.3.2. Explosive-related compound suite

The second experiment in the bunker involved three analytes related to the manufacture of explosive materials: diethyl phthalate (a plasticizer), butyrolactone, and isophorone (both solvents). These were found as components of explosive materials previously analyzed using laboratory PLOT-cryo.[31] The compounds were introduced to the bunker in three diffusers. A

fourth diffuser with a small amount of naphthalene was also included as a standard to confirm proper functionality of the unit.

The concentrations of the compounds inside the bunker were calculated based on their vapor pressures and quantities used: 46 mg/m^3 diethyl phthalate (saturation), 221 mg/m^3 isophorone, and 419 mg/m^3 butyrolactone. Sampling times were 30 seconds and 3 minutes; both intervals were sufficient to detect diethyl phthalate and isophorone. In these two collections, five days apart, the bunker temperature was 38 °C and RH was 20 % and 15 %. Butyrolactone was not detected in any sample, even after increasing collection time up to 15 minutes in hot, dry weather. It is the most volatile of the three compounds, and it may have diffused out of the bunker before the first sample was taken.

6.3.3. Decomposition compound suite

In the third experiment, a suite of eight compounds associated with protein decomposition were used to simulate a cargo container containing a cadaver, the presence of which could be the result of an accident or a crime. The compounds were phenyl sulfide, trimethyl pyridine, dimethyl trisulfide, dimethyl disulfide, methyl thioacetate, allyl methyl sulfide, 1,5-pentanediamine (cadaverine), and 1,4-butanediamine (putrescine). These compounds were chosen because they were identified as decomposition markers during previous PLOT-cryo experiments.[36]

The eight compounds were added to the bunker in the same experiment, each in its own diffuser. A two minute sampling interval detected allyl methyl sulfide and dimethyl disulfide, two of the more volatile analytes. After increasing collection time to 15 minutes, both previous analytes plus methyl thioacetate and dimethyl trisulfide were detected. The other four less volatile compounds were not detected in any sample. Bunker temperatures during these

experiments were low (in October shade), ranging from 11 to 23 °C. Higher temperatures would increase the likelihood of detecting some of the lower volatility compounds. Internal temperatures around 70 °C have been considered typical for real cargo containers, but temperatures likely vary widely dependent on their environments.[22] These compounds should be tested again under different conditions; other markers of decomposition, or real decomposing material, would also be interesting subjects of future work.

6.3.4. Simulated gasoline spill

In the fourth and final experiment, approximately 250 mL of gasoline was placed in the bunker in a quarter baking sheet. This represented a ruptured fuel tank on a car being transported by freight. Gasoline is also relevant as a possible fuel used in crude explosive devices. Portable PLOT-cryo detected gasoline components with a sample collection time of 10 seconds with a low bunker temperature (17 °C).

Because gasoline is a complex mixture of hundreds of components, a comparison could be made between the composition of the collected vapor sample and the liquid gasoline itself. As expected and described throughout this thesis, the contents of the vapor were different than the composite liquid gasoline. Samples collected from the bunker were enriched in the more volatile components of gasoline, especially aromatic compounds, and contained little to no lower volatility species (Figure 6.4).

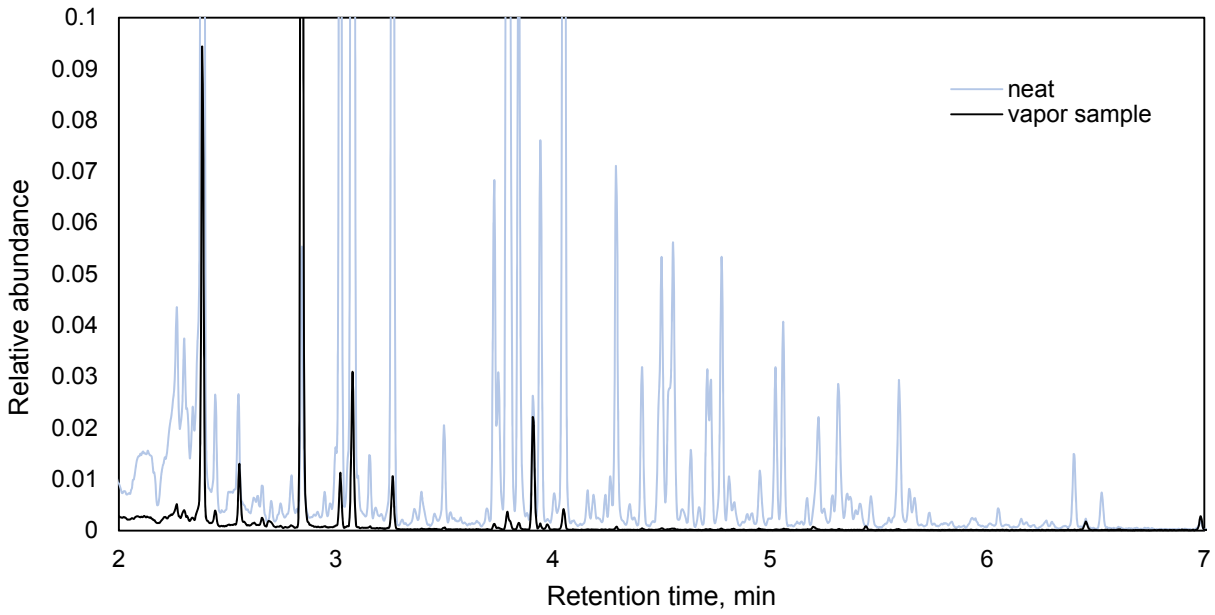

Figure 6.4. More volatile, less retained gasoline components were enriched in the vapor sample (black) compared to the composition of neat gasoline (blue). Note that the y axis range is 0-0.1.

Another ten second vapor collection taken three weeks after the introduction of the gasoline sample (and in colder weather, 9 °C) did not detect any gasoline compounds, suggesting that the compounds volatile enough to be detected in a short sampling time had leaked away.

6.4. Conclusion

Bolstering the safety and security of transportation infrastructure internationally is one important motivation for the development of field portable vapor sampling technology. These experiments were the first demonstrations of portable PLOT-cryo technology deployed in a field environment. Using an old Army communications bunker as a simulated shipping container, the portable PLOT-cryo unit detected naphthalene, two explosives-related compounds (diethyl phthalate, isophorone), four decomposition markers (allyl methyl sulfide, methyl thioacetate,

dimethyl disulfide, dimethyl trisulfide), and a simulated gasoline spill. The sampling intervals required for detection were mostly two minutes or less.

The background signal of the bunker – vapor chemistry present in the absence of any added analyte – was primarily attributable to ketone decomposition products of the polyurethane insulation used in its construction. Background compounds were often collected in greater abundance than the analytes, and the analytical challenge this presents must be considered. Background vapor signatures of shipping containers are very likely to vary based on the construction and contents.

Some overall conclusions can be drawn from this series of experiments about the effects of field conditions – temperature, both inside and outside the bunker, and relative humidity –, as well as the environment inside the bunker, including any effect of sampling location. Across all experiments, temperatures inside the bunker ranged from 2.2 to 43 °C. Temperatures outside the bunker ranged from 3 to 37 °C. Relative humidity ranged from 9 % to 92 %.

Qualitative observations were made of the effects of temperature and ambient relative humidity on the environment inside the bunker as well as on the performance of the portable PLOT-cryo unit. The primary factor influencing detection ability was the temperature inside the bunker, as expected. Temperatures observed in real shipping containers are typically higher than the temperatures observed during these experiments. High humidity (RH > 90 %) required longer sampling times in the naphthalene experiment. This could be an effect of water vapor outcompeting the analyte for adsorption to the capillary trap; water content inside the bunker likely also affected the concentration of analyte present in the vapor in the first place.

The minimal change in the mass of analyte observed during all experiments indicated that the true concentration of analyte in the vapor was consistently lower than the presented value.

Wall losses and lack of airtightness also likely affected the vapor concentration present. The estimated concentrations given in this article are not of much value; these serve as upper bounds only. Compound vapor pressure is a more useful metric.

Across all the experiments, the analyte-containing diffusers were located on the floor in the center of the bunker, which was sampled from a limited number of locations. There was no observable effect of port location. Another study has shown that in real circumstances, port location may matter.[19] The environment inside the bunker was not intentionally mixed, but changes in temperature may have caused small convection currents. In a real cargo container, any crates or other contents could serve as diffusion barriers and make port location a crucial variable. This study is merely a necessary first step towards understanding the variables affecting compound detection.

These results indicate that portable PLOT-cryo is a good candidate for in-the-field chemical screening of cargo in transit, not limited only to seaports but also cargo transported by plane or truck. The current observations are mostly qualitative. The lack of controlled conditions inherent in a field study means extensive work will be required to fully characterize the capabilities and limits of the technology. Designing the unit for thermal desorption and testing it coupled to a field analysis method—such as micro GC or direct mass spectrometry—would both support portability. This work has initiated further development of portable PLOT-cryo for continually enhanced sensitivity and a broad array of applications in forensics and beyond.

6.5. References

13. Li, Z., Suslick, K. S., A hand-held optoelectronic nose for the identification of liquors. *ACS Sensors* 2018, *3* (1), 121-127.

19. Hargather, M. J., Staymates, M. E., Madalis, M. J., Smith, D. J., Settles, G. S., The internal aerodynamics of cargo containers for trace chemical sampling and detection. *IEEE Sensors Journal* 2011, *11* (5), 1184-1193.

22. Staples, E. J., Viswanathan, S., Detection of contrabands in cargo containers using a high-speed gas chromatograph with surface acoustic wave sensor. *Industrial & Engineering Chemistry Research* 2008, *47* (21), 8361-8367.

23. Truong, T., Porter, N., Lee, E., Thomas, R. J., The applicability of field-portable GC–MS for the rapid sampling and measurement of high-boiling-point semivolatile organic compounds in environmental samples. *Spectroscopy* 2016, *14* (3), 20-26.

30. Lovestead, T. M., Bruno, T. J., Determination of cannabinoid vapor pressures to aid in vapor phase detection of intoxication. *Forensic Chemistry* 2017, *5* (Supplement C), 79-85.

31. Lovestead, T. M., Bruno, T. J., Trace headspace sampling for quantitative analysis of explosives with cryoadsorption on short alumina porous layer open tubular columns. *Analytical Chemistry* 2010, *82*, 5621-5627.

33. Burger, J. L., Lovestead, T. M., Bruno, T. J., Composition of the C6+ fraction of natural gas by multiple porous layer open tubular capillaries maintained at low temperatures. *Energy & Fuels* 2016, *30* (3), 2119-2126.

34. Lovestead, T. M., Bruno, T. J., Detecting gravesoil with headspace analysis with adsorption on short porous layer open tubular (PLOT) columns. *Forens Sci Int* 2011, *204*, 156-161.

35. Nichols, J. E., Harries, M. E., Lovestead, T. M., Bruno, T. J., Analysis of arson fire debris by low temperature dynamic headspace adsorption porous layer open tubular columns. *Journal of Chromatography A* 2014, *1334*, 126-138.

36. Lovestead, T. M., Bruno, T. J., Detection of poultry spoilage markers from headspace analysis with cryoadsorption on a short alumina PLOT column. *Food Chem* 2010, *121*, 1274-1282.

37. Bruno, T. J., Field portable low temperature porous layer open tubular cryoadsorption headspace sampling and analysis Part I: Instrumentation. *Journal of Chromatography A* 2016, *1429*, 65-71.

38. Harries, M., Bukovsky-Reyes, S., Bruno, T. J., Field portable low temperature porous layer open tubular cryoadsorption headspace sampling and analysis Part II: Applications. *Journal of Chromatography A* 2016, *1429*, 72-78.

147. UN-Business Action Hub., IMO (International Maritime Organization) profile. https://business.un.org/en/entities/13.

148. Security and Accountability for Every Port Act. *Public Law 109-347*, 109th Congress, 2006.

149. Hutchins, R., Debate reignites over container scanning of US imports. *Journal of Commerce* 2016.

150. Scan Containers Absolutely Now (SCAN) Act. 113th Congress, 2014.

151. Scan Containers Absolutely Now (SCAN) Act. 114th Congress, 2016.

152. Counter-Terrorism Committee Executive Directorate. *Physical protection of critical infrastructure against terrorist attacks*; United Nations Security Council: 2017.

153. Miller, E. *Terrorist Attacks Targeting Critical Infrastructure in the United States, 1970-2015*; START: College Park, MD, 2016.

154. US Customs and Border Protection, CSI: Container Security Initiative. https://www.cbp.gov/border-security/ports-entry/cargo-security/csi/csi-brief.

155. Rouhi, A. M., Detecting illegal substances. *Chemical & Engineering News* 1997.

156. U.S. Customs and Border Protection. *Inspection and Detection Technology: Multi-Year Investment and Management Plan (FY 2016-2021)*; 2016.

157. Dworzanski, J. P., Kim, M.-G., Peter Snyder, A., Arnold, N. S., Meuzelaar, H. L. C., Performance advances in ion mobility spectrometry through combination with high speed vapor sampling, preconcentration and separation techniques. *Analytica Chimica Acta* 1994, *293* (3), 219-235.

158. Antoine, C., Tensions des vapeurs; nouvelle relation entre les tensions et les températures [Vapor pressure: a new relationship between pressure and temperature]. *Comptes Rendus des Séances de l'Académie des Sciences (in French)* 1888, *107*, 681–684, 778–780, 836–837.

159. Yaws, C. L., *The Yaws Handbook of Vapor Pressure*. 2nd ed.; Gulf Professional Publishing: Oxford, 2015.

160. Linstrom, P. J., Mallard, W.G., NIST Chemistry WebBook, NIST Standard Reference Database Number 69, June 2005, National Institute of Standards and Technology, Gaithersburg MD, 20899 (http://webbook.nist.gov).

Chapter 7: Thesis Conclusions and Recommendations for Future Research

This thesis investigates the utility of vapor-liquid equilibria measurements to improve both forensic vapor analysis and the development of alternative liquid fuels. It also introduces one method for determining the vapor-liquid equilibrium of multicomponent mixtures to increase success in both areas. First, Chapters 2 and 3 describe the characterization of the volatility and composition of several alternative liquid fuels and bio oils using the advanced distillation curve (ADC) method. Next, motivated by the need to better relate the compositions of the vapor and liquid phases, a new method for measuring the VLE of complex, multicomponent fluids like these alternative fuels is introduced in Chapter 4: the advanced distillation curve with reflux (ADCR). Finally, our knowledge of VLE gained through ADC and ADCR made possible further development of a forensic vapor analysis technique, portable PLOT-cryoadsorption (PLOT-cryo). Portable PLOT-cryo leverages principles of phase equilibrium to characterize a condensed phase sample using its vapor composition. This technology is discussed in Chapters 5 and 6.

The pyrolysis fuels and oils studied in this thesis are in various stages of development. The fluids made from polypropylene, described in Chapter 2, are high in energy content and have the appropriate volatility to be tested as blends with petroleum fuels. Upgrading and refining them to reduce alkene content is also recommended. The challenges presented by the nonhomogeneous oils measured in Chapter 3 should be addressed, especially because these fluids are far from the only pyrolysis fluids that cannot be homogenized; they contain multiple organic phases separated by a water layer. ADC is currently the only distillation method to be used to examine nonhomogeneous pyrolysis fluids for alternative fuel development. Improving

the method as described in that chapter is the next step for this research. The two bio oils used as a case study in Chapter 3 are not ideal candidates for further development into alternative fuels.

The cornerstone of this thesis is the development of a metrology for multicomponent mixture VLE. The advanced distillation curve with reflux was shown to reliably measure simple mixtures chosen to demonstrate the approach. Although the ADCR as introduced in Chapter 4 has already proven to be a useful tool, future improvements can be made. The equilibrium stage effect in the present design may be eliminated by choosing different materials in the apparatus and using an additional heat source to maintain the head temperature at or above the temperature of the kettle. Also, having demonstrated success measuring simple mixtures with the ADCR, VLE measurements of fluids with increasing complexity are an obvious future direction, though challenging with respect to data processing. Finally, a connection of ADCR measurements with vapor analysis should be explored.

The vapor characterization work described in this thesis used portable PLOT-cryoadsorption for forensic and environmental applications. Portable PLOT-cryo shows great promise as an additional tool in the arsenal of cargo screening approaches necessary to strive to meet 100 % screening goals set by law enforcement agencies. As with any novel technology, more questions remain than can be addressed here. Future work on portable PLOT-cryo should strive to decrease collection times and fully characterize its limits of detection. Alternate adsorbent phases and additional analytes should be tested. Beyond continued characterization at the research laboratory level, technology transfer is necessary to bring portable vapor sampling via PLOT-cryo into practice in the forensics community. This includes two steps: first, making the instruments available on a larger scale so that law enforcement agencies, for instance, can acquire them; second, educating that population about the theory, operation, and applications of

portable PLOT-cryo. Both steps have been initiated, the former by a small business licensing the patents and the latter through workshops taught in partnership with the National Courts and Sciences Institute, and these efforts should continue to grow.

ADC and ADCR are important tools for the development of alternative fuels and to better understand thermal weathering of fluids for applications in the forensic and environmental sciences, including the use of vapor analysis in these areas. One of the initial motivations for this thesis work was to increase the rigor of forensic vapor analysis by characterizing the relationship between the vapor and condensed phases of a piece of evidence, especially arson fire debris evidence. ADCR has the potential not only to provide the vapor-liquid equilibrium of a thermally weathered sample (such as an ignitable liquid), but also to connect these with the composition of the neat fluid used prior to the fire. Such an application of ADCR to ignitable liquids and weathered fire debris samples also characterized by portable PLOT-cryo would be of enormous benefit to the forensics community. All three of these technologies together have the potential to revolutionize both alternative fuels development and forensic science.

BIBLIOGRAPHY

1. National Research Council, *Strengthening Forensic Science in the United States: A Path Forward*. The National Academies Press: Washington, DC, 2009.

2. American Trucking Association, Reports, trends & statistics: fuel consumption. http://www.trucking.org/News_and_Information_Reports_Energy.aspx.

3. Sharma, B. K., Moser, B. R., Vermillion, K. E., Doll, K. M., Rajagopalan, N., Production, characterization and fuel properties of alternative diesel fuel from pyrolysis of waste plastic grocery bags. *Fuel Processing Technology* 2014, *122*, 79-90.

4. Kunwar, B., Chandrasekaran, S. R., Moser, B. R., Deluhery, J., Kim, P., Rajagopalan, N., Sharma, B. K., Catalytic thermal cracking of postconsumer waste plastics to fuels: 2. Pilot-scale thermochemical conversion. *Energy & Fuels* 2017, *31* (3), 2705-2715.

5. Han, Y., McIlroy, D. N., McDonald, A. G., Hydrodeoxygenation of pyrolysis oil for hydrocarbons production using nanosprings based catalysts. *J Anal Appl Pyrolysis* 2016, *117*, 94-105.

6. Anuar Sharuddin, S. D., Abnisa, F., Wan Daud, W. M. A., Aroua, M. K., A review on pyrolysis of plastic wastes. *Energy Conversion and Management* 2016, *115*, 308-326.

7. Elliott, D. C., Wang, H., French, R., Deutch, S., Iisa, K., Hydrocarbon liquid production from biomass via hot-vapor-filtered fast pyrolysis and catalytic hydroprocessing of the bio-oil. *Energy & Fuels* 2014, *28* (9), 5909-5917.

8. Zacher, A. H., Elliott, D. C., Olarte, M. V., Santosa, D. M., Preto, F., Iisa, K., Pyrolysis of woody residue feedstocks: Upgrading of bio-oils from mountain-pine-beetle-killed trees and hog fuel. *Energy & Fuels* 2014, *28* (12), 7510-7516.

9. *ASTM D86, Standard test method for distillation of petroleum products at atmospheric pressure*. ASTM International: West Conshohocken, PA, 2004.

10. Al Ghafri, S. Z., Maitland, G. C., Trusler, J. P. M., Experimental and modeling study of the phase behavior of synthetic crude oil+CO2. *Fluid Phase Equilibria* 2014, *365*, 20-40.

11. Turek, E. A., Metcalfs, R. S., Yarborough, L., Robinson, R. L., Jr., Phase Equilibria in CO2 - Multicomponent Hydrocarbon Systems: Experimental Data and an Improved Prediction Technique. *Society of Petroleum Engineers Journal* 1984, *24* (3).

12. US Environmental Protection Agency, Method 5021A: Volatile organic compounds in various sample matrices using equilibrium headspace analysis. July 2014.

13. Li, Z., Suslick, K. S., A hand-held optoelectronic nose for the identification of liquors. *ACS Sensors* 2018, *3* (1), 121-127.

14. Baránková, E., Dohnal, V., Effect of additives on volatility of aroma compounds from dilute aqueous solutions. *Fluid Phase Equilibria* 2016, *407*, 217-223.

15. Omar, J., Olivares, M., Alonso, I., Vallejo, A., Aizpurua-Olaizola, O., Etxebarria, N., Quantitative analysis of bioactive compounds from aromatic plants by means of dynamic headspace extraction and multiple headspace extraction-gas chromatography-mass spectrometry. *Journal of Food Science* 2016, *81* (4), C867-C873.

16. Kaiser, R., Environmental Scents at the Ligurian Coast. *Perfumer & Flavorist* 1997, *22*, 7–18.

17. Zhang, C.-Y., Zhang, Q., Zhong, C.-H., Guo, M.-Q., Analysis of volatile compounds responsible for kiwifruit aroma by desiccated headspace gas chromatography–mass spectrometry. *Journal of Chromatography A* 2016, *1440*, 255-259.

18. Sghaier, L., Vial, J., Sassiat, P., Thiebaut, D., Watiez, M., Breton, S., Rutledge Douglas, N., Cordella Christophe, B. Y., An overview of recent developments in volatile compounds analysis from edible oils: Technique-oriented perspectives. *European Journal of Lipid Science and Technology* 2016, *118* (12), 1853-1879.

19. Hargather, M. J., Staymates, M. E., Madalis, M. J., Smith, D. J., Settles, G. S., The internal aerodynamics of cargo containers for trace chemical sampling and detection. *IEEE Sensors Journal* 2011, *11* (5), 1184-1193.

20. Holland, P. M., Mustacich, R. V., Everson, J. F., Foreman, W., Leone, M., Sanders, A. H., Naumann, W. J., *Correlated column micro gas chromatography instrumentation for the vapor detection of contraband drugs in cargo containers*. SPIE's 1994 International Symposium on Optics, Imaging, and Instrumentation, SPIE: 1994; p 8.

21. Neudorfl, P., Hupe, M., Pilon, P., Lawrence, A. H., Drolet, G., Su, C.-W., Rigdon, S. W., Kunz, T. D., Ulwick, S., Hoglund, D. E., Wingo, J. J., Demirgian, J. C., Shier, P., *Detection of cocaine in cargo containers by high-volume vapor sampling: field test at Port of Miami*. Enabling Technologies for Law Enforcement and Security, SPIE: 1997; p 9.

22. Staples, E. J., Viswanathan, S., Detection of contrabands in cargo containers using a high-speed gas chromatograph with surface acoustic wave sensor. *Industrial & Engineering Chemistry Research* 2008, *47* (21), 8361-8367.

23. Truong, T., Porter, N., Lee, E., Thomas, R. J., The applicability of field-portable GC–MS for the rapid sampling and measurement of high-boiling-point semivolatile organic compounds in environmental samples. *Spectroscopy* 2016, *14* (3), 20-26.

24. Bellar, T. A., Lichtenberg, J. J., Kroner, R. C., The occurrence of organohalides in chlorinated drinking waters. *Journal - American Water Works Association* 1974, *66* (12), 703-706.

25. Hu, H.-C., Chai, X.-S., Determination of methanol in pulp washing filtrates by desiccated full evaporation headspace gas chromatography. *Journal of Chromatography A* 2012, *1222* (Supplement C), 1-4.

26. Hu, H.-C., Chai, X.-S., Wei, C.-H., Barnes, D., Increasing the sensitivity of headspace analysis of low volatility solutes through water removal by hydrate formation. *Journal of Chromatography A* 2014, *1343*, 42-46.

27. Mills, G. A., Walker, V., Headspace solid-phase microextraction procedures for gas chromatographic analysis of biological fluids and materials. *Journal of Chromatography A* 2000, *902* (1), 267-287.

28. Hryniuk, A., Ross, B. M., Detection of acetone and isoprene in human breath using a combination of thermal desorption and selected ion flow tube mass spectrometry. *International Journal of Mass Spectrometry* 2009, *285* (1), 26-30.

29. Di Francesco, F., Fuoco, R., Trivella, M. G., Ceccarini, A., Breath analysis: trends in techniques and clinical applications. *Microchemical Journal* 2005, *79* (1), 405-410.

30. Lovestead, T. M., Bruno, T. J., Determination of cannabinoid vapor pressures to aid in vapor phase detection of intoxication. *Forensic Chemistry* 2017, *5* (Supplement C), 79-85.

31. Lovestead, T. M., Bruno, T. J., Trace headspace sampling for quantitative analysis of explosives with cryoadsorption on short alumina porous layer open tubular columns. *Analytical Chemistry* 2010, *82*, 5621-5627.

32. Bruno, T. J., Simple, quantitative headspace analysis by cryoadsorption on a short alumina PLOT column. *J Chromatogr Sci* 2009, *47* (7), 569-74.

33. Burger, J. L., Lovestead, T. M., Bruno, T. J., Composition of the C6+ fraction of natural gas by multiple porous layer open tubular capillaries maintained at low temperatures. *Energy & Fuels* 2016, *30* (3), 2119-2126.

34. Lovestead, T. M., Bruno, T. J., Detecting gravesoil with headspace analysis with adsorption on short porous layer open tubular (PLOT) columns. *Forens Sci Int* 2011, *204*, 156-161.

35. Nichols, J. E., Harries, M. E., Lovestead, T. M., Bruno, T. J., Analysis of arson fire debris by low temperature dynamic headspace adsorption porous layer open tubular columns. *Journal of Chromatography A* 2014, *1334*, 126-138.

36. Lovestead, T. M., Bruno, T. J., Detection of poultry spoilage markers from headspace analysis with cryoadsorption on a short alumina PLOT column. *Food Chem* 2010, *121*, 1274-1282.

37. Bruno, T. J., Field portable low temperature porous layer open tubular cryoadsorption headspace sampling and analysis Part I: Instrumentation. *Journal of Chromatography A* 2016, *1429*, 65-71.

38. Harries, M., Bukovsky-Reyes, S., Bruno, T. J., Field portable low temperature porous layer open tubular cryoadsorption headspace sampling and analysis Part II: Applications. *Journal of Chromatography A* 2016, *1429*, 72-78.

39. Ott, L. S., Smith, B.L., Bruno, T.J., Composition-explicit distillation curves of mixtures of diesel fuel with biomass-derived glycol ester oxygenates: a fuel design tool for decreased particulate emissions. *Energy & Fuels* 2008, *22*, 2518-2526.

40. Bruno, T. J., Smith, B. L., Enthalpy of combustion of fuels as a function of distillate cut: application of an advanced distillation curve method. *Energy & Fuels* 2006, *20*, 2109-2116.

41. Smith, B. L., Bruno, T.J., Advanced distillation curve measurement with a model predictive temperature controller. *Int J Thermophys* 2006, *27*, 1419-1434.

42. Ott, L. S., Bruno, T.J., Corrosivity of fluids as a function of distillate cut: application of an advanced distillation curve method. *Energy & Fuels* 2007, *21*, 2778 - 2784.

43. Ott, L. S., Smith, B.L., Bruno, T.J., Advanced distillation curve measurement: application to a bio-derived crude oil prepared from swine manure. *Fuel* 2008, *87*, 3379-3387.

44. Lovestead, T. M., Bruno, T.J., Application of the advanced distillation curve method to aviation fuel avgas 100LL. *Energy & Fuels* 2009, *23*, 2176-2183.

45. Bruno, T. J., Ott, L.S., Smith, B.L., Lovestead, T.M., Complex fluid analysis with the advanced distillation curve approach. *Analytical Chemistry* 2010, *82*, 777-783.

46. Huber, M. L., Smith, B.L., Ott, L.S., Bruno, T.J., Surrogate mixture model for the thermophysical properties of synthetic aviation fuel S-8: Explicit application of the advanced distillation curve. *Energy & Fuels* 2008, *22*, 1104 - 1114.

47. Carpenter, D., Westover, T. L., Czernik, S., Jablonski, W., Biomass feedstocks for renewable fuel production: a review of the impacts of feedstock and pretreatment on the yield and product distribution of fast pyrolysis bio-oils and vapors. *Green Chemistry* 2014, *16* (2), 384-406.

48. Hsieh, P. Y., Bruno, T. J., Pressure-controlled advanced distillation curve analysis and rotational viscometry of swine manure pyrolysis oil. *Fuel* 2014, *132*, 1-6.

49. Gug, J., Cacciola, D., Sobkowicz, M. J., Processing and properties of a solid energy fuel from municipal solid waste (MSW) and recycled plastics. *Waste Manag* 2015, *35*, 283–292.

50. Subramanian, P., Plastics recycling and waste management in the US. *Resour Conserv Recycl* 2000, *28* (3), 253–263.

51. Wang, H., Wang, L., Shahbazi, A., Life cycle assessment of fast pyrolysis of municipal solid waste in North Carolina of USA. *Journal of Cleaner Production* 2015, *87*, 511-519.

52. Hadler, A. B., Ott, L. S., Bruno, T. J., Study of azeotropic mixtures with the advanced distillation curve approach. *Fluid Phase Equilibria* 2009, *281*, 49-59.

53. Smith, B. L., Bruno, T.J., Improvements in the measurement of distillation curves - part 3: Application to gasoline and gasoline + methanol mixtures. *Ind Eng Chem Res* 2007, *46*, 297-309.

54. Ott, L. S., Smith, B.L., Bruno, T.J., Experimental test of the Sydney Young equation for the presentation of distillation curves. *J Chem Thermodynam* 2008, *40*, 1352-1357.

55. Young, S., Correction of boiling points of liquids from observed to normal pressures. *Proc Chem Soc* 1902, *81*, 777.

56. Bruno, T. J., Wolk, A., Naydich, A., Composition-explicit distillation curves for mixtures of gasoline and diesel fuel with gamma-valerolactone. *Energy & Fuels* 2010, *24* (4), 2758-2767.

57. Bruno, T. J., Svoronos, P.D.N, *CRC Handbook of Basic Tables for Chemical Analysis, 3rd. ed*. Taylor and Francis CRC Press: Boca Raton, 2011.

58. NIST/EPA/NIH mass spectral library with search program. National Institute of Standards and Technology SRD Program, Ed. Gaithersburg, MD, 2014.

59. Haynes W. M. (editor), *CRC Handbook of Chemistry and Physics, 97th ed.* Taylor and Francis CRC Press: Boca Raton, FL, 2017.

60. Orbital Engine Company. *A literature review based assessment on the impacts of a 20% ethanol gasoline fuel blend on the Australian vehicle fleet*; 2002.

61. Orbital Engine Company. *Market barriers to the uptake of biofuels study: A testing based assessment to determine the impacts of a 20 % ethanol gasoline fuel blend on the Australian passenger fleet*; 2003.

62. Burger, J. L., Gough, R. V., Bruno, T. J., Characterization of dieseline with the advanced distillation curve method: hydrocarbon classification and enthalpy of combustion. *Energy & Fuels* 2013, *27*, 878 - 795.

63. Windom, B. C., Lovestead, T.M., Bruno, T.J., Application of the advanced distillation curve method to the development of unleaded aviation gasoline. *Energy & Fuels* 2010, *24*, 3275 - 3284.

64. Mueller, C. J., Canella, W. J., Bruno, T. J., Bunting, B., Dettman, H. D., Franz, J. A., Huber, M. L., Natarajan, M., Pitz, W. J., Ratcliff, M. A., Wright, K., Methodology for formulating diesel surrogate fuels with accurate compositional, ignition quality and volatility characteristics. *Energy & Fuels* 2012, *26*, 3284-3303.

65. Windom, B. C., Huber, M. L., Bruno, T. J., Lown, A. L., Lira, C. T., Measurements and modeling study on a high aromatic diesel fuel. *Energy & Fuels* 2012, *26*, 1787-1797.

66. *ASTM D5186, Standard test method for determination of the aromatic content and polynuclear aromatic content of diesel fuels and aviation turbine fuels by supercritical fluid chromatography*. ASTM International: West Conschoken, PA, 2009.

67. *ASTM D613, Standard test method for cetane number of diesel fuel*. ASTM International: West Conshohocken, PA, 2010.

68. Bruno, T. J., Smith, B.L., Evaluation of the physicochemical authenticity of aviation kerosene surrogate mixtures Part I: Analysis of volatility with the advanced distillation curve *Energy & Fuels* 2010, *24*, 4266-4276.

69. Bruno, T. J., Huber, M.L., Evaluation of the physicochemical authenticity of aviation kerosene surrogate mixtures Part II: Analysis and prediction of thermophysical properties. *Energy & Fuels* 2010, *24*, 4277-4284.

70. *ASTM D4814, Standard specification for automotive spark-ignition engine fuel*. ASTM International: West Conshohocken, PA, 2015.

71. Bruno, T. J., Method and apparatus for precision in-line sampling of distillate. *Sep Sci Technol* 2006, *41* (2), 309-314.

72. Smith, B. L., Bruno, T.J., Improvements in the measurement of distillation curves - part 4: Application to the aviation turbine fuel Jet-A. *Ind Eng Chem Res* 2007, *46*, 310-320.

73. Rowley, R. L., Wilding, W. V., Oscarson, J. L., Zundel, N. A., Marshall, T. L., Daubert, T. E., Danner, R. P., DIPPR data compilation of pure compound properties. Design Institute for Physical Properties AIChE, New York, 2004.

74. Bruno, T. J., Wolk, A., Naydich, A., Stabilization of biodiesel fuel at elevated temperature with hydrogen donors: evaluation with the advanced distillation curve method. *Energy & Fuels* 2009, *23*, 1015-1023.

75. Ott, L. S., Bruno, T.J., Variability of biodiesel fuel and comparison to petroleum-derived diesel fuel: application of a composition and enthalpy explicit distillation curve method. *Energy & Fuels* 2008, *22*, 2861-2868.

76. Burger, J. L., Widegren, J. A., Lovestead, T., M., Bruno, T. J., 1H and 13C NMR analysis of gas turbine fuels as applied to the advanced distillation curve method. *Energy & Fuels* 2015, *29* (8), 4874-4885.

77. Agency for Toxic Substances and Disease Registry, Toxicological Profiles. http://www.atsdr.cdc.gov/toxprofiles/.

78. de Klerk, A., *Fischer-Tropsch Refining*. Wiley-VCH: Weinheim, Germany, 2011.

79. *ASTM D975, Standard specification for diesel fuel oils*. ASTM International: West Conshohocken, PA, 2015.

80. Bruno, T. J., Wolk, A., Naydich, A., Composition-explicit distillation curves for mixtures of gasoline with four-carbon alcohols (butanols). *Energy & Fuels* 2009, *23*, 2295-2306.

81. Smith, B. L., Ott, L.S., Bruno, T.J., Composition-explicit distillation curves of diesel fuel with glycol ether and glycol ester oxygenates: a design tool for decreased particulate emissions. *Environ Sci Tech* 2008, *42* (20), 7682-7689.

82. Newalkar, G., Iisa, K., D'Amico, A. D., Sievers, C., Agrawal, P., Effect of temperature, pressure, and residence time on pyrolysis of pine in an entrained flow reactor. *Energy & Fuels* 2014, *28* (8), 5144-5157.

83. Bruno, T. J., Smith, B.L., Improvements in the measurement of distillation curves - part 2: Application to aerospace/aviation fuels RP-1 and S-8. *Ind Eng Chem Res* 2006, *45*, 4381-4388.

84. Bruno, T. J., Improvements in the measurement of distillation curves - part 1: A composition-explicit approach. *Ind Eng Chem Res* 2006, *45*, 4371-4380.

85. Burger, J. L., Gough, R. V., Lovestead, T., M., Bruno, T. J., Characterization of the effects of cetane number improvers on diesel fuel volatility by use of the advanced distillation curve method. *Energy & Fuels* 2014, *24*, 2437-2445.

86. Hofmann, N., A geographical profile of livestock manure production in Canada, 2006. *EnviroStats* 2008, *2* (4), 12-16.

87. Ocean Recovery Alliance. *Plastics-to-fuel project developer's guide*; American Chemistry Council: Los Angeles, 2015.

88. Ott, L. S., Smith, B.L., Bruno, T.J., Advanced distillation curve measurements for corrosive fluids: application to two crude oils. *Fuel* 2008, *87*, 3055-3064.

89. Young, S., *Fractional distillation*. Macmillan and Co., Ltd.: London, 1903.

90. *ASTM E1064, Standard test method for water in organic liquids by coulometric Karl Fischer titration*. ASTM International: West Conshohocken, PA, 2012.

91. Bruno, T. J., Wolk, A., Naydich, A., Analysis of fuel ethanol plant liquor with the composition explicit distillation curve approach. *Energy & Fuels* 2009, *23* (6), 3277-3284.

92. Hsieh, P. Y., Bruno, T. J., Measuring sulfur content and corrosivity of North American petroleum with the advanced distillation curve method. *Energy & Fuels* 2014, *28*, 1868-1883.

93. Lou, R., Wu, S., Lyu, G., Quantified monophenols in the bio-oil derived from lignin fast pyrolysis. *J Anal Appl Pyrol* 2015, *111*, 27-32.

94. Yu, Y., Chua, Y. W., Wu, H., Characterization of pyrolytic sugars in bio-oil produced from biomass fast pyrolysis. *Energy & Fuels* 2016, *30* (5), 4145-4149.

95. Elkasabi, Y., Chagas, B. M. E., Mullen, C. A., Boateng, A. A., Hydrocarbons from spirulina pyrolysis bio-oil using one-step hydrotreating and aqueous extraction of heteroatom compounds. *Energy & Fuels* 2016, *30* (6), 4925-4932.

96. Outcalt, S. L., Lee, B.-C., A small-volume apparatus for the measurement of phase equilibria. *J Res Natl Inst Stand Technol* 2004, *109*, 525-531.

97. Mansfield, E., Bell, I. H., Outcalt, S. L., Bubble-point measurements of n-propane + n-decane binary mixtures with comparisons of binary mixture interaction parameters for linear alkanes. *J Chem Eng Data* 2016, *61*, 2573-2579.

98. Dejoz, A., González-Alfaro, V., Miguel, P. J., Vázquez, M. I., Isobaric Vapor−Liquid Equilibria for Binary Systems Composed of Octane, Decane, and Dodecane at 20 kPa. *Journal of Chemical & Engineering Data* 1996, *41* (1), 93-96.

99. Ma, X.-B., Liu, X.-G., Li, Z.-H., Xu, G.-H., Vapor–liquid equilibria for the ternary system methanol + dimethyl carbonate + dimethyl oxalate and constituent binary systems at different temperatures. *Fluid Phase Equilibria* 2004, *221* (1), 51-56.

100. Outcalt, S. L., Lemmon, E. W., Bubble-point measurements of eight binary mixtures for organic Rankine cycle applications. *Journal of Chemical & Engineering Data* 2013, *58* (6), 1853-1860.

101. Muhammad, F., Oliveira, M. B., Pignat, P., Jaubert, J.-N., Pinho, S. P., Coniglio, L., Phase equilibrium data and modeling of ethylic biodiesel, with application to a non-edible vegetable oil. *Fuel* 2017, *203*, 633-641.

102. Matthews, M. A., Li, F., Towler, B. F., Bell, D. A., Vapor liquid equilibrium measurements with semi-continuous mixtures. *Fluid Phase Equilibria* 1995, *111*, 101-111.

103. Angelos, C. P., Bhagwat, S.V., Matthews, M.A., Measurement and modeling of phase equilibria with synthetic multicomponent mixtures. *Fluid Phase Equilibria* 1992, *72*, 182-209.

104. Li, H., Jakobsen, J. P., Wilhelmsen, Ø., Yan, J., PVTxy properties of CO2 mixtures relevant for CO2 capture, transport and storage: Review of available experimental data and theoretical models. *Applied Energy* 2011, *88* (11), 3567-3579.

105. Ioffe, B. V., Vittenburg, A.G., Manatov, I.A., *Head-Space Analysis and Related Methods in Gas Chromatography*. Wiley-Interscience: 1984.

106. Ghasemi, E., Sillanpaa, M., Optimization of headspace solid phase microextraction based on nano-structured ZnO combined with gas chromatography-mass spectrometry for preconcentration and determination of ultra-traces of chlorobenzenes in environmental samples. *Talanta* 2014, *130*, 322-327.

107. Higashikawa, F. S., Cayuela, M. L., Roig, A., Silva, C. A., Sánchez-Monedero, M. A., Matrix effect on the performance of headspace solid phase microextraction method for the analysis of target volatile organic compounds (VOCs) in environmental samples. *Chemosphere* 2013, *93* (10), 2311-2318.

108. Lorenzo, N., Wan, T., Harper, R. J., Hsu, Y.-L., Chow, M., Rose, S., Furton, K. G., Laboratory and field experiments used to identify Canis lupus var. familiaris active odor signature chemicals from drugs, explosives, and humans. *Analytical and Bioanalytical Chemistry* 2003, *376* (8), 1212-1224.

109. National Center for Forensic Science University of Central Florida, Ignitable Liquids Reference Collection Database. http://ilrc.ucf.edu/.

110. Birks, H. L., Cochran, A. R., Williams, T. J., Jackson, G., The surprising effect of temperature on the weathering of gasoline. *Forensic Chemistry* 2017, *4*, 32-40.

111. Martín-Alberca, C., Ortega-Ojeda, F., García-Ruiz, C., *Analytical tools for the analysis of fire debris. A review: 2008-2015*, Vol. 928, 2016.

112. Baerncopf, J. M., McGuffin, V. L., Smith, R. W., Association of ignitable liquid residues to neat ignitable liquids in the presence of matrix interferences using chemometric procedures. *Journal of Forensic Sciences* 2011, *56* (1), 70-81.

113. Ferris, A. M., Rothamer, D. A., Methodology for the experimental measurement of vapor–liquid equilibrium distillation curves using a modified ASTM D86 setup. *Fuel* 2016, *182*, 467-479.

114. Windom, B. C., Bruno, T.J., Improvements in the measurement of distillation curves-part 5: Reduced pressure distillation curve method. *Ind Eng Chem Res* 2011, *50*, 1115-1126.

115. Anitescu, G., Bruno, T. J., Biodiesel fuels from supercritical fluid processing: quality evaluation with the advanced distillation curve method and cetane numbers. *Energy & Fuels* 2012, *26*, 5256-5264.

116. Burger, J., Harries, M., Bruno, T. J., Characterization of four diesel fuel surrogates by the advanced distillation curve method. *Energy & Fuels* 2016, *30* (4), 2813–2820.

117. Burger, J. L., Bruno, T. J., Application of the advanced distillation curve method to the variability of jet fuels. *Energy & Fuels* 2012, *26*, 3661-3671.

118. Hsieh, P. Y., Abel, K., Bruno, T. J., Analysis of marine diesel fuel with the advanced distillation curve method. *Energy & Fuels* 2013, *27*, 804-810.

119. Lovestead, T. M., Windom, B.C., Riggs, J.R., Nickell, C, Bruno, T.J., Assessment of the compositional variability of RP-1 and RP-2 with the advanced distillation curve approach. *Energy & Fuels* 2010, *24*, 5611-5623.

120. Windom, B. C., Bruno, T. J., Application of pressure-controlled advanced distillation curve analysis: virgin and waste oils. *Ind Eng Chem Res* 2013, *52*, 327-337.

121. Bruno, T. J., Allen, S., Weathering patterns of ignitable liquids with the advanced distillation curve method. *J Res Nat Inst Stds Tech (US)* 2012, *117*, 29-51.

122. Bruno, T. J., Lovestead, T. M., Huber, M. L., Prediction and preliminary standardization of fire debris analysis constituents with the advanced distillation curve method. *J Forensic Sci* 2011, *56*, S191 - S202.

123. Bruno, T. J., Ott, L.S., Lovestead, T.M., Huber, M.L., Relating complex fluid composition and thermophysical properties with the advanced distillation curve approach. *Chemical Eng Tech* 2010, *33* (3), 363-376.

124. Bruno, T. J., Abel, K., Riggs, J. R., Comparison of JP-8 and JP-8+100 with the advanced distillation curve approach. *Energy & Fuels* 2012, *26*, 5843 - 5850.

125. Burger, J. L., Schneider, N., Bruno, T. J., Application of the advanced distillation curve method to fuels for advanced combustion gasoline engines. *Energy & Fuels* 2015, *29*, 4227 - 4235.

126. Harries, M., Sharma, B. K., Bruno, T. J., Application of the advanced distillation curve method for the characterization of two alternative transportation fuels prepared from the pyrolysis of polyethylene bags. *Energy & Fuels* 2016, *30*, 9671-9678.

127. Lovestead, T. M., Bruno, T.J., Comparison of the hypersonic vehicle fuel JP-7 to the rocket propellants RP-1 and RP-2 with the advanced distillation curve method. *Energy & Fuels* 2009, *23* (7), 3637-3644.

128. Lovestead, T. M., Windom, B.C., Bruno, T.J., Investigating the unique properties of Cuphea derived biodiesel fuel with the advanced distillation curve method. *Energy & Fuels* 2010, *24*, 3665-3675.

129. Windom, B. C., Bruno, T. J., Pressure controlled advanced distillation curve analysis of biodiesel fuels: assessment of thermal decomposition. *Energy & Fuels* 2012, *26*, 2407 - 2415.

130. Lemmon, E. W., McLinden, M.O., Huber, M.L., REFPROP, Reference fluid thermodynamic and transport properties, NIST Standard Reference Database 23, V9.1. National Institute of Standards and Technology, Gaithersburg, MD: 2013.

131. Huber, M. L., Lemmon, E.W., Bruno, T.J., Surrogate mixture models for the thermophysical properties of aviation fuel Jet-A. *Energy & Fuels* 2010, *24*, 3565-3571.

132. Mueller, C. J., Cannella, W. J., Bays, J. T., Bruno, T. J., DeFabio, K., Dettman, H. D., Gieleciak, R. M., Huber, M. L., Kweon, C.-B., McConnell, S. S., Pitz, W. J., Ratcliff, M. A., Diesel surrogate fuels for engine testing and chemical-kinetic modeling: Compositions and properties. *Energy & Fuels* 2016, *30* (2), 1445-1461.

133. Kunz, O., Klimeck, R., Wagner, W., Jaesche, M., The GERG-2004 Wide-Range Reference Equation of State for Natural Gases and Other Mixtures; GERG Technical Monograph Fortschr.-Ber. VDI; VDI-Verlag:Dusseldorf, Germany. 2007.

134. Lemmon, E. W., Jacobsen, J. T., A generalized thermodynamic model for the thermodynamic properties of mixtures. *Int J Thermophys* 1999, *20* (3), 825-835.

135. Peng, D.-Y., Robinson, D. B., A new two-constant equation of state. *Ind Eng Chem Fundam* 1976, *15* (1), 59-64.

136. Personal communication to M. Harries from M.L. Huber, NIST, Boulder, CO. 2016.

137. Lemmon, E. W., McLinden, M. O., *Method for estimating mixture equation of state parameters*. Proc Thermophysical Properties and Transfer Processes of New Refrigerants Conference, Paderborn, Germany, International Institute of Refrigeration: Paderborn, Germany, 2001; pp 23-30.

138. Young, S., *Distillation principles and processes*. Macmillan and Co., Ltd.: London, 1922.

139. Organisation for Economic Co-operation and Development, *OECD Guideline for the testing of chemicals, No. 103, boiling point*. Paris, France, 1995.

140. Bruno, T. J., Svoronos, P.D.N., *CRC Handbook of Fundamental Spectroscopic Correlation Charts*. Taylor and Francis CRC Press: Boca Raton, 2006.

141. Bruno, T. J., Simple, quantitative headspace analysis by cryoadsorption on a short alumina PLOT column. *J Chromatogr Sci* 2009, *47*, 5069-5074.

142. United States Code of Federal Regulations, Title 40: Protection of Environment, Part 136 – Guidelines establishing test procedures for the analyses of pollutants, Appendix B to Part 136 – definition and procedure for the determination of Method Detection Limit. 1999.

143. National Advisory Committee for Acute Exposure Guideline Levels for Hazardous Substances, Acute Exposure Guideline Levels (AEGLs) for 1,3,5-trimethylbenzene, 1,2,4-trimethylbenzene, 1,2,3-trimethylbenzene. US Environmental Protection Agency, Washington, DC, 2007.

144. American Conference of Governmental Industrial Hygienists, Trimethyl benzene isomers. In *Documentation of the Threshold Limit Values and Biological Exposure Indices*, Cincinnati, OH, 2002.

145. National Institute for Occupational Safety and Health, NIOSH recommendations for occupational safety and health: Compendium of policy documents and statements. US Department of Health and Human Services, Cincinnati, OH, 1992.

146. Office of Emergency and Remedial Response, Guidance for Performing Site Inspections Under CERCLA. US Environmental Protection Agency, Washington, DC, 1992.

147. UN-Business Action Hub., IMO (International Maritime Organization) profile. https://business.un.org/en/entities/13.

148. Security and Accountability for Every Port Act. *Public Law 109-347*, 109th Congress, 2006.

149. Hutchins, R., Debate reignites over container scanning of US imports. *Journal of Commerce* 2016.

150. Scan Containers Absolutely Now (SCAN) Act. 113th Congress, 2014.

151. Scan Containers Absolutely Now (SCAN) Act. 114th Congress, 2016.

152. Counter-Terrorism Committee Executive Directorate. *Physical protection of critical infrastructure against terrorist attacks*; United Nations Security Council: 2017.

153. Miller, E. *Terrorist Attacks Targeting Critical Infrastructure in the United States, 1970-2015*; START: College Park, MD, 2016.

154. US Customs and Border Protection, CSI: Container Security Initiative. https://www.cbp.gov/border-security/ports-entry/cargo-security/csi/csi-brief.

155. Rouhi, A. M., Detecting illegal substances. *Chemical & Engineering News* 1997.

156. U.S. Customs and Border Protection. *Inspection and Detection Technology: Multi-Year Investment and Management Plan (FY 2016-2021)*; 2016.

157. Dworzanski, J. P., Kim, M.-G., Peter Snyder, A., Arnold, N. S., Meuzelaar, H. L. C., Performance advances in ion mobility spectrometry through combination with high speed vapor sampling, preconcentration and separation techniques. *Analytica Chimica Acta* 1994, *293* (3), 219-235.

158. Antoine, C., Tensions des vapeurs; nouvelle relation entre les tensions et les températures [Vapor pressure: a new relationship between pressure and temperature]. *Comptes Rendus des Séances de l'Académie des Sciences (in French)* 1888, *107*, 681–684, 778–780, 836–837.

159. Yaws, C. L., *The Yaws Handbook of Vapor Pressure*. 2nd ed.; Gulf Professional Publishing: Oxford, 2015.

160. Linstrom, P. J., Mallard, W.G., NIST Chemistry WebBook, NIST Standard Reference Database Number 69, June 2005, National Institute of Standards and Technology, Gaithersburg MD, 20899 (http://webbook.nist.gov).

APPENDIX

Headspace analysis: Static

Reprinted from Harries and Bruno, Headspace Analysis: Static, Journal of Analytical Science 3rd ed, 2018.

1. Introduction

Headspace analysis is a technique for sampling and examining the volatiles in a solid or liquid sample. The term headspace refers to the volume of vapor above a condensed phase sample. For most headspace analyses, the sample and its associated headspace are held within an enclosed container (Figure 1). It is often the volatiles that are of primary importance when, for example, the chemical composition of the mixture giving rise to the aroma of the sample is to be determined. In other circumstances, examination of the headspace rather than the condensed phase sample greatly decreases the analytical complications that result from a complex matrix and still yields information relating to the whole sample.

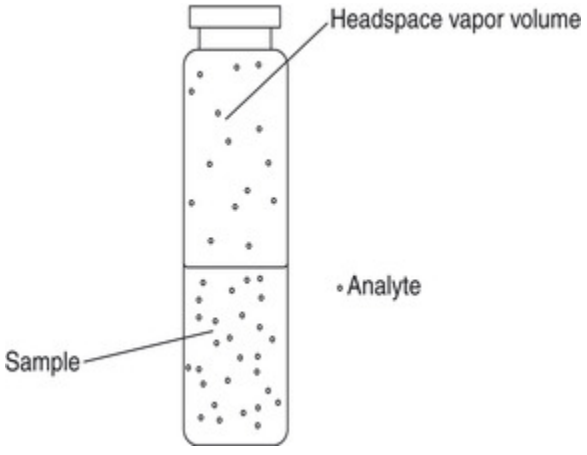

Figure 1. The fundamental concept of headspace analysis.

2. Principles

Once collected, a headspace sample can be examined by any appropriate analytical method, although the technique is most often associated with gas chromatography (GC), or gas chromatography with mass spectrometry detection (GC-MS). The simplest approach to headspace sampling is to use a gas-tight syringe to withdraw some of the headspace contained in a closed volume above the sample and subsequently inject it into the analytical instrumentation. Alternatively, an automated system can be used in which the sample can be conditioned in various ways according to the capabilities of the instrumentation prior to introduction into the analytical system using autosampler syringe technology or a sample transfer line. The results obtained depend upon the analytical technique chosen to supplement the headspace sampling procedure.

Static and dynamic headspace sampling techniques may be distinguished as shown diagrammatically in Figure 2. Static methods involve the removal of a small fraction of the headspace in equilibrium with the condensed phase. Dynamic methods involve the continuous removal of headspace from above the sample followed by a concentration of the vapors either cryogenically or using a porous adsorbent. The concentrated sample from the dynamic sampling may then be revaporized (from a cryogenic trap) or desorbed (from a solid adsorbent thermally or by use of a solvent) and analyzed by an appropriate technique. Less commonly, solvents can be used to collect and preconcentrate headspace; two examples of such techniques are continuous flow thin layer headspace, which concentrates headspace analytes in a thin layer of a flowing liquid, and single drop microextraction (SDME), during which a drop of solvent suspended from a syringe is exposed to the headspace of a sample of interest. The analytes

concentrated in the solvent can then be analyzed by the appropriate technique, including voltammetry, nuclear magnetic resonance (NMR), GC-MS, and so forth.

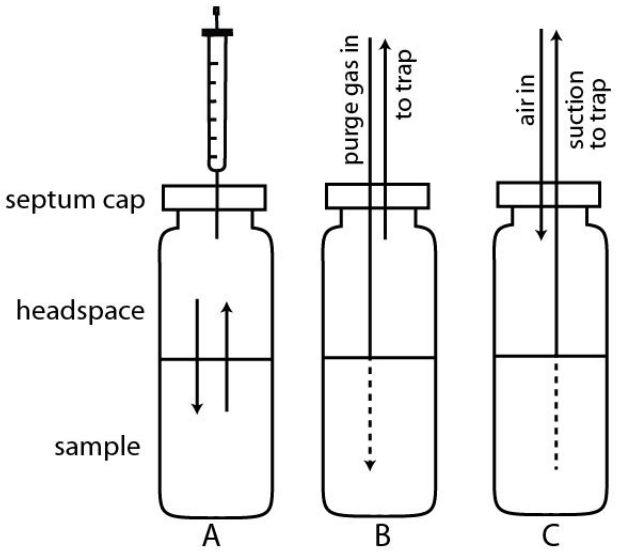

Figure 2. Concepts of static headspace (A) in which equilibrium is established, and dynamic headspace using purge gas (B) and suction (C).

Qualitative headspace analysis is used in many applications to determine differences between selected samples, to identify a mixture by comparison to a known sample, and to assess the importance of specific compounds in defining the aroma character of certain materials. This approach is often termed 'fingerprinting,' as in many instances the composition is not fully characterized. Additional qualitative data can be obtained using knowledge of GC retention data or with GC–MS techniques to definitively identify components in a headspace sample.

Quantitative relationships exist between the concentrations of volatiles in equilibrium with liquid samples, and these form the basis of quantitative theory for headspace techniques. The sensitivity of headspace analysis is influenced principally by two sample-related parameters:

the partition coefficient (K) of the analyte between the phases and the phase ratio (β) of sample to vapor.

The partition coefficient (or distribution coefficient) K is the parameter of fundamental importance, and it is defined as the ratio of concentration of analyte (a) in the sample phase (s) C_a^s to that in the vapor phase (v) C_a^v at equilibrium (eqn [1]):

$$[1].\ K = \frac{C_a^s}{C_a^v}$$

The phase ratio, β, is defined as the ratio of volume of the vapor phase V^v to the volume of the sample phase V^s (eqn [2]):

$$[2].\ \beta = \frac{V^v}{V^s}$$

Using these two dimensionless parameters and additional algebra not shown here, we can develop a simple expression for the sensitivity of a method applied to a given sample with original concentration C_a^0. There are many ways to define and evaluate sensitivity; in this context, it refers to the ability of the method to correctly detect or measure the value of interest. Because C_a^v is related to the analytical response to the collected headspace sample, we can use it as a measure of sensitivity (eqn [3]):

$$[3].\ C_a^v = \frac{C_a^0}{K+\beta}$$

Equation [3] shows that for a given concentration of an analyte in the original sample, C_a^0, the analytical response, which is proportional to C_a^v, will depend upon K and β. With a large value of K (e.g. 5260 for ethanol in water at 25 °C), the phase ratio has minimal influence. Conversely, for a small value of K (e.g. 4 for benzene in water at 25 °C), the phase ratio has a significant bearing upon the sensitivity. Chemical methods for modifying the partition characteristics of the system are appropriate in some cases. Perhaps the most well-known

practice is “salting out,” the addition of salts to the liquid phase to induce a higher concentration of organics in the vapor phase. In addition, as it does in any analytical method, the sensitivity of the detector used and the capacity of the analytical system for the sample will influence the sensitivity that can be achieved.

As mentioned, quantitative analysis using headspace techniques is dependent on the partition of the analyte between the sample and vapor phases. Although it is the vapor phase that is sampled and analyzed, the concentration of the analyte in the sample phase is usually the desired quantity. The four approaches to quantitative headspace analysis discussed below (total vaporization, matrix-matched analyte standards, multiple headspace extraction, and standards addition) enable the determination of this value.

3. Quantitative Headspace Analysis

3.1. Total Vaporization

Total vaporization of the analyte into the vapor phase is the simplest approach to quantification but can only be achieved with samples that are particularly suitable. For example, a polymeric matrix containing residual water could be heated to 150°C to effectively drive all the water into the vapor. Headspace analysis of the vapor phase in conjunction with external calibration will give the concentration of water in the vapor phase. From this and knowledge of the vapor phase volume, the total amount of water present in the sample can be calculated. This is expressed in the trivial equality between the mass of analyte in the sample and its mass in the vapor after total vaporization is achieved (eqn [4]):

$$[4].\ M_a^s = M_a^v$$

which becomes (eqn [5]):

$$[5].\ M_a^s = C_a^v V^v$$

where V^v is total vapor volume. Conversely, of course, with a known sample mass and volume, the concentration of analyte in the sample may be calculated.

3.2. Matrix-Matched Analyte Standards

In most practical cases, the analyte will not be totally vaporized, but rather it will be distributed between the condensed and vapor phases. Calibration with matrix-matched standards involves preparing known concentrations of analyte in a matrix identical to that of the sample. These standards are then analyzed under identical conditions to the sample and to construct a calibration graph. This procedure is practical for liquid samples and is applied as described in eqn [6]:

$$[6].\ C_a^s = C_a^{std} \frac{A_a}{A_{std}}$$

where C_a^{std} is the concentration of analyte in the prepared standard, A_a is the analytical response to the analyte in the sample, and A_{std} is the analytical response to the analyte in the prepared standard. For solid samples, preparation of valid matrix-matched standards is more difficult because the analyte in the real sample may be bound in a different form from that in the standard. These so-called matrix effects are difficult to overcome; however, the multiple headspace extraction method may be applied to solid samples.

3.3. Multiple Headspace Extraction

Multiple headspace extraction is a valuable quantitation method for quantification of volatiles in solid samples or for quantifying highly volatile analytes for which the preparation of accurate standards is experimentally difficult. If headspace is extracted multiple times from one

sample, the analyte concentration progressively decreases until no analyte is detected. Summing the results from all extractions produces the total analyte concentration in the sample. While it would be time intensive to conduct the necessary extractions to reach zero analyte, simpler practical approaches using the same concept exist: multiple headspace extraction is a variant of methods known as stepwise gas extraction and discontinuous gas extraction.

The practical approach to quantification via this method is to conduct a limited series of headspace analyses on the same sample which is conditioned to equilibrium between each extraction. From the progressive decrease in measured concentrations, the total analyte concentration in the sample can be calculated.

With a continuous gas extraction, the concentration of analyte present at time *t* is expressed (eqn [7]):

$$[7].\ C = C_a^o e^{-kt}$$

in which C_a^o is the initial concentration and *k* is an exponent that includes the partition coefficient *K*. (The mathematical derivation, and the omitted steps in deriving all the equations used in this entry, can be found in detail in the texts cited in Further Reading.) In practice, the total concentration in the sample can be calculated from the analysis of only two extractions. This is described in eqn [8] for the case where concentration is proportional to analytical response (substitute *C* for *A* in all other cases):

$$[8].\ \sum A_n = \frac{A_1^2}{A_1 - A_2}$$

3.4. Standard Addition

Finally, standard addition is a method used to quantify headspace analysis in cases where a standard solution of the analyte can be added to the sample in such a way that it exists in an

identical form in relation to the matrix as the analyte itself. Analysis of the original sample and the sample spiked with a known quantity of analyte can then provide a value for the concentration of analyte in the original sample (C_a^s).

The analytical response to the original sample (A_a), the analytical response to the standard-added sample (A_a^*), and the known concentration of the standard solution (C_{std}), are needed to calculate C_a^s. When the volume of the standard solution added is small (as is typical in practice), eqn [9] describes this relationship.

$$[9].\ C_a^s = \frac{A_a C_{std}}{A_a^* - A_a}$$

The choice of quantification in headspace analysis depends on the sample and the analyte. Procedures include total vaporization, the use of matrix-matched standards, multiple extractions, and standard additions. A method using an internal standard may also be used, provided that the equilibrium constants for the standard and the analyte are known.

4. Apparatus

Headspace analysis in its simplest form requires only a vial of suitable volume with a septum turn closure through which a sample of the vapor may be collected using a gas-tight syringe. This method of sampling can be effective for simple applications to volatile analytes where a qualitative or semiquantitative analysis is required.

Headspace preconcentration can be accomplished with a range of static approaches for more demanding applications involving trace quantities or involatile analytes. Preconcentration collects a larger amount of analyte than direct sampling with a syringe and is thus more sensitive. Such methods include solid phase microextraction (SPME), passive samplers (often used in the field, including in some standard EPA test methods), and the carbon strip (used in arson fire

debris analysis). A variety of adsorbent materials are available for use with these methods, such as porous polymers, silica, alumina, and carbon. Resources to assist with the choice of an adsorbent are given in Further Reading—see the CRC Handbook of Basic Tables for Chemical Analysis.

Depending on the chosen sampling method and the desired analysis, an adsorbent used for preconcentration may be thermally desorbed by rapid heating inside the inlet of an analytical instrument; desorption is also often accomplished by solvent elution. Solvent elution, producing a sample in liquid form, is more versatile, as it can be stored or injected multiple times and analyzed by more than one analytical instrument; however, for analysis of very low concentration solutes (trace levels), use of solvent may not be appropriate as it could dilute the analyte collected on the adsorbent.

Commercially available systems for static headspace collection exist from several major instrument manufacturers. These systems can provide the means for automatic conditioning of samples and features like vial shaking, constant equilibration times, and method development options (whereby parameters can be tuned to a variety of samples). Automated methods to introduce samples into analytical instrumentation include automated syringe technology, sample valve and loop techniques, and direct coupling using pressure-balanced sampling.

Headspace sampling methods and equipment for a wide range of specific applications are described in the literature. For example, apparatus have been designed and reported for sampling the headspace of canned foods and whole cheeses and from single cigarettes. Some applications are better suited to static or dynamic sampling methods; for example, PLOT-cryoadsorption, a dynamic headspace method, is optimal in special cases of extremely low volatility solutes like drug compounds and plasticizers used in explosives.

5. Applications

While we discuss the applications below in the context of static methods, we note that dynamic purge and trap methods can be used with many of these examples as well. See the separate article on purge and trap methods for additional details. Headspace techniques have been used for examining a wide variety of samples including environmental samples of soil, water, and air, biological fluids, foodstuffs and related materials, forensic samples, pharmaceuticals, natural products, and polymers. Such samples are examined to ensure environmental protection, to diagnose medical conditions, to establish compliance with regulations in the food, pharmaceutical, and packaging industries, to evaluate evidence in criminal investigations, and for the direct determination of volatiles influencing taste and aroma. All these applications benefit from the advantages of headspace analysis, either by removing some of the matrix effects or because of its direct relation to aroma volatiles. As mentioned above, static headspace analysis is closely associated with purge and trap and other dynamic techniques which extract headspace from a sample using purge gas. This is an overview of some major applications.

Environmental samples of soil, water, and air are frequently analyzed (sometimes for enforcement of regulation) using headspace techniques. Soils, estuarine sediments, and industrial wastes (wastewater) are screened for volatile organics including chlorinated hydrocarbons, benzene, and other aromatics. Groundwater samples have been examined for a wide range of volatile substances including chlorinated hydrocarbons, carbon disulfide, components of gasoline from fuel spills, and methyl-mercury. The latter analysis was carried out using GC with atomic emission detection. Headspace sampling techniques have been used to test drinking water for

volatile constituents including halocarbons, aromatics, and chloral hydrate. Dissolved gases and light hydrocarbons have been determined in seawater. In some cases, headspace methods have lower limits of detection than direct injection procedures, and the problems associated with aqueous samples (column overloading and detector memory effects) can be eliminated. Headspace sampling is also used to monitor workplace and domestic environments for hazards. Several examples are solvents in waste gases, vulcanization volatiles in the rubber industry, and alkylated benzenes and formaldehyde from particle board products.

Biological samples of urine, blood, expired air, and tissue have been examined using headspace sampling approaches, often for clinical reasons. Blood has been examined for alcohol, cyanide, methyl sulfide, and formaldehyde levels, the last as a measure of methanol intoxication. Use of headspace methods for blood samples overcomes the difficulties associated with the alternative, direct injection of two-phase samples. Urine is screened for chlorinated organic compounds, methanol, acetone, methyl ethyl ketone, and phenols; these and other volatile substances in urine can be a guide to acute poisoning or to detect stimulants. Breath has been examined for markers of illness.

Like blood, milk is a two-phase suspension which creates some analytical difficulties for direct injection methods; headspace techniques have been used to overcome these and to determine the odor components that have a bearing upon milk quality in processing and storage.

Trace components in alcoholic drinks can be determined following headspace concentration procedures, although great care is required to establish that the major components present in the sample are not influencing the partition of the analyte of interest between the liquid and headspace phases.

Solid samples can of course also be analyzed using headspace techniques. When solids such as polymers and tablet formulations of pharmaceuticals dissolve completely, they can be dealt with as solutions. For insoluble solids, the headspace can be characterized for volatiles, but quantification, which has been discussed above, is less straightforward.

Headspace analysis lends itself naturally to the determination of the volatile aroma compounds of natural products, their essential oils and extracts. Fruits, tobacco, hops, mushrooms, and various plants have been examined to determine the volatiles present. Such investigations provide information relating to the important chemistry of aroma, taste, and flavor; food quality and freshness can also be assessed. This has advanced the understanding of the development of odor in fresh, processed, and preserved food products as well as in flowers, from which fragrances are extracted and developed. Consequently, criteria of quality have been established, and the changes in volatile composition occurring as a result of aging, storage, and processing procedures have been characterized. As diverse examples, headspace techniques have been used to examine truffle aroma, volatiles in canned salmon, kiwi fruit flowers, butter, and spoiled poultry. Synthesis of nature-identical flavors has been significantly advanced by the results of headspace analysis in this area of aroma and flavor research.

Volatile components of packaging materials in foods can be detected and quantified using headspace techniques, including monomeric residues in polymeric products. Monomer impurities may be undesirable with respect to subsequent usage, especially as packaging for food because of the off odors and toxicity produced by the volatile species present. As an example, vinyl chloride as a component of poly(vinyl chloride) (PVC) has been determined in olive oil after storage in PVC containers.

Headspace techniques can be used to determine a number of thermodynamically important properties relating to vapor–liquid equilibria. The technique has been used to develop distillation procedures specifically where the selection of solvents in extractive distillation is required. Vapor pressures of pure substances and activity coefficients may also be determined using headspace techniques.

Several of the above applications of headspace analysis present unique challenges. Two examples are the detection of low volatility analytes and the presence of water in the sample.

To determine involatile components in a sample using headspace, sampling can be preceded by a chemical treatment (derivatization) to produce a volatile compound from the analyte of interest. It is thus possible to determine fluoride in fluorinated milk following initial treatment to produce volatile trifluorosilane. Information about derivatizing reagents can be found in the CRC Handbook of Basic Tables for Chemical Analysis (Further Reading). Sample adulteration is undesirable for a number of reasons, and recent advances have been made to increase the effectiveness of headspace methods on low volatility samples. Dynamic methods like PLOT-cryoadsorption are very sensitive to involatile analytes and circumvent the need for derivatization by use of a low-temperature adsorbent capillary trap to capture the vapors above explosives, weathered fuels, and drug compounds, for example.

The challenges presented by aqueous matrices can be addressed with selectively permeable membranes (like Nafion) or through desiccated headspace, the addition of anhydrous salts to the sample to form hydrate precipitates and remove the liquid water from the sample. Care must be taken to control the hydrate formation reaction, which is exothermic. The addition of water scavengers is rarely used and produces contaminants. Salting out does not remove any water from the sample but decreases the solubility of the desired volatiles in the water, enriching

the headspace. This method has limited benefit. It is not desirable to alter a sample by removal or addition of any part of it; however, well-characterized alterations may be advantageous for difficult aqueous samples.

Finally, standard methods for headspace analysis exist for many of the above applications. Details are given in Table 1.

Table 1. A selection of standard methods using both static and dynamic headspace techniques; many more are available through the sources below. Sources: ASTM, American Society for Testing and Materials; SASO, Saudi Arabian Standards Organization; US EPA, United States Environmental Protection Agency.

	Determination of residual volatiles
ASTM D4443	Standard Test Method for Determining Residual Vinyl Chloride Monomer Content in PPB Range in Vinyl Chloride Homo- and Co-Polymers by Headspace Gas Chromatography
ASTM D3749	Standard Test Method for Residual Vinyl Chloride Monomer in Poly(Vinyl Chloride) Resins by Gas Chromatographic Headspace Technique
	Fire debris samples
ASTM E1413	Standard Practice for Separation of Ignitable Liquid Residues from Fire Debris Samples by Dynamic Headspace Concentration
ASTM E1412	Standard Practice for Separation of Ignitable Liquid Residues from Fire Debris Samples by Passive Headspace Concentration with Activated Charcoal
ASTM E1388	Standard Practice for Static Headspace Sampling of Vapors from Fire Debris Samples
	Recommended methods and apparatus
ASTM D5116	Standard Guide for Small-Scale Environmental Chamber Determinations of Organic Emissions from Indoor Materials/Products
ASTM D4526	Standard Practice for Determination of Volatiles in Polymers by Static Headspace Gas Chromatography
ASTM F2714	Standard Test Method for Oxygen Headspace Analysis of Packages Using Fluorescent Decay
	Soil and water samples
US EPA Method 5021A	Volatile Organic Compounds in Various Sample Matrices Using Equilibrium Headspace Analysis
ASTM D3871	Standard Test Method for Purgeable Organic Compounds in Water Using Headspace Sampling
ASTM D6520	Standard Practice for the Solid Phase Micro Extraction (SPME) of Water and its Headspace for the Analysis of Volatile and Semi-Volatile Organic Compounds
ASTM D6889	Standard Practice for Fast Screening for Volatile Organic Compounds in Water Using Solid Phase Microextraction (SPME)
ASTM D8028	Standard Test Method for Measurement of Dissolved Gases Methane, Ethane, Ethylene, and Propane by Static Headspace Sampling and Flame Ionization Detection (GC/FID)
	Foodstuffs
SASO 440	Methods of Test for Vegetables, Fruits and Their Products, First Part: Organoleptic Examination, Determination of Net Weight and Drained Weight, Determination of Apparent Viscosity, Determination of Headspace, Determination of Extraneous Matter and Defective Fruits

Further Reading

ASTM International, https://www.astm.org/.

Baránková, E. and Dohnal, V. (2016). Effects of additives on volatility of aroma compounds from dilute aqueous solutions. Fluid Phase Equilibria 407, 217-223.

Bruno, T. J., Svoronos, P.D.N, *CRC Handbook of Basic Tables for Chemical Analysis, 3rd. ed*. Taylor and Francis CRC Press: Boca Raton, 2011.

Index to EPA test methods, https://www.epa.gov/measurements/index-epa-test-methods.

Hu, H.-C. and Chai, X.-S. (2012). Determination of methanol in pulp washing filtrates by desiccated full evaporation headspace gas chromatography. Journal of Chromatography A 1222 (Supplement C), 1-4.

Ioffe, B. V. and Vitenberg, A. G. (1984). Head-space analysis and related methods in gas chromatography. New York: Wiley.

Kocúrová, L., Balogh, I.S., and Andruch, V. (2013). A glance at achievements in the coupling of headspace and direct immersion single-drop microextraction with chromatographic techniques. Journal of Separation Science 36, 3758-3768.

Kolb, B. and Ettre, L. (1997). Static headspace–gas chromatography: theory and practice. (2nd ed.). New York: Wiley.

Lovestead, T. M. and Bruno, T. J. (2010). Trace headspace sampling for quantitative analysis of explosives with cryoadsorption on short alumina porous layer open tubular columns. Analytical Chemistry 82, 5621-5627.

Lovestead, T.M., Bruno, T.J. (2017). Determination of cannabinoid vapor pressures to aid in vapor phase detection of intoxication. Forensic Chemistry 5, 79-85.

Mills, G. A. and Walker, V. (2000). Headspace solid-phase microextraction procedures for gas chromatographic analysis of biological fluids and materials. Journal of Chromatography A 902, 267-287.

Risticevic, S., Lord, H., Górecki, T., Arthur, C.L., and Pawliszyn, J. (2010). Protocol for solid-phase microextraction method development. Nature Protocols 5(1), 122-139.

Saudi Standards, Metrology, and Quality Org (SASO) standard specifications, https://www.saso.gov.sa/en/standards/Pages/default.aspx.

Sghaier, L., Vial, J., Sassiat, P., et al. (2016). An overview of recent developments in volatile compounds analysis from edible oils: Technique-oriented perspectives. European Journal of Lipid Science and Technology 118, 1853-1879.

Souza-Silva, E.A., Gionfriddo, E., and Pawliszyn, J. (2015). A critical review of the state of the art of solid-phase microextraction of complex matrices II. Food analysis. Trends in Analytical Chemistry 71, 236-248.

Tiscione, N.B., Yeatman, D.T., Shan, X., and Kahl, J.H. (2013). Identification of volatiles by headspace gas chromatography with simultaneous flame ionization and mass spectrometric detection. Journal of Analytical Toxicology 37, 573-579.

Truong, T.V., Porter, N.L., Lee, E.D., and Thomas, R.J. (2016). The applicability of field-portable GC-MS for the rapid sampling and measurement of high-boiling-point semivolatile organic compounds in environmental samples. The Application Notebook September 2016, 30-36.

Urbanowicz, M., Zabiegała, B., and Namieśnik, J. (2011). Solventless sample preparation techniques based on solid- and vapour-phase extraction. Analytical and Bioanalytical Chemistry 399(1), 277-300.

van Boxtel, N., Wolfs, K., Van Schepdael, A., and Adams, E. (2015). Applications of acetone acetals as water scavengers and derivatization agents prior to the gas chromatographic analysis of polar residual solvents in aqueous samples. Journal of Chromatography A 1425, 62-72.

Headspace analysis: Dynamic

Reprinted from Harries and Bruno, Headspace Analysis: Dynamic, Journal of Analytical Science 3rd ed, 2018.

1. Introduction

Headspace analysis is a technique for sampling and examining the volatiles in a solid or liquid sample. The term headspace refers to the volume of vapor above a condensed phase sample. Purge and trap refers to the headspace technique in which volatile organic compounds (VOCs) are purged out of the sample matrix by an inert gas and carried onto a sorbent trap, where they are concentrated and later introduced into an instrument (e.g., gas chromatography (GC) or GC/mass spectrometry (MS)) for analysis. After its introduction in the 1970s, purge and trap quickly gained widespread acceptance and was adopted by regulatory agencies as a standard method. Today, it is still the workhorse for the analysis of low-concentration VOCs in solids and liquids. Low volatility solutes can also be collected and concentrated using purge and trap. Differing instrumentation and procedures may be used for liquid and solid samples, tailored to the application. This article discusses its basic theory, instrumentation, operational procedures, quantification methods, and selected applications.

2. Principles

Purge and trap is also known as dynamic headspace extraction, which is closely related to static headspace extraction. In both techniques, organic compounds migrate from the condensed phase of the sample matrix into its headspace. This is illustrated in Figure 1. In static headspace, equilibrium is often reached between the sample and its headspace. In purge and trap, an inert sweep gas is used to continuously remove the analytes out of the sample, thus creating non-

equilibrium and a potentially higher concentration gradient between phases. An alternative to the use of the inert sweep gas is to draw headspace from the sample by suction, with the withdrawn volume replaced by air through a vent line. This dynamic withdrawal of analyte enhances mass transfer. Consequently, purge and trap is generally more sensitive than static headspace analysis (see the article on this topic). It is suitable for trace analysis with detection limits at parts per billion to parts per trillion levels. On the other hand, static headspace is often used as a complementary screening method for high-concentration samples, and typically requires simpler equipment.

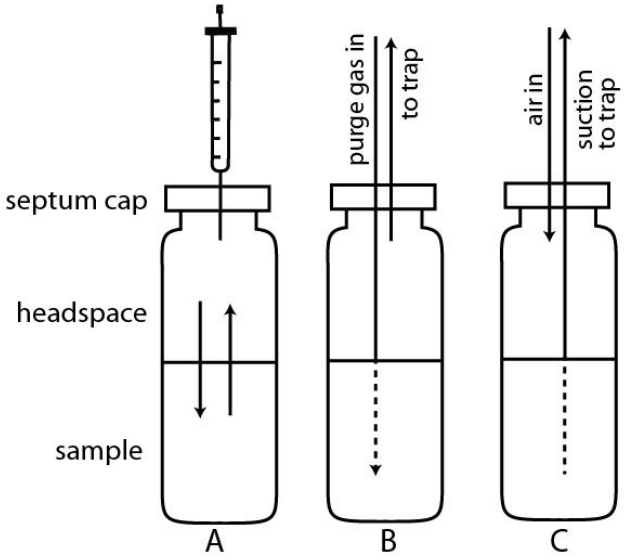

Figure 1. Concepts of static headspace (A) and dynamic headspace using purge gas (B) and suction (C).

There are three main processes in purge and trap methods: extraction (purging), simultaneous adsorption (trapping), and subsequent desorption (by use of an elution solvent or heating, sometimes called thermal desorption). The overall purge-and-trap performance depends on the efficiency of each individual process.

Purging efficiency (the fraction of analytes removed from the sample) depends upon the properties of the analytes, sample temperature, flow rate, duration of the purging, and sample matrix. When working in an aqueous matrix, purging is most efficient for VOCs that are insoluble or slightly soluble in water. Purging at ambient temperature is adequate for these compounds. Water-soluble VOCs (e.g., ketones, alcohols, aldehydes, and some ethers) are more difficult to purge, and detection limits can be an order of magnitude higher if purged under the same conditions as those for the nonpolar VOCs. Purging efficiency can also be improved by using elevated temperatures. Acceptable recovery can be obtained for many water-soluble compounds when purged at 80°C. Purge time and flow rate are both aspects of sampling that are tunable depending on the application. Purge time is typically on the order of minutes; in rare cases, samples are purged for only a few seconds or for hours. For most compounds, the optimum flow rate is in the range of 20–40 ml min^{-1}. High flow rates can improve the recovery of compounds that are hard to purge. Very low flow rates should be avoided for such compounds. At high flow rates, however, gaseous compounds (boiling point lower than 35°C, e.g., chloromethane) can be lost from the trap due to breakthrough, which can be detected by bubbling the gas leaving the trap through a vial of solvent or by connecting multiple traps in series. Matrix effects are common for complex samples such as soils, sludges, foods, polymers, and matrices containing adsorbent carbon such as fire debris. Appropriate quantification methods that can compensate for the matrix effects should be used accordingly (discussed later).

Trapping efficiency is dependent on the properties of the target compounds and the sorbent materials used in the trap. Generally, compounds with lower boiling points are not only present at lower concentrations (that is, trace levels) in the vapor phase, but they are also more difficult to trap and require the use of “stronger” sorbents. For the purpose of this discussion,

strong and weak sorbents can be classified by thermodynamic (enthalpic) and kinetic (rate and diffusion) processes. A strong sorbent is associated with a large, negative enthalpy of interaction of the vapor components with the surface. Additionally, a strong sorbent is associated with rapid mass transfer onto the sorbent. Trapping is also more efficient at lower temperatures.

3. Instrumentation

The fundamental components of a purge and trap headspace sampling apparatus are the sample (enclosed with some headspace in a container such as an autosampler vial) with an inlet and outlet, a source of purge gas or suction, the adsorbent trap(s) through which headspace vapor passes, and the corresponding transfer lines to connect these. The operator may optionally bubble the purge gas exiting the trap through a vial of solvent (or pass the flow through a secondary sorbent trap) to detect breakthrough, that is, any analyte that was not trapped.

Depending on the application and quantity of sample, the container used may be a small vial, a clean steel paint can, or an even larger volume. For select applications, especially sampling in the field, headspace vapors are collected in situ. In situ applications could include sampling vapor inside of a suitcase or a shipping container.

The trap can contain one sorbent phase (selected for general purpose usage or tailored to the type of analyte expected) or several different sorbents with different trapping abilities. The different sorbents can be layered in a single trap, arranged in series from the weakest at the inlet to the strongest at the outlet. This is shown schematically in Figure 2. During purging, the analyte-laden gas reaches the weak sorbent first, which traps the less volatile compounds. More volatile compounds break through the weak sorbent and subsequently are trapped by strong sorbent. During desorption (solvent or thermal), the trap is heated and backflushed. In this way,

the less volatile compounds never come in contact with strong sorbents, avoiding irreversible adsorption.

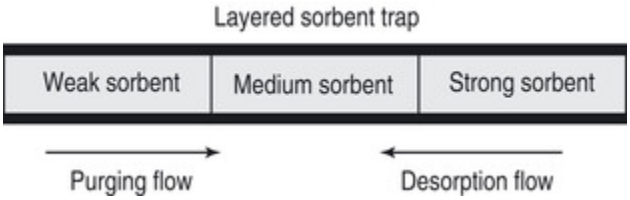

Figure 2. Schematic diagram of a multilayer sorbent trap, used with backflushed desorption.

Several different sorbent phases can also be used to collect headspace from a single sample in parallel, for example, when porous layer open tubular capillaries are used as traps for the purge and trap method PLOT-cryoadsorption.

The selection of the trap should be based on the target analytes. Table 1 describes some of the major sorbents used. Conventional, general-purpose traps can contain a porous polymer, silica gel, and activated carbon (charcoal) in series, each material filling one-third of the trap. The most common porous polymer used is Tenax TA, which is a 2,6-diphenylene oxide polymer. It is hydrophobic and has relatively weak trapping ability. It can only trap compounds with boiling points higher than 35 °C, and more volatile species and polar compounds are retained poorly. Tenax GR is a composite material of Tenax TA blended with graphitized carbon. Both sorbents have the advantage of stability under high temperatures up to 350 °C.

Silica gel is a hydrophilic sorbent with trapping capacity stronger than Tenax TA. Note that silica gel can be catalytic toward some samples (it is a Lewis acid) and it is sensitive to alkaline samples (actually dissolving in strong base). Charcoal is a very strong sorbent used for trapping the highly volatile species (e.g., dichlorodifluoromethane, boiling point −29°C) that

break through Tenax and silica gel. Charcoal is hydrophobic and therefore does not retain much water. If the compounds to be analyzed have boiling temperatures above 35 °C, Tenax is a sufficient adsorbent.

Other commonly-used sorbent materials include granulized carbon black (GCB or Carbopack), carbon molecular sieves (Carbosieve), and Carboxen. These carbon-based materials are hydrophobic. Alumina, silica, clay, and polymeric phases are also good sorbents for some applications.

Another factor in the adsorbent capability of these materials is temperature. Decreasing temperature increases the efficiency with which volatile analytes are retained; this is most commonly accomplished by chilling the trap inside a cryostat to sub-zero temperatures. Cryotrapping is a headspace preconcentration technique that uses an uncoated length of tubing chilled to approximately -150 °C to capture headspace volatiles. It is worth noting that cryo-enhancement is unique to dynamic headspace methods and cannot be used with static approaches.

Table 1. The following table provides a listing of the major types of sorbents used in sampling, concentrating, odor profiling, and air and water pollution research. These materials are useful in a wide variety of research and control applications. Many can be obtained commercially in different sizes, depending upon the application involved. The purpose of this table is to aid in the choice of a sorbent for a given analysis. Additional resources like this are available in numerous reference materials, including those in the Further Reading. From the Handbook of Basic Tables for Chemical Analysis (Further Reading).

Sorbent	Desorption Solvents	Applications
activated carbon	carbon disulfide, methylene chloride, diethyl ether, diethyl ether with 1% methanol, diethyl ether with 5% 2-propanol (caution: CS_2 and CH_3OH can react in the presence of charcoal)	used for common volatile organics; examples include methylene chloride, vinyl chloride, chlorinated aliphatics, aromatics, acetates
Notes:	Metallic or salt impurities in the sorbent can sometimes cause the irreversible adsorption of electron-rich oxygen functionalities; examples include 1-butanol, 2-butanone, and 2-ethoxyacetate; recovery rate is often poor for polar compounds.	
graphitized carbon-black	carbon disulfide, methylene chloride, diethyl ether (or thermal desorption can be used)	used for common volatile aliphatic and aromatic compounds, organic acids and alcohols, and chlorinated aliphatics
Notes:	These sorbents are hydrophobic and are not very sensitive to moisture; the possibility of thermal desorption makes them of value for "trace-level" analyses.	
silica gel	methanol, ethanol, water, diethyl ether	used for polar compound collection and concentration; examples include alcohols, phenols, chlorophenols, chlorinated aromatics, aliphatic and aromatic amines, nitrogen dioxide
Notes:	Useful for compounds which can't be recovered from the charcoal sorbents; the most serious problem with silica is the effect of water, which can cause desorption of the analytes of interest, and the heating effect involved can sometimes initiate reactions such as polymerization of the analyte. Silica gel cannot be used with highly alkaline samples.	
Sorbent	Desorption Solvents	Applications
activated alumina	water, diethyl ether, methanol	used for polar compounds such as alcohols, glycols, ketones, aldehydes; has also been used for polychlorinated biphenyls and phthalates
Notes:	Similar in application to silica gel.	
porous polymers	hexane, diethyl ether, alcohols (thermal desorption also possible in some cases)	used for a wide range of compounds which include phenols, acidic and basic organics, pesticides, priority pollutants
Notes:	The most commonly used porous polymer sorbent is Tenax-TA, although the Porapak and Chromosorb Century series have also been used; Tenax-TA has been used with thermal desorption methods, but can release toluene, benzene, and trichloroethylene residues at the higher temperatures; in addition to Tenax-TA, XAD 2-8, Porapak-N, Chromosorbs 101, 102, 103, and 106 have found applications, sometimes in "stacked" sampling devices (for example, a sorbent column of Tenax-TA and Chromosorb 106 in tandem); Chromosorb 106, a very low polarity polymer, has the lowest retention of water with respect to organic materials, and is well suited for use as a back-up sorbent.	
bonded phases	methanol, hexane, diethyl ether	used for specialized applications in pesticides, herbicides, and polynuclear aromatic hydrocarbons
Notes:	Most expensive of the common sorbents; useful for the collection of organic samples from water.	
Sorbent	Desorption Solvents	Applications
molecular sieves	carbon disulfide, hexane diethyl ether	have been used for the collection of aldehydes, alcohols, and for acrolein
Notes:	Molecular sieve 13-X is the main molecular sieve to be used as a trapping adsorbent; the sorbents will also retain water.	

The transfer lines are usually made of inert materials such as deactivated (silanized) fused silica or silica-lined stainless steel tubing. These have minimal active sites for adsorption. The lines can be heated to avoid analyte condensation; alternatively, to collect any analyte that condenses, when solvent elution is used the solvent can be flowed through the transfer lines as well as the trap.

4. Operational Procedures

Analyzing a sample by purge and trap headspace collection is a multistep process which includes purging, desorption, and trap reconditioning. The procedure described here is general to all purge and trap apparatus; for specific operations of a commercial instrument, refer to the manufacturer's literature.

To begin collection by purge and trap, an aliquot of sample is placed into the container which will be purged. In the laboratory, this container can be as small as an automatic sampler vial or as large as an oil drum. An inert purge gas (nitrogen or helium) passes through the sample, purges the VOCs out of the matrix, and carries them to the trap. Alternatively, suction is applied to the end of the trap opposite the sample and filtered air is drawn through the container, pulling headspace into the trap. Analytes are retained by the sorbents while the gas is vented. Purge time and flow rate can be adjusted and tuned to the specific application. The sample container may be heated to enhance purging efficiency, and the trap may be cooled to enhance adsorption.

Once the headspace sample is collected, the analyte(s) are stripped from the adsorbent trap in one of two ways: thermal desorption or solvent elution. In both cases, the trap is often

preheated before desorption to increase efficiency (in the case of solvent elution) and to improve the delivery of the sample to the inlet of an instrument (in the case of thermal desorption).

Thermal desorption is accomplished by heating the trap to a temperature appropriate for the sorbent phase and backflushing with the desorb (carrier) gas. Thermal desorption efficiency is affected by temperature, trap heating rate, and desorption gas flow rate. Analytes are released faster at a higher temperature, which is limited by the thermal stability of the sorbent and solute materials. For on-line purge and trap sampling, the purge and trap setup must be synchronized with the analytical instrument, and the operational parameters of the two units must be compatible. Gas chromatography (GC) coupled with a detector is frequently used to analyze thermally desorbed headspace samples. The GC run and data acquisition are initiated simultaneously at the onset of desorption (except when a secondary trap is used, see below). Desorption time is typically 2–4 min. Desorption is fast at a flow rate of ~40 ml min^{-1} and this produces a sharp injection for the GC. Packed columns can directly accept such a high flow. However, other types of columns can offer analytical advantages but are not able to accept the optimal flow rate for desorption. In these cases, a split injector may be used to divert excess flow away from the GC. However, this also decreases the quantity of sample that enters the GC, leading to decreased sensitivity. The other solution is to desorb at a low flow rate (typically 4 ml min^{-1}) for 5 min. Desorption is slow under such conditions and the desorbed analytes need to be refocused. A secondary cryogenic trap is often used for this purpose, in a process called cryofocusing. The cryotrap is a piece of uncoated silica tubing cooled to −150°C with liquid nitrogen or a vortex tube. Once desorption from the primary trap is finished, the cryogenic trap is rapidly heated to 250°C, and the chromatographic run and data acquisition are started at the same time.

Solvent elution may use a syringe, a syringe pump or a pressurized vial to push an appropriate solvent or solvent mixture through the (heated or ambient temperature) trap and collect the solution into an autosampler vial. Larger quantities of solvent ensure maximum retrieval of analyte from the trap; however, dilution of the sample is a drawback here. Smaller quantities of solvent are less diluent to a sample that may have components at low concentrations (trace). The sample solution can then be analyzed off-line by any suitable analytical technique or instrument; the sample may also be stored for future analysis.

After desorption, either thermally or with solvent, the trap must be reconditioned by baking at a temperature higher than the desorption temperature and flushing with purge gas. Reconditioning reduces sample carryover and possible trap contamination, and in the case of solvent elution, strips residual solvent from the trap to reactivate it before reuse. After reconditioning, the trap heater is turned off and purge flow is stopped. Once the trap has cooled down, it is ready for the next sample. Traps cannot be reused indefinitely; however, simple quality checks can be used to determine whether a trap is still functioning properly.

The dynamic headspace extraction approach, from collection through reconditioning, can be made field portable. Specialized apparatus exist for the in situ sampling of headspace for the field detection of analytes like explosives, cadavers, drugs, and environmental pollutants.

5. Methods of Quantification

The most commonly used quantification methods in purge and trap are external standard calibration and internal standard calibration. External standards refer to target compounds of known concentrations that are prepared and analyzed separately from the samples. A calibration curve or calibration factor (CF) is obtained by plotting the peak area count (or height) of the

analyte versus its concentration in the standards. The analyte concentration in the sample is equal to its peak area divided by the CF. External standard calibration works well for relatively clean samples where matrix has no or little effects on analyte recovery.

An internal standard is a compound that is not a sample analyte but is similar to the analytes in analytical behavior. It is spiked into each sample and calibration solution at a fixed concentration. The calibration curve is a plot of area ratio of analyte to internal standard versus the analyte concentration in the calibration solutions. The slope of the plot is called the response factor (RF). When a sample is analyzed, the peak areas of the analytes and the internal standard are obtained. The analyte concentration in the sample can be calculated from the area ratio divided by the RF. The advantage of using internal standards is that it compensates for the variations in experimental conditions such as sample volume and analyte recovery. It is especially desirable for complex samples where purging efficiency varies with matrices. The main limitations of internal standards are that they must not exist in the original sample and that they must not interfere with the analysis of the target analytes. For environmental samples, fluorinated compounds can be chosen as internal standards since their presence in the environment is uncommon. The use of MS detectors has made the use of internal standard in purge and trap more feasible because internal standards that may coelute with the analytes in a chromatogram can be differentiated by their difference in mass. Stable isotopically labeled compounds are widely used as internal standards in purge and trap with GC–MS. In general, they offer superior precision and accuracy, because these isotope analogs are almost identical to the target compounds in physical and chemical properties, mimicking the behavior of the analytes in every step of the analysis.

6. Applications and Trends

Purge and trap has been widely used in environmental, biological, pharmaceutical, food, forensic, and other types of analyses. Determination of volatile pollutants in water and soil remains its most common application, for example, the detection of banned pesticides and fuel additives. Several US Environmental Protection Agency standard test methods rely on the method for air, water, and soil testing.

Dynamic headspace extraction is used in quality control and aroma analysis of food products, including the detection of byproducts that indicate undesirable microbial growth. It has been used to investigate differences in aroma and flavor among different varieties of fruits and wine. Purge and trap has been deployed in the lab and in the field for forensic applications to detect accelerant residue on arson fire debris, decomposition products, components of explosive materials, and illicit drugs, among others. Some applications of headspace analysis present unique challenges; two examples are the detection of low volatility analytes and the presence of water in the sample.

To determine involatile components in a sample using headspace, sampling can be preceded by a chemical treatment (derivatization) to produce a volatile compound from the analyte of interest. It is thus possible to determine fluoride in fluorinated milk following initial treatment to produce volatile trifluorosilane. Sample adulteration is undesirable for several reasons. A dynamic headspace approach known as PLOT-cryoadsorption circumvents the need for derivatization using a low-temperature adsorbent capillary trap to capture the vapors above such samples as explosives, weathered fuels, and drug compounds.

Water vapor present in the headspace can pose an analytical challenge. Although water has little effect on analyte desorption from the trap, at a certain level it can cause damage to

some analytical instruments or interfere with analysis. It can also plug the column when a cryogenic interface is used. Therefore, water removal is critical in purge and trap.

There are several approaches for water removal: for example, permeation and condensation. Permaselective membrane (e.g., Nafion tubing) is effective in removing water while retaining the VOCs. However, some polar compounds such as alcohols also go through the membrane along with water vapors. Thus, this method is not suitable for polar analytes. A condensation device is more commonly used when coupling trap desorption with gas chromatography. It has less effect on the recovery of polar, water-soluble analytes, although there is always the possibility of losing such compounds. The device is a piece of tubing made of inert material (e.g., nickel). It is placed between the trap and the GC, and is maintained at ~30°C during trap heating, serving as a cold spot in the heated transfer lines. Water is condensed on it and removed from the GC carrier gas. After sample desorption, the device is heated and water vapor is vented. A third method of water removal is the addition of anhydrous salts to the sample that contains moisture. The salts together with water form hydrates, which precipitate out of solution, decreasing the amount of water vapor collected during sampling.

Finally, headspace techniques can be used to determine a number of thermodynamically important properties relating to vapor–liquid equilibria. The technique has been used to develop distillation procedures specifically where the selection of solvents in extractive distillation is required. Vapor pressures of pure substances and activity coefficients may also be determined using headspace techniques.

Further Reading

Abeel S.M., Vickers A.K., and Decker D. (1994). Trends in purge and trap. Journal of Chromatographic Science 32(8), 328-338.

ASTM International, https://www.astm.org/.

Baránková, E. and Dohnal, V. (2016). Effects of additives on volatility of aroma compounds from dilute aqueous solutions. Fluid Phase Equilibria 407, 217-223.

Bellar, T.A., Lichtenberg, J.J., and Kroner, K.C. (1974). The occurrence of organohalides in chlorinated drinking waters, Journal American Water Works Association 66, 703-706.

Bellar T.A. and Lichtenberg J.J. (1974). Determining volatile organics at microgram-per-liter levels by gas chromatography. Journal American Water Works Association 66(12), 739-744.

Bruno, T.J. (1994). Chromatographic cryofocusing and cryotrapping with the vortex tube. Journal of Chromatographic Science 32, 112-115.

Bruno, T.J. (2009). Simple, quantitative headspace analysis by cryoadsorption on a short alumina PLOT column. Journal of Chromatographic Science 47(7), 569-74.

Bruno, T. J., Svoronos, P.D.N, *CRC Handbook of Basic Tables for Chemical Analysis, 3rd. ed*. Taylor and Francis CRC Press: Boca Raton, 2011.

Bruno, T. J. (2016). Field portable low temperature porous layer open tubular cryoadsorption headspace sampling and analysis part I: Instrumentation. Journal of Chromatography A 1429, 65-71.

Index to EPA test methods, https://www.epa.gov/measurements/index-epa-test-methods.

Harries, M., Bukovsky-Reyes, S., and Bruno, T. J. (2016). Field portable low temperature porous layer open tubular cryoadsorption headspace sampling and analysis part II: Applications. Journal of Chromatography A 1429, 72-78.

Index to EPA test methods, https://www.epa.gov/measurements/index-epa-test-methods.

Ioffe, B. V. and Vitenberg, A. G. (1984). Head-space analysis and related methods in gas chromatography. New York: Wiley.

Lovestead, T. M. and Bruno, T. J. (2010). Detection of poultry spoilage markers from headspace analysis with cryoadsorption on a short alumina PLOT column. Food Chemistry 121, 1274-1282.

Lovestead, T. M. and Bruno, T. J. (2011). Detecting gravesoil with headspace analysis with adsorption on short porous layer open tubular (PLOT) columns. Forensic Science International 204, 156-161.

Lovestead, T.M., Bruno, T.J. (2017). Determination of cannabinoid vapor pressures to aid in vapor phase detection of intoxication. Forensic Chemistry 5, 79-85.

Lovestead, T. M. and Bruno, T. J. (2010). Trace headspace sampling for quantitative analysis of explosives with cryoadsorption on short alumina porous layer open tubular columns. Analytical Chemistry 82, 5621-5627.

Nichols, J. E., Harries, M. E., Lovestead, T. M., and Bruno, T. J. (2014). Analysis of arson fire debris by low temperature dynamic headspace adsorption porous layer open tubular columns. Journal of Chromatography A 1334, 126-138.

Sghaier, L., Vial, J., Sassiat, P., et al. (2016). An overview of recent developments in volatile compounds analysis from edible oils: Technique-oriented perspectives. European Journal of Lipid Science and Technology 118, 1853-1879.

Slack G., Snow N., and Kou D. (2003). Extraction of volatile organic compounds from solids and liquids. In Mitra, S. (ed.) Sample preparation techniques in analytical chemistry, pp 183-226. Hoboken, New Jersey: Wiley.

Tiscione, N.B., Yeatman, D.T., Shan, X., and Kahl, J.H. (2013). Identification of volatiles by headspace gas chromatography with simultaneous flame ionization and mass spectrometric detection. Journal of Analytical Toxicology 37, 573-579.

Truong, T.V., Porter, N.L., Lee, E.D., and Thomas, R.J. (2016). The applicability of field-portable GC-MS for the rapid sampling and measurement of high-boiling-point semivolatile organic compounds in environmental samples. The Application Notebook September 2016, 30-36.